Kunz lecture notes for Les Houches 2019: Waves and Instabilities

Ideal MHD equations: $$\frac{\partial\rho}{\partial t} + \vec{\nabla}\cdot(\rho\vec{u}) = 0$$

$$\rho\left(\frac{\partial}{\partial t} + \vec{u}\cdot\vec{\nabla}\right)\vec{u} = -\vec{\nabla}\left(p + \frac{B^2}{8\pi}\right) + \frac{\vec{B}\cdot\vec{\nabla}\vec{B}}{4\pi} - \rho\vec{\nabla}\Phi$$

$$\frac{\partial\vec{B}}{\partial t} = \vec{\nabla}\times\left(\vec{u}\times\vec{B}\right) = -\vec{u}\cdot\vec{\nabla}\vec{B} + \vec{B}\cdot\vec{\nabla}\vec{u} - \vec{B}\,\vec{\nabla}\cdot\vec{u}$$

if incompressible, $\vec{\nabla}\cdot\vec{u}=0$, which determines the pressure p; if adiabatic, then $\frac{3}{2}p\left(\frac{\partial}{\partial t}+\vec{u}\cdot\vec{\nabla}\right)\ln\frac{p}{\rho^{5/3}} = 0$

Standard notation: ρ = mass density ($\Sigma_s m_s n_s$)

$\vec{u}$ = fluid velocity ($\Sigma_s m_s n_s \vec{u}_s / \Sigma_s m_s n_s$)

p = thermal pressure ($\Sigma_s p_s = \Sigma_s n_s T_s$)

$\vec{B}$ = magnetic field (Φ = potential, e.g., gravitational)

Other forms, after defining $\frac{d}{dt} \equiv \frac{\partial}{\partial t} + \vec{u}\cdot\vec{\nabla}$ as the Lagrangian (or comoving) derivative:

$$\frac{d\rho}{dt} = -\rho\vec{\nabla}\cdot\vec{u}$$

$$\frac{d\vec{u}}{dt} = -\frac{1}{\rho}\vec{\nabla}\left(p + \frac{B^2}{8\pi}\right) + \frac{\vec{B}\cdot\vec{\nabla}\vec{B}}{4\pi\rho} - \vec{\nabla}\Phi$$

$$\frac{d\vec{B}}{dt} = \vec{B}\cdot\vec{\nabla}\vec{u} - \vec{B}\,\vec{\nabla}\cdot\vec{u}$$

$$\left(\frac{3}{2}p\frac{d}{dt}\ln\frac{p}{\underset{\uparrow\ \gamma=5/3}{\rho^{5/3}}} = 0\right)$$

We'll also write $\vec{B} = B\hat{b}$. Then

$$\frac{d\ln B}{dt} = \left(\hat{b}\hat{b} - \overleftrightarrow{I}\right) : \vec{\nabla}\vec{u} \quad \text{and} \quad \frac{d\hat{b}}{dt} = \left(\overleftrightarrow{I} - \hat{b}\hat{b}\right) : \left(\hat{b}\cdot\vec{\nabla}\vec{u}\right).$$

First, we'll do waves. Then, Lagrangian perturbation theory. Then, some instabilities. Then we'll go into non-ideal MHD and pick up some additional waves and instabilities. Let's start simple...

MHD WAVES

Consider a uniform, stationary, MHD fluid, threaded by a uniform magnetic field. To orient our coordinate system, we will use $\vec{B} = B_0\hat{z}$, with the directions ⊥ to the field being x and y. Perturb the fluid with small displacements, which we take (freely) to be sinusoidal:

$$\rho = \rho_0 + \delta\rho\, e^{i\vec{k}\cdot\vec{r} - i\omega t}$$
$$\vec{B} = B_0\hat{z} + \vec{\delta B}\, e^{i\vec{k}\cdot\vec{r} - i\omega t}$$
$$\vec{u} = 0 + \vec{\delta u}\, e^{i\vec{k}\cdot\vec{r} - i\omega t}$$
$$p = p_0 + \delta p\, e^{i\vec{k}\cdot\vec{r} - i\omega t}$$

$\vec{k}$ = wavevector

ω = frequency

Small? What's "small"? By "small", I mean that all nonlinearities $\sim\delta^2$ will be dropped. The result is linear theory. Before we do this, note that, when computing actual observed quantities, we should take the real part (e.g. $e^{i\vartheta} \to \cos\vartheta$, $ie^{i\vartheta} \to -\sin\vartheta$, etc.)

First, simplest geometry: $\vec{k} = k\hat{z}$. My notation is usually "$k_{\parallel}$" in this case, to remind me that k is parallel to the guide field. This notation is used in a lot of plasma physics, but less so in astronomy. Our linearized MHD equs. are then

$$-i\omega \frac{\delta\rho}{\rho_0} + ik_{\parallel}\delta u_{\parallel} = 0$$

$$-i\omega \vec{\delta u} = -\frac{ik_{\parallel}\hat{z}}{\rho_0}\left(\delta p + \frac{B_0 \delta B_{\parallel}}{4\pi}\right) + \frac{ik_{\parallel}B_0}{4\pi\rho_0}\vec{\delta B}$$

$$-i\omega \frac{\vec{\delta B}}{B_0} = ik_{\parallel}\vec{\delta u} - \hat{z}\, ik_{\parallel}\delta u_{\parallel} \longrightarrow \delta B_{\parallel} = 0 \quad \left(\text{as is required by } \vec{k}\cdot\vec{\delta B} = 0\right)$$

Note that we don't need to know δp and $\delta\rho$ to solve for the perpendicular ($\perp$) dynamics:

$$\left.\begin{aligned} -i\omega \vec{\delta u_{\perp}} &= \frac{ik_{\parallel}B_0}{4\pi\rho_0}\vec{\delta B_{\perp}} \\ -i\omega \frac{\vec{\delta B_{\perp}}}{B_0} &= ik_{\parallel}\vec{\delta u_{\perp}} \end{aligned}\right\} \left(\omega^2 - k_{\parallel}^2 v_A^2\right)\frac{\vec{\delta B_{\perp}}}{B_0} = 0$$

$$\Downarrow$$

$$\boxed{\begin{gathered} \omega = \pm k_{\parallel} v_A \\ \text{with } v_A \equiv \frac{B_0}{\sqrt{4\pi\rho_0}} \end{gathered}}$$

These are "Alfvén waves", which are polarized across the guide field and which propagate at speed v_A, the "Alfvén speed".

These waves are not associated with any motion along the field nor any changes in density.

Using $\frac{\delta p}{p_0} = \gamma \frac{\delta \rho}{\rho_0}$, the other modes are sound waves: $\boxed{\omega = \pm k_{\parallel} c_s}$,

with $c_s \equiv \left(\frac{\gamma p_0}{\rho_0}\right)^{1/2}$ being the "sound speed". The fifth mode is $\boxed{\omega = 0}$,

and corresponds to a relabeling of fluid elements. It's called the "entropy mode."

Now, let's have $\vec{k} = k_{\parallel}\hat{z} + \vec{k}_{\perp}$ — a more general wavevector. Then our linearized eqns. are

$$Ⓐ \quad -i\omega \frac{\delta \rho}{\rho_0} + i k_{\parallel} \delta u_{\parallel} + i\vec{k}_{\perp} \cdot \vec{\delta u}_{\perp} = 0$$

$$-i\omega \delta\vec{u} = -\frac{i\vec{k}}{\rho_0}\left(\delta p + \frac{B_0 \delta B_{\parallel}}{4\pi}\right) + \frac{i k_{\parallel} B_0}{4\pi \rho_0} \delta\vec{B}$$

$$-i\omega \frac{\delta \vec{B}}{B_0} = i k_{\parallel} \delta\vec{u} - \hat{z}\left(i k_{\parallel} \delta u_{\parallel} + i\vec{k}_{\perp} \cdot \delta\vec{u}_{\perp}\right)$$

$$Ⓑ \quad -i\omega \frac{\delta \vec{B}_{\perp}}{B_0} = i k_{\parallel} \delta\vec{u}_{\perp} \quad \text{and} \quad Ⓒ \quad -i\omega \frac{\delta B_{\parallel}}{B_0} = -i\vec{k}_{\perp} \cdot \delta\vec{u}_{\perp}$$

$$Ⓓ \quad -i\omega \delta\vec{u}_{\perp} = -\frac{i\vec{k}_{\perp}}{\rho_0}\left(\delta p + \frac{B_0 \delta B_{\parallel}}{4\pi}\right) + \frac{i k_{\parallel} B_0}{4\pi \rho_0} \delta\vec{B}_{\perp} \quad \text{and}$$

$$Ⓔ \quad -i\omega \delta u_{\parallel} = -\frac{i k_{\parallel}}{\rho_0}\left(\delta p + \frac{B_0 \delta B_{\parallel}}{4\pi}\right) + \frac{i k_{\parallel} B_0}{4\pi \rho_0} \delta B_{\parallel} .$$

$\vec{k}_\perp \cdot$ Ⓓ $+ k_\parallel$ Ⓔ $\Rightarrow \; -i\omega\left(\vec{k}_\perp \cdot \delta\vec{u}_\perp + k_\parallel \delta u_\parallel\right) = -i\frac{k^2}{\rho_0}\left(\delta p + \frac{B_0 \delta B_\parallel}{4\pi}\right)$

use Ⓐ : $\frac{-i\omega}{i}\left(\frac{i\omega\,\delta\rho}{\rho_0}\right) = -i\frac{k^2}{\rho_0}\left(\delta p + \frac{B_0 \delta B_\parallel}{4\pi}\right)$

use $\frac{\delta p}{p_0} = \gamma \frac{\delta\rho}{\rho_0}$ (which loses the entropy mode)

$$\Rightarrow \left(\omega^2 - k^2 c_s^2\right)\frac{\delta\rho}{\rho_0} = k^2 v_A^2 \frac{\delta B_\parallel}{B_0}$$

Now, Ⓓ with Ⓑ gives: $\left(\omega^2 - k_\parallel^2 v_A^2\right)\frac{\delta\vec{B}_\perp}{B_0} = -k_\parallel \vec{k}_\perp\left(c_s^2 \frac{\delta\rho}{\rho_0} + v_A^2 \frac{\delta B_\parallel}{B_0}\right)$

$$\left(\omega^2 - k_\parallel^2 v_A^2\right)\frac{\delta\vec{B}_\perp}{B_0} = -k_\parallel \vec{k}_\perp \frac{\delta B_\parallel}{B_0}\left[c_s^2 \frac{k^2 v_A^2}{\omega^2 - k^2 c_s^2} + v_A^2\right]$$

Note that the parallel and perpendicular components are now coupled!

$$\left(\omega^2 - k_\parallel^2 v_A^2\right)\frac{\delta\vec{B}_\perp}{B_0} = -k_\parallel \vec{k}_\perp v_A^2\left[\frac{\omega^2}{\omega^2 - k^2 c_s^2}\right]\frac{\delta B_\parallel}{B_0}$$

Before we go any further, note that, if $c_s^2/v_A^2 \gg 1$, then we have $\omega^2 - k_\parallel^2 v_A^2 \approx 0$, and so we get back something like an Alfvén wave in this limit. Proceeding by using $\frac{\delta B_\parallel}{B_0} = \frac{-\vec{k}_\perp \cdot \delta\vec{B}_\perp}{k_\parallel B_0}$, we have

$$\left[\overleftrightarrow{I}\left(\omega^2 - k_\parallel^2 v_A^2\right) - \vec{k}_\perp \vec{k}_\perp v_A^2 \frac{\omega^2}{\omega^2 - k^2 c_s^2}\right] \cdot \frac{\delta \vec{B}_\perp}{B_0} = 0.$$

Taking the determinant and setting it to zero gives the dispersion relation

$$\boxed{\left(\omega^2 - k_\parallel^2 v_A^2\right)\underbrace{\left[\omega^2 - k_\parallel^2 v_A^2 - k_\perp^2 v_A^2 \cdot \frac{\omega^2}{\omega^2 - k^2 c_s^2}\right]}_{} = 0.}$$

you'll often see this part as

$$\omega^4 - \omega^2 k^2 \left(c_s^2 + v_A^2\right) + k_\parallel^2 v_A^2 k^2 c_s^2,$$

but I prefer it in this form because it's easier to take $\beta \equiv \frac{c_s^2}{v_A^2}$ limits.

Note that we recover the Alfvén-wave solution $\omega^2 = k_\parallel^2 v_A^2$. Nice.

Now we also have

$$\boxed{\omega^2 = \frac{k^2\left(c_s^2 + v_A^2\right)}{2} \pm \sqrt{\frac{k^4\left(c_s^2 + v_A^2\right)^2}{4} - k_\parallel^2 v_A^2 k^2 c_s^2}.}$$

These are "magnetosonic modes" — the $\oplus$ solution being the "fast wave" and the $\ominus$ solution being the "slow wave".

Note that, in the high-β limit, we have

$$\omega_+^2 \approx k^2 c_s^2 \qquad \text{and} \qquad \omega_-^2 \approx k_\parallel^2 v_A^2$$

SOUND! ALFVÉN!

The difference between the slow mode in this limit and the shear-Alfvén wave is that the latter involves no compressive fluctuations, being polarized with $\delta B_\parallel = 0$ exactly. This is sometimes called a "pseudo-Alfvén wave". (Note that the $\beta \gg 1$ slow mode is $\omega^2 = k_\parallel^2 v_A^2 + k_\parallel^2 v_A^2 \dfrac{k_\perp^2}{\beta k^2} + O\left(\dfrac{1}{\beta^2}\right)$.)

Here are some pictures of these waves: ($\vec{\xi}$ is a displacement)

Alfvén :

NB. can have $k_\perp \neq 0$ AW:

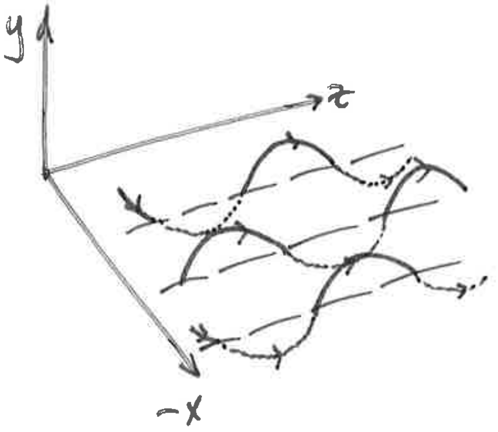

Sound:

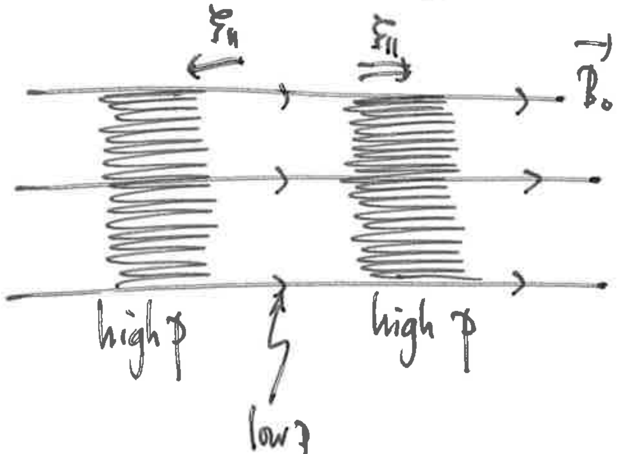

fast w/ $k_\parallel = 0$:

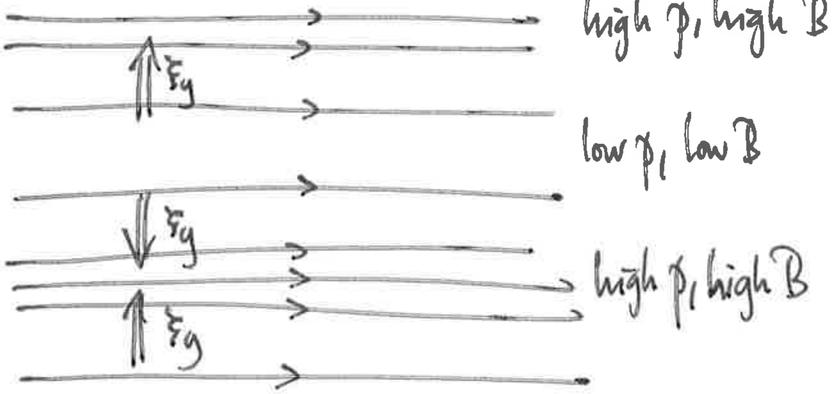

Fast:

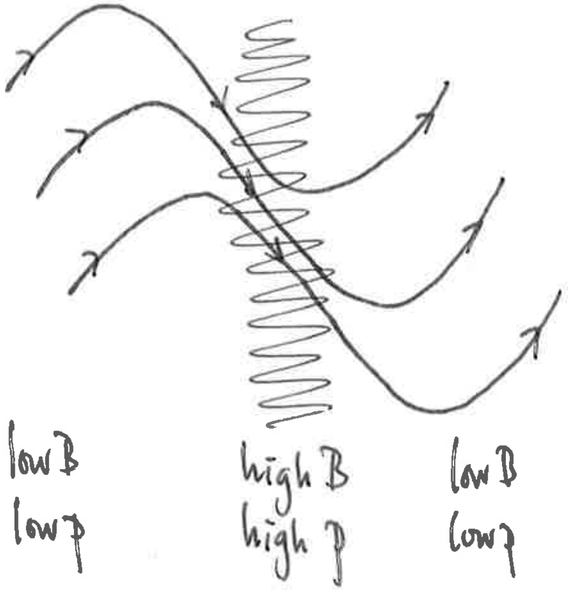

Slow:

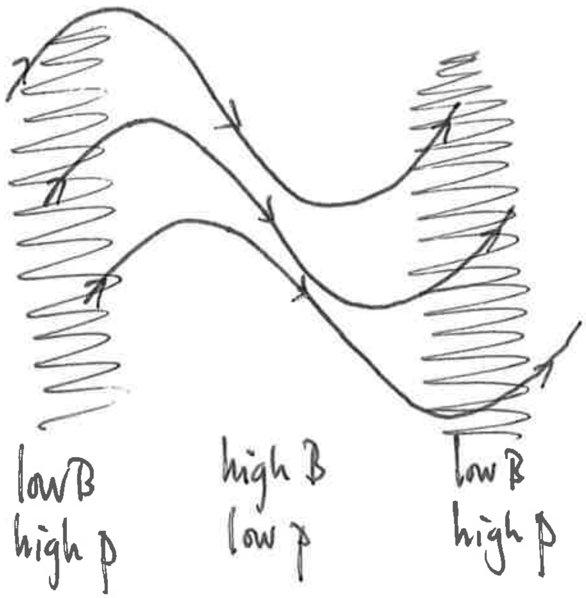

Slow with $k_\parallel/k_\perp \ll 1$:

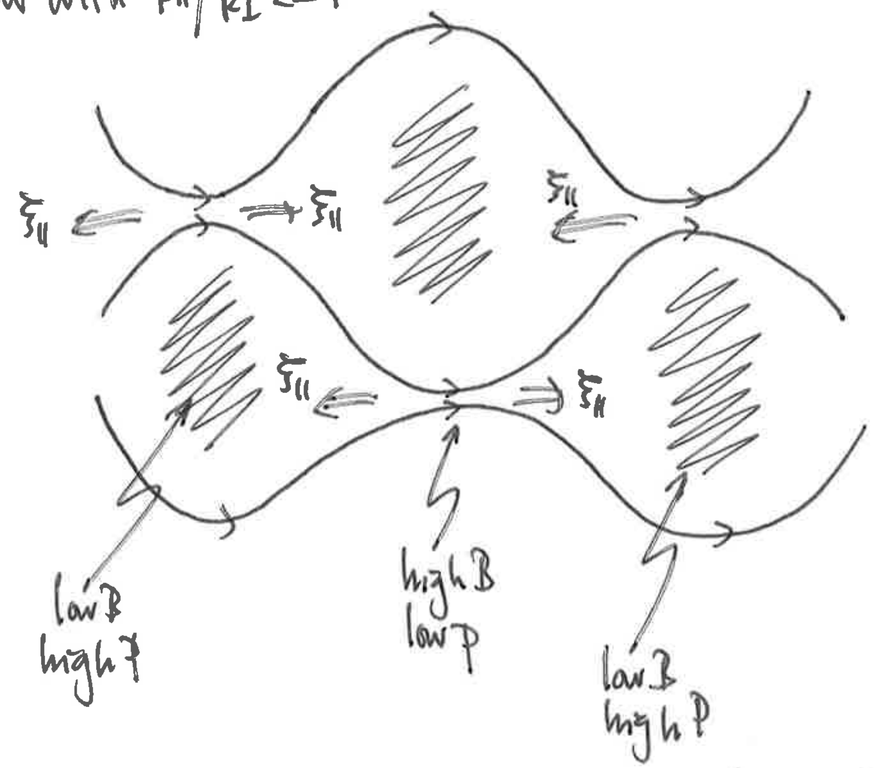

Now, this last limit, $k_\parallel/k_\perp \ll 1$, is quite useful for studies of Alfvénic turbulence, which generically evolves towards having fluctuations with $k_\parallel/k_\perp \ll 1$. In this limit, the AW is still just $\omega = \pm k_\parallel V_A$. But the magnetosonic modes become

$$\begin{tikzcd}[column sep=small] & \omega^2 \simeq \dfrac{k_\perp^2 (c_s^2+V_A^2)}{2}\left[1 \pm \left(1 - \dfrac{2k_\parallel^2 V_A^2 k_\perp^2 c_s^2}{k_\perp^4 (c_s^2+V_A^2)^2}\right)\right] \arrow[dl, "\oplus\ \text{FAST}"'] \arrow[dr, "\ominus\ \text{SLOW}"] & \\ \begin{array}{l} k_\perp^2 (c_s^2+V_A^2) \\ = k_\perp^2 V_A^2 (1+\beta) \end{array} & & k_\parallel^2 V_A^2 \left(\dfrac{c_s^2}{c_s^2+V_A^2}\right) = k_\parallel^2 V_A^2 \left(\dfrac{\beta}{1+\beta}\right) \end{tikzcd}$$

Let's look at the slow mode in this limit. Recall from the linear calculation that

$$\delta p = c_s^2 \delta\rho = \rho_0 c_s^2 \left(\frac{k^2 V_A^2}{\omega^2 - k^2 c_s^2}\right) \frac{\delta B_\parallel}{B_0} \Rightarrow \frac{\delta\rho}{\rho_0} + \left(\frac{k^2 V_A^2}{k^2 c_s^2 - \omega^2}\right)\frac{\delta B_\parallel}{B_0} = 0.$$

With $k_\perp \gg k_\parallel$ and $\omega^2 \simeq k_\parallel^2 V_A^2 \left(\frac{\beta}{1+\beta}\right)$, this becomes

$$\frac{\delta\rho}{\rho} + \frac{k_\perp^2 V_A^2}{k_\perp^2 c_s^2 - \frac{k_\parallel^2 V_A^2 \beta}{1+\beta}} \frac{\delta B_\parallel}{B_0} \simeq \underbrace{\frac{\delta\rho}{\rho} + \frac{1}{\beta}\frac{\delta B_\parallel}{B_0}}_{\text{pressure balance!}} = 0.$$

Slow modes with $k_\parallel / k_\perp \ll 1$ are pressure-balanced structures.

LAGRANGIAN VS. EULERIAN PERTURBATIONS

Thus far, I have used "Eulerian" perturbation theory, in which perturbations are denoted by a "δ". This measures the change in a quantity at a particular point in space. For ex., if the equilibrium density at $\vec{r}$, $\rho(\vec{r})$, is changed at time t by some disturbance to become $\rho'(t,\vec{r})$, then we denote the Eulerian perturbation of the density by

$$\rho'(t,\vec{r}) - \rho(\vec{r}) \equiv \delta\rho \ll \rho(\vec{r}).$$

Again, these perturbations are taken <u>at fixed position</u>. There is an alternative treatment, called "Lagrangian" perturbation theory, which concerns the evolution of small perturbations about a background state <u>within a particular fluid element</u> as it undergoes a displacement $\vec{\xi}$. For ex., if a particular fluid element is displaced from its equilibrium position $\vec{r}$ to position $\vec{r}+\vec{\xi}$, then the density of that fluid element changes by an amount

$$\rho'(t,\vec{r}+\vec{\xi}) - \rho(\vec{r}) \equiv \Delta\rho.$$

This is a Lagrangian perturbation. To linear order, δ and Δ are related by

$$\Delta\rho \simeq \rho'(t,\vec{r}) + \vec{\xi}\cdot\vec{\nabla}\rho(\vec{r}) - \rho(\vec{r}) = \delta\rho + \vec{\xi}\cdot\vec{\nabla}\rho.$$

There are many situations in which a Lagrangian approach is easier to use than is an Eulerian approach; there are also some situations in which doing so is absolutely necessary (e.g., see §IIe of Balbus (1988, ApJ, 328, 395) and §Ic of Balbus & Soker (1989, ApJ, 341, 611) for discussions of the perils of Eulerian perturbations in the context of local thermal instability.

Q: it is possible to have zero Eulerian perturbation and yet have finite Lagrangian perturbation. What does this mean physically? Is there a real physical change in the system?

The Lagrangian velocity perturbation $\Delta\vec{u}$ is given by

$$\Delta\vec{u} \equiv \frac{d\vec{\xi}}{dt} = \left(\frac{\partial}{\partial t} + \vec{u}\cdot\vec{\nabla}\right)\vec{\xi},$$

where $\vec{u}$ is a background velocity. It is the instantaneous time rate of change of the displacement of a fluid element, taken relative to the unperturbed flow. Because $\Delta\vec{u} = \delta\vec{u} + \vec{\xi}\cdot\vec{\nabla}\vec{u}$, we have

$$\delta\vec{u} = \frac{\partial\vec{\xi}}{\partial t} + \vec{u}\cdot\vec{\nabla}\,\vec{\xi} - \vec{\xi}\cdot\vec{\nabla}\vec{u}.$$

Exercise. Let $\vec{u} = R\Omega(R)\hat{\varphi}$, as in a differentially rotating disk in cylindrical coordinates. Consider a displacement $\vec{\xi}$ with radial and azimuthal components ξ_R and ξ_φ, each depending upon R and φ. Show that

$$\frac{d\xi_R}{dt} = \delta u_R \quad \text{and} \quad \frac{d\xi_\varphi}{dt} = \delta u_\varphi + \xi_R \frac{d\Omega}{d\ln R}.$$

You can think of δ and Δ as difference operators, since we're only working to linear order:

$$\delta\left(\frac{1}{\rho}\right) = \frac{1}{\rho+\delta\rho} - \frac{1}{\rho} \simeq -\frac{\delta\rho}{\rho^2}.$$

But you must be very careful when mixing Eulerian and Lagrangian points of view. Prove the following commutation relations:

i. $[\delta, \partial/\partial t] = 0$

ii. $[\delta, \partial/\partial x_i] = 0$

iii. $[\Delta, \partial/\partial t] = -\frac{\partial \xi^j}{\partial t}\frac{\partial}{\partial \xi_j}$

iv. $[\Delta, \partial/\partial x_i] = -\frac{\partial \xi^j}{\partial x^i}\frac{\partial}{\partial x^j}$

v. $[\Delta, d/dt] = 0$

vi. $[\delta, d/dt] = -\xi^j \frac{\partial}{\partial x^j}\frac{d}{dt}$

viii. $\left[\frac{\partial}{\partial x^i}, \frac{d}{dt}\right] = \frac{\partial u^j}{\partial x^i}\frac{\partial}{\partial x^j}$

You can use these to show that

$$\frac{\Delta\rho}{\rho} = -\vec{\nabla}\cdot\vec{\xi}$$

$$\frac{\Delta T}{T} = -(\gamma-1)\vec{\nabla}\cdot\vec{\xi}$$

$$\delta\vec{B} = \vec{B}\cdot\vec{\nabla}\vec{\xi} - \vec{B}\,\vec{\nabla}\cdot\vec{\xi}$$

SOME MHD INSTABILITIES

- **Kelvin-Helmholtz instability (KHI).** Using Lagrangian perturbation, this is quite easy. Consider two uniform fluids separated by a discontinuous interface at $z=0$. The fluid above the interface ($z>0$) has density ρ_2 and equilibrium velocity $\vec{u}_0 = U\hat{x}$. The fluid below the interface ($z<0$) has density ρ_1 and is stationary. (We can always transform to a frame in which this fluid is stationary, so why not take advantage of that?) There is a uniform magnetic field $\vec{B}_0 = B_{0x}\hat{x} + B_{0y}\hat{y}$ oriented parallel to the interface that permeates all of the fluid, which we take to be perfectly conducting. Assume the fluid is incompressible.

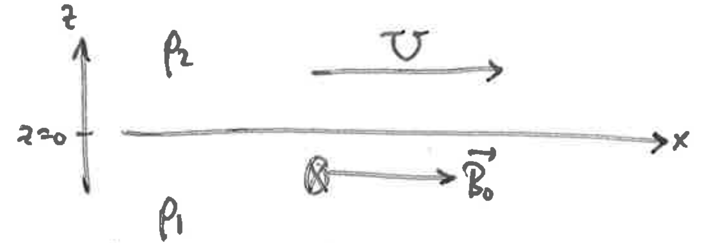

We seek the dispersion relation governing small-amplitude perturbations. Take the momentum equation and apply Δ:

$$\Delta\left[\rho\frac{d\vec{u}}{dt} = -\vec{\nabla}\left(p + \frac{B^2}{8\pi}\right) + \frac{\vec{B}\cdot\vec{\nabla}\vec{B}}{4\pi}\right]$$

$$\Rightarrow \rho\frac{d^2\vec{\xi}}{dt^2} = -\vec{\nabla}\delta\left(p + \frac{B^2}{8\pi}\right) + \frac{\vec{B}_0\cdot\vec{\nabla}\,\delta\vec{B}}{4\pi},$$

since $\vec{\nabla}B_0 = \vec{\nabla}p_0 = 0$. Use linearized induction equation, $\delta\vec{B} = (\vec{B}_0\cdot\vec{\nabla})\vec{\xi}$ (since $\vec{\nabla}B_0 = 0$ and $\vec{\nabla}\cdot\vec{u} = \vec{\nabla}\cdot\vec{\xi} = 0$), to obtain

$$\circledast \qquad \left[\frac{d^2}{dt^2} - \frac{(\vec{B}_0\cdot\vec{\nabla})^2}{4\pi\rho}\right]\vec{\xi} = -\frac{1}{\rho}\vec{\nabla}\,\delta\left(p + \frac{B^2}{8\pi}\right) \equiv -\frac{1}{\rho}\vec{\nabla}\,\delta\Pi.$$

Take $\vec{\nabla}\cdot$ of this:

$$\left[\frac{d^2}{dt^2} - \frac{(\vec{B}_0\cdot\vec{\nabla})^2}{4\pi\rho}\right]\vec{\nabla}\cdot\vec{\xi} = -\frac{1}{\rho}\nabla^2\delta\Pi = 0 \text{ by incompressibility}$$

$$\Rightarrow \nabla^2\delta\Pi = \left(-k_x^2 - k_y^2 + \frac{\partial^2}{\partial z^2}\right)\delta\Pi = 0 \Rightarrow \delta\Pi \propto \exp\left(ik_x x + ik_y y - |kz|\right)$$

where $k = \sqrt{k_x^2 + k_y^2}$. Adopt solutions $\xi \sim e^{-i\omega t}$. Then equation ⊛ above and below the interface becomes

$$\left[(-i\omega + ik_x U)^2 + (\vec{k}\cdot\vec{V}_{A0})_2^2\right]\xi_{z2} = +\frac{1}{\rho_2}|k|\,\delta\Pi_2,$$

$$\left[(-i\omega)^2 \qquad + (\vec{k}\cdot\vec{V}_{A0})_1^2\right]\xi_{z1} = -\frac{1}{\rho_1}|k|\,\delta\Pi_1,$$

respectively. At the interface, $\xi_{z1} = \xi_{z2}$ and $\Delta\Pi_1 = \Delta\Pi_2$. Because $\vec{\nabla}p_0 = 0$, the latter implies $\delta\Pi_1 = \delta\Pi_2$. Matching these, we find

$$(\omega - k_x U)^2\rho_2 + \omega^2\rho_1 = \frac{(\vec{k}\cdot\vec{B}_0)^2}{2\pi}$$

$$\Rightarrow \boxed{\omega = k_x U\frac{\rho_2}{\rho_1+\rho_2}\left\{1 \pm \left(\frac{\rho_1}{\rho_2}\right)^{1/2}\left[\frac{(\vec{k}\cdot\vec{B}_0)^2}{\pi\bar{\rho}\,k_x^2U^2} - 1\right]^{1/2}\right\}}$$

where $\bar{\rho} \equiv \frac{2\rho_1\rho_2}{\rho_1+\rho_2}$ is the reduced mass density. For stability, the discriminant must be >0; thus,

$$\boxed{\frac{(\vec{k}\cdot\vec{B}_0)^2}{4\pi\bar{\rho}} > \left(\frac{k_x U}{2}\right)^2}$$ Kelvin-Helmholtz stability.

magn. tension > velocity shear

Note that, if $B_{0x}=0$, then this reads $\left(\frac{k_y}{k_x}\right)^2 \frac{B_{0y}^2}{4\pi\bar{\rho}} > \left(\frac{U}{2}\right)^2$, which is always unstable for small enough $|k_y/k_x|$, no matter how strong is B_{0y}.

The physics: an upwardly displaced distortion of the interface into region 2 causes a constriction of the velocity there, and the fluid must move faster to conserve its mass. But when it moves faster, the pressure must drop (Bernoulli!). The opposite happens below the interface. Now there is a pressure gradient pushing upwards, reinforcing the displacement, and the process runs away. <u>That's</u> why pressure perturbations were vital in ⊛.

Question: Does this instability occur in a linear shear flow? (i.e., $\vec{u}_0 = Sz\hat{x}$) No! Drop the magnetic field for simplicity. With $\vec{u}_0 = u_0(z)\hat{x}$, one can show from (using $\vec{\nabla}\cdot\delta\vec{u}=0$)

$$\left.\begin{aligned} &ik_x\delta u_x + \delta u_z' = 0 \\ &-i(\omega-k_xu_0)\delta u_x + \delta u_z u_0' = -ik_x\delta p/\rho \\ &-i(\omega-k_xu_0)\delta u_z = -\delta p'/\rho \end{aligned}\right\} \quad \delta u_z'' - k_x^2\delta u_z = \frac{k u_0''\delta u_z}{\omega-k_xu_0}.$$ Now,

Multiply this by $\delta u_z^{*(\leftarrow \text{c.c.})}$ and integrate between upper and lower boundaries $\pm L$.

$$\int_{-L}^{L} dz \left(\delta u_z^* \delta u_z'' - k_x^2 |\delta u_z|^2\right) = \int_{-L}^{L} dz \, \frac{k_x u_0'' |\delta u_z|^2}{\omega - k_x u_0}$$

$$\downarrow$$

$$= \underbrace{\delta u_z^* \delta u_z' \Big|_{-L}^{+L}}_{\substack{=0 \text{ if periodic,} \\ \text{or if } \delta u_z \text{ or } \delta u_z' \\ \text{vanishes at boundaries}}} - \int_{-L}^{L} dz \, |\delta u_z'|^2$$

$$\Rightarrow \quad -\int_{-L}^{L} dz \left[|\delta u_z'|^2 + k_x^2 |\delta u_z|^2 + \frac{k_x u_0'' |\delta u_z|^2}{\omega - k_x u_0} \right] = 0$$

If the system is unstable, ω must have an imaginary part, ω_I. Writing $\omega = \omega_R + i\omega_I$, the imaginary part of the above equation is

$$\omega_I k_x \int_{-L}^{+L} dz \left(\frac{|\delta u_z|^2 u_0''}{|\omega - k_x u_0|^2} \right) = 0$$

$\Rightarrow$ u_0'' must be positive over part of the integration range, and negative over the rest; i.e., u_0'' must pass through zero.

Thus, instability requires an inflection point!
(J.W.S. Rayleigh, Proc. London Math. Soc. 9, 57 (1880))

- **Rayleigh-Taylor instability (RTI).** Consider two fluids seperated by a discontinuous interface at $z=0$ in the presence of a constant gravitational field $\vec{g} = -g\hat{z}$. The fluid above the interface ($z>0$) has uniform density ρ_2; the fluid below the interface ($z<0$) has uniform density ρ_1. Both fluids are initially stationary. There is a uniform magnetic field $\vec{B}_0 = B_{0x}\hat{x} + B_{0y}\hat{y}$ oriented parallel to the interface that permeates all of the fluid, which we take to be perfectly conducting. Again, assume $\vec{\nabla}\cdot\vec{u} = 0$.

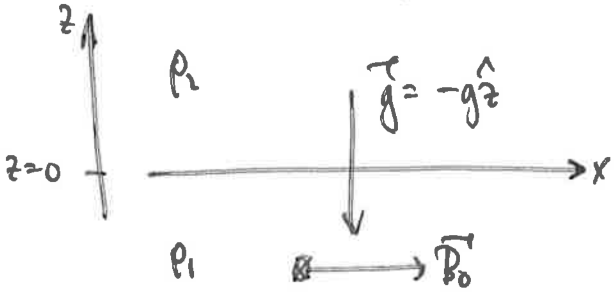

Either side of the interface, $-\frac{1}{\rho}\frac{dp}{dz} = g$

$$\Rightarrow g = -\frac{1}{\rho_1}\frac{dp_1}{dz} = -\frac{1}{\rho_2}\frac{dp_2}{dz}.$$

As before,

$$\Delta\left[\rho\frac{d\vec{u}}{dt} = -\vec{\nabla}\left(p + \frac{B^2}{8\pi}\right) + \frac{\vec{B}\cdot\vec{\nabla}\vec{B}}{4\pi} + \rho\vec{g}\right]$$

$$\Rightarrow \rho\frac{d^2\vec{\xi}}{dt^2} = -\vec{\nabla}\delta\left(p + \frac{B^2}{8\pi}\right) + \frac{\vec{B}_0\cdot\vec{\nabla}\delta\vec{B}}{4\pi} - \vec{\xi}\cdot\vec{\nabla}(\vec{\nabla}p) \underbrace{+\,\Delta\rho\,\vec{g}}_{\substack{=(\Delta\rho - \vec{\xi}\cdot\vec{\nabla}\rho)\vec{g} \\ = \delta\rho\,\vec{g} = 0 \text{ (incomp.)}}}$$

Following the KHI calculation, this gives

$$\left[-\omega^2 + (\vec{k}\cdot\vec{V}_{A0})_2^2\right]\xi_{z2} = +\frac{1}{\rho_2}|k|\,\delta\Pi_2 ,$$

$$\left[-\omega^2 + (\vec{k}\cdot\vec{V}_{A0})_1^2\right]\xi_{z1} = -\frac{1}{\rho_1}|k|\,\delta\Pi_1 .$$

Likewise, $\xi_{z1} = \xi_{z2}$ and $\Delta\Pi_1 = \Delta\Pi_2$ at the interface. But because $\vec{\nabla}p_0 \neq 0$, we have

$$\Delta\Pi_1 = \Delta\Pi_2 \Rightarrow \delta\Pi_1 - \xi_{z1}\rho_1 g = \delta\Pi_2 - \xi_{z2}\rho_2 g$$

$$\xi_{z1} = \xi_{z2} \Rightarrow \delta\Pi_1 - \delta\Pi_2 = (\rho_1 - \rho_2)\xi_z g .$$

$$\Rightarrow -\rho_1\left[-\omega^2 + (\vec{k}\cdot\vec{V}_{A0})_1^2\right]\xi_z - \rho_2\left[-\omega^2 + (\vec{k}\cdot\vec{V}_{A0})_2^2\right]\xi_z$$

$$= |k|(\rho_1 - \rho_2)\xi_z g ,$$

or

$$\omega^2(\rho_1 + \rho_2) - \frac{(\vec{k}\cdot\vec{B}_0)^2}{2\pi} = |k|(\rho_1 - \rho_2) g .$$

$$\Rightarrow \boxed{\omega = \pm\left[\frac{(\vec{k}\cdot\vec{B}_0)^2}{2\pi(\rho_1+\rho_2)} + |k| g\,\frac{\rho_1 - \rho_2}{\rho_1 + \rho_2}\right]^{1/2}}$$

For stability, the discriminant must be >0; thus,

$$\boxed{\rho_1 > \rho_2 - \frac{(\vec{k}\cdot\vec{B}_0)^2}{2\pi|k|g}.}$$ Rayleigh-Taylor stability

For instability, the fluid on top must be heavy enough for the gravitational force acting on a density fluctuation of wavelength $2\pi/|k|$ to overcome the stabilizing magnetic tension. (Note that, if $\vec{B}_0$ is not oriented along the interface, no amount of magnetic field can stabilize the system.)

- Convective instability. The RTI is but one example of convective instability; here we'll generalize the calculation for a continuously stratified MHD fluid. We will still have $-\frac{1}{\rho}\frac{dp}{dz} = g =$ constant as our equilibrium state, but will allow perturbations throughout the fluid:

$$\rho = \rho_0(z) + \delta\rho \ , \quad p = p_0(z) + \delta p \ , \quad \vec{u} = 0 + \delta\vec{u} .$$

For simplicity, let's ignore the magnetic field — it'll simply act to stabilize the system via its tension (as least as long as $B_0 =$ constant). The linearized equs. are then

$$\frac{\partial}{\partial t}\delta\rho + \rho_0(z)\,\vec{\nabla}\cdot\delta\vec{u} + \delta\vec{u}\cdot\vec{\nabla}\rho_0 = 0$$

$$\rho_0\frac{\partial}{\partial t}\delta\vec{u} = -\vec{\nabla}\delta p - \delta\rho\, g\hat{z}$$

$$\frac{\partial}{\partial t}\left(\frac{\delta p}{p_0} - \gamma\frac{\delta\rho}{\rho_0}\right) + \delta\vec{u}\cdot\vec{\nabla}\ln p_0\rho_0^{-\gamma} = 0$$

Solutions to this set of equs. are $\propto e^{-i\omega t}$:

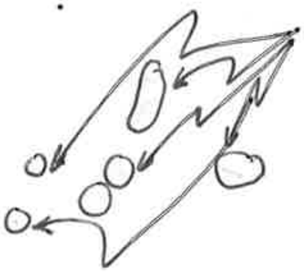

I got chocolate on my finger.

$$-i\omega\frac{\delta\rho}{\rho_0} + \vec{\nabla}\cdot\delta\vec{u} + \delta u_z\frac{d\ln\rho_0}{dz} = 0,$$

$$-i\omega\delta\vec{u} = -\frac{1}{\rho_0}\vec{\nabla}\delta p - \frac{\delta\rho}{\rho_0}g\hat{z} ,$$

$$-i\omega\left(\frac{\delta p}{p_0} - \gamma\frac{\delta\rho}{\rho_0}\right) + \delta u_z\frac{d\ln p_0\rho_0^{-\gamma}}{dz} = 0 .$$

In general, we cannot Fourier transform these equs. in z, because the coefficients in front of the perturbed quantities are z-dependent. But we can do so in the horizontal (say, x) direction:

$$-i\omega \frac{\delta\rho}{\rho_0} + ik_x \delta u_x + \frac{d\,\delta u_z}{dz} + \delta u_z \frac{d\ln\rho_0}{dz} = 0,$$

$$-i\omega\,\delta u_x = -ik_x \frac{\delta p}{\rho_0},$$

$$-i\omega\,\delta u_z = -\frac{1}{\rho_0}\frac{d\,\delta p}{dz} - \frac{\delta\rho}{\rho_0} g,$$

$$-i\omega\left(\frac{\delta p}{p_0} - \gamma\frac{\delta\rho}{\rho_0}\right) + \delta u_z \frac{d\ln p_0\rho_0^{-\gamma}}{dz} = 0,$$

where now the fluctuations are z-dependent Fourier amplitudes. Denoting $\delta\vec{u} = -i\omega\vec{\xi}$, and dropping the equilibrium "0" subscripts for notational ease, we have

Ⓐ $$\frac{\delta\rho}{\rho} + ik_x\xi_x + \xi_z' + \xi_z \frac{d\ln\rho}{dz} = 0,$$

Ⓑ $$-\omega^2\xi_x = -ik_x\frac{\delta p}{\rho},$$

Ⓒ $$-\omega^2\xi_z = -\frac{1}{\rho}\frac{d}{dz}\delta p - \frac{\delta\rho}{\rho}g,$$

Ⓓ $$\frac{\delta p}{p} = \gamma\frac{\delta\rho}{\rho} - \xi_z\frac{d\ln p\rho^{-\gamma}}{dz}.$$

Ⓑ and Ⓓ $\Rightarrow$ $$-\omega^2 \xi_x = -ik_x \frac{P}{\rho}\left[\gamma \frac{\delta\rho}{\rho} - \xi_z \frac{d\ln P\rho^{-\gamma}}{dz}\right]$$

and Ⓐ $\Rightarrow$ $$-\omega^2\xi_x = +ik_x \frac{P}{\rho}\gamma\left[+ik_x\xi_x + \xi_z' + \xi_z\frac{d\ln\rho}{dz}\right] + ik_x\frac{P}{\rho}\xi_z\frac{d\ln P\rho^{-\gamma}}{dz}$$

$$\Rightarrow (-\omega^2 + k_x^2 a^2)\xi_x = ik_x a^2 \xi_z' + \frac{ik_x a^2}{\gamma}\frac{d\ln P}{dz}\xi_z ,$$

where $a^2 \equiv \gamma P/\rho$. Note: $g = \frac{-a^2}{\gamma}\frac{d\ln P}{dz}$, so this is

Ⓔ $$\boxed{(-\omega^2+k_x^2a^2)\xi_x = ik_x a^2\xi_z' - ik_x\xi_z g}$$

Ⓐ $\Rightarrow$ $$\frac{\delta\rho}{\rho} = -\xi_z' - \xi_z\frac{d\ln\rho}{dz} - \frac{ik_x\left[ik_xa^2\xi_z' - ik_x\xi_z g\right]}{-\omega^2+k_x^2a^2}$$

$$\Rightarrow \boxed{\frac{\delta\rho}{\rho} = \frac{\omega^2\xi_z' + \left[(\omega^2-k_x^2a^2)\frac{d\ln\rho}{dz} - k_x^2 g\right]\xi_z}{k_x^2a^2-\omega^2}}$$ Ⓒ

$$\Rightarrow \frac{\delta P}{P} = \frac{1}{k_x^2a^2-\omega^2}\left[\gamma\omega^2\xi_z' + \gamma\left((\omega^2-k_x^2a^2)\frac{d\ln\rho}{dz} - k_x^2 g\right)\xi_z + (\omega^2-k_x^2a^2)\frac{d\ln P\rho^{-\gamma}}{dz}\xi_z\right]$$

$$= \frac{1}{k_x^2a^2-\omega^2}\left[\gamma\omega^2\xi_z' + \omega^2\frac{d\ln P}{dz}\xi_z\right]$$

$$= \frac{\omega^2}{k_x^2a^2-\omega^2}\left[\gamma\xi_z' + \frac{d\ln P}{dz}\xi_z\right]$$ ✪

into ⓒ:

$$+\omega^2\xi_z = +g\left[\frac{\omega^2\xi_z' + (\omega^2 - k_x^2a^2)\frac{d\ln\rho}{dz}\xi_z - k_x^2 g\,\xi_z}{k_x^2a^2-\omega^2}\right]$$

$$+\frac{1}{\rho}\frac{d}{dz}\left[\frac{\omega^2 p}{k_x^2a^2-\omega^2}\left(\xi_z'\gamma + \xi_z\frac{d\ln p}{dz}\right)\right]$$

$$= \frac{\frac{\omega^2}{\rho}\frac{dp}{dz}\left(\xi_z'\gamma+\xi_z\frac{d\ln p}{dz}\right)}{k_x^2a^2-\omega^2} + \frac{p}{\rho}\frac{\omega^2}{k_x^2a^2-\omega^2}\left(\gamma\xi_z''+\xi_z'\frac{d\ln p}{dz}+\xi_z\frac{d^2\ln p}{dz^2}\right)$$

$$-\frac{\omega^2 p}{\rho}\frac{k_x^2}{(k_x^2a^2-\omega^2)^2}\frac{da^2}{dz}\left(\xi_z'\gamma+\xi_z\frac{d\ln p}{dz}\right)$$

$$\Rightarrow \omega^2\xi_z = \frac{g}{k_x^2a^2-\omega^2}\left[\omega^2\xi_z' - k_x^2 g\,\xi_z + (\omega^2-k_x^2a^2)\frac{d\ln\rho}{dz}\xi_z\right]$$

$$+\frac{\omega^2}{k_x^2a^2-\omega^2}(-g)\left[\xi_z'\gamma+\xi_z\frac{d\ln p}{dz}\right]$$

$$+\left(\frac{a^2}{\gamma}\right)\frac{\omega^2}{k_x^2a^2-\omega^2}\left[\xi_z''\gamma+\xi_z'\frac{d\ln p}{dz}+\xi_z\frac{g\gamma}{a^2}\frac{d\ln T}{dz}\right]$$

$$-\frac{\omega^2}{\gamma}\frac{a^2k_x^2a^2}{(k_x^2a^2-\omega^2)^2}\frac{d\ln T}{dz}\left[\xi_z'\gamma+\xi_z\frac{d\ln p}{dz}\right]$$

Multiply by $\frac{k_x^2a^2-\omega^2}{\omega^2a^2}$ and group:

$$\xi_z'': \ 1.$$

$$\xi_z': \ \cancel{\frac{g}{a^2}} - \frac{g\gamma}{a^2} + \cancel{\frac{1}{\gamma}\frac{d\ln p}{dz}} - \frac{k_x^2a^2}{\cancel{\gamma}}\frac{1}{(k_x^2a^2-\omega^2)}\frac{d\ln T}{dz}\cancel{\gamma}$$

$$= \frac{d\ln p}{dz} - \left(\frac{k_x^2a^2}{k_x^2a^2-\omega^2}\right)\frac{d\ln T}{dz} = \frac{d\ln p/dz}{k_x^2a^2-\omega^2}\left[k_x^2a^2-\omega^2 - k_x^2a^2\frac{d\ln T}{d\ln p}\right]$$

$$= \frac{d\ln p/dz}{k_x^2a^2-\omega^2}\left[-\omega^2 + k_x^2a^2\frac{d\ln p}{d\ln p}\right] = \frac{\omega^2\frac{d\ln p}{dz} - k_x^2a^2\frac{d\ln p}{dz}}{\omega^2-k_x^2a^2}$$

$$\xi_z: \ -\frac{(k_x^2a^2-\omega^2)}{a^2} - \frac{k_x^2g^2}{\omega^2a^2} - g\frac{d\ln p}{dz}\frac{k_x^2a^2\cancel{-\omega^2}}{\omega^2a^2}$$

$$-\cancel{\frac{g}{a^2}\frac{d\ln p}{dz}} + \frac{a^2}{\gamma}\cancel{\frac{1}{a^2}\frac{g\gamma}{a^2}\frac{d\ln T}{dz}} - \frac{k_x^2a^2}{\gamma(k_x^2a^2-\omega^2)}\frac{d\ln T}{dz}\frac{d\ln p}{dz}$$

$$= \frac{-1}{k_x^2a^2-\omega^2}\left[\frac{k_x^2a^2}{\gamma}\frac{d\ln T}{dz}\frac{d\ln p}{dz} + \frac{gk_x^2}{\omega^2}\frac{d\ln p}{dz}(k_x^2a^2-\omega^2) + \frac{k_x^2g^2}{a^2\omega^2}(k_x^2a^2-\omega^2) + \frac{(k_x^2a^2-\omega^2)^2}{a^2}\right]$$

$$= \frac{1}{\omega^2-k_x^2a^2}\left[\frac{\omega^4}{a^2} - 2\omega^2k_x^2 + k_x^4a^2 - \frac{k_x^2g^2}{a^2} - \cancel{gk_x^2\frac{d\ln p}{dz}} + \frac{k_x^2a^2}{\gamma}\frac{d\ln T}{dz}\frac{d\ln p}{dz} + \frac{gk_x^4a^2}{\omega^2}\frac{d\ln p}{dz} + \frac{k_x^4\cancel{a^2}g^2}{\cancel{a^2}\omega^2}\right]$$

$$\downarrow$$

$$-k_x^2g\left(\frac{d\ln p}{dz} - \cancel{\frac{d\ln p}{dz}}\right)$$

So,

$$\boxed{\begin{aligned} &\xi_z'' + \xi_z' \left[\frac{\omega^2 \frac{d\ln p}{dz} - k_x^2 a^2 \frac{d\ln \rho}{dz}}{\omega^2 - k_x^2 a^2} \right] \\ &+ \xi_z \frac{1}{\omega^2 - k_x^2 a^2} \left[\frac{\omega^4}{a^2} - 2\omega^2 k_x^2 + k_x^4 a^2 - k_x^2 g \frac{d\ln p}{dz}\left(1 - \frac{1}{\gamma}\right) \right. \\ &\qquad \left. + g \frac{k_x^4 a^2}{\omega^2} \frac{d\ln \rho}{dz} + \frac{k_x^4 g^2}{\omega^2} \right] = 0. \end{aligned}}$$

This is UGLY!!! And we can't solve it analytically anyhow. It's just a stratified fluid — why is it so complicated?! The reason is twofold: (1) this equation mixes up buoyancy and sound waves — distinct physical effects; and (2) the sound and buoyancy frequencies are functions of height. Let's fix this by adopting an ordering: let

$$\frac{d\xi_z}{dz} \sim ik_z\xi_z = ik_zH\left(\frac{\xi_z}{H}\right) \gg \frac{\xi_z}{H},$$

where $H \equiv \left|\frac{dz}{d\ln p}\right| \sim \left|\frac{dz}{d\ln \rho}\right|$. In other words, we assume that ξ_z varies on a scale $\ll$ the scale of the background. This is a WKB approach. So...

Let $\epsilon \equiv \frac{1}{k_zH} \ll 1$. Also, $k_x \sim k_z$. Now, we must make a decision about the size of ω, by comparing it with

$\frac{a}{H} = \frac{\gamma g}{a} = \sqrt{\frac{\gamma g}{H}}$. There are two choices of interest:

(i) $\omega \sim a/H$

(ii) $\omega \sim ka \sim \frac{(a/H)}{\epsilon} \gg \frac{a}{H}$.

First, write $\frac{d\xi_z}{dz} = ik_z\xi_z$ with $k_zH \equiv \frac{1}{\epsilon}$;  becomes

$$-k_z^2\xi_z + ik_z\xi_z\left[\frac{\omega^2\frac{d\ln p}{dz} - k_x^2a^2\frac{d\ln\rho}{dz}}{\omega^2-k_x^2a^2}\right]$$

$$+\frac{\xi_z}{\omega^2-k_x^2a^2}\left[\frac{\omega^4}{a^2} - 2\omega^2k_x^2 + k_x^4a^2 - k_x^2 g\frac{d\ln p}{dz}\left(1-\frac{1}{\gamma}\right)\right.$$

$$\left.+\frac{gk_x^4a^2}{\omega^2}\frac{d\ln\rho}{dz} + \frac{k_x^4g^2}{\omega^2}\right]=0.$$

Now, (i) $\omega \sim a/H$ gives $k_x^2a^2 \gg \omega^2$ and so the dominant terms are

$$-k_z^2\xi_z + \xi_z(-k_x^2) - \xi_z\frac{gk_x^2}{\omega^2}\frac{d\ln\rho}{dz} - \xi_z\frac{k_x^2g^2}{a^2\omega^2} = 0$$

$$\Rightarrow \quad k^2 + \frac{gk_x^2}{\omega^2}\left[\underbrace{\frac{d\ln\rho}{dz} + \frac{g}{a^2}}_{\frac{d\ln\rho}{dz} - \frac{1}{\gamma}\frac{d\ln p}{dz} = -\frac{1}{\gamma}\frac{d\ln p\rho^{-\gamma}}{dz}}\right] = 0.$$

$$\Rightarrow \boxed{\omega^2 = \frac{k_x^2}{k^2}\,\frac{g}{\gamma}\,\frac{d\ln P\rho^{-\gamma}}{dz} = -\frac{k_x^2}{k^2}\,\frac{1}{\gamma\rho}\,\frac{dP}{dz}\,\frac{d\ln P\rho^{-\gamma}}{dz} \equiv \frac{k_x^2}{k^2}\,N^2}$$

where N^2 is the square of the Brunt - Väisälä frequency. If $N^2>0$, these are called <u>internal waves</u> or <u>g-modes.</u>

Note that different wavenumbers have different velocities (i.e., dispersion) and that ω depends on the direction of $\vec{k}$: $\frac{\partial\omega}{\partial\vec{k}} = \frac{\omega}{k^2}\frac{k_z}{k_x}\left(k_z\hat{x} - k_x\hat{z}\right)$, so that $\vec{k}\cdot\frac{\partial\omega}{\partial\vec{k}} = 0$.

We'll return to the physical cause of these waves later, after the "Boussinesq approximation" is introduced, but, for now, note that $N^2<0$ (i.e., upwardly decreasing entropy) gives instability. Go boil some water and think about it.

(ii) $\omega\sim ka \gg a/H$. This gives the following dominant terms:

$$-k_z^2 + \frac{1}{\omega^2 - k_x^2a^2}\underbrace{\left[\frac{\omega^4}{a^2} - 2\omega^2k_x^2 + k_x^4a^2\right]}_{(\omega^2-k_x^2a^2)^2/a^2} = 0$$

$$\Rightarrow \boxed{\omega^2 = (k_x^2+k_z^2)\,a^2}$$ <u>Sound waves!</u>

Now, sound waves are often a nuisance in many calculations. They mostly play a rather boring role, and often serve only to make the algebra more tedious. There is something called the Boussinesq approximation, which rigorously filters out sound waves. Let's see how this works in our convection problem...

Return to $\circledast$ with $\omega \sim \epsilon k a$:

$$\frac{\delta p}{p} \simeq \frac{\omega^2}{k_x^2 a^2}\, i k_z \xi_z \gamma \quad \text{if} \quad k_z \neq 0;$$

$$\simeq \underbrace{\frac{\omega^2}{k_x^2 a^2}}_{\sim \epsilon^2 \ll 1} \frac{d\ln p}{dz}\, \xi_z \quad \text{otherwise.}$$

So, perhaps we should have dropped perturbations to the gas pressure at some point. Where? In the momentum equation? Hmm... careful. Consider Ⓑ with $\frac{\delta P}{P} \simeq \frac{\omega^2}{k_x^2 a^2} i k_z \xi_z \gamma$

$\Rightarrow \xi_x = -\xi_z \frac{k_z}{k_x}$, or $\vec{k}\cdot\vec{\xi} = 0$. Looks like pressure fluctuations are enforcing (near) incompressibility. Best not to drop them! And ⓒ?

$$-\omega^2 \xi_z = -i k_z \frac{p}{\rho} \frac{\omega^2}{k_x^2 a^2}\, i k_z \xi_z \gamma - \frac{\delta\rho}{\rho} g$$

same order!

Okay. So, pressure fluctuations are small, but not so small that they can be dropped from the momentum eqn. What about the entropy eqn?

$$Ⓓ \Longrightarrow \underset{\underset{\sim \frac{\xi_z}{H}\frac{\omega^2}{k_x^2 a^2}}{\uparrow}}{\frac{\delta P}{P}} = \gamma \frac{\delta\rho}{\rho} - \underset{\underset{\sim \frac{\xi_z}{H}, \text{ required for internal waves}}{\uparrow}}{\xi_z} \frac{d \ln P\rho^{-\gamma}}{dz}$$

or $\sim i k_z \xi_z \gamma \frac{\omega^2}{k_x^2 a^2}$, either way... it's small. So, drop δP from entropy equation! What does that leave us with?

$$\gamma \frac{\delta\rho}{\rho} \simeq \xi_z \frac{d \ln P\rho^{-\gamma}}{dz}$$

$\Longrightarrow \frac{\delta\rho}{\rho} \sim \frac{\xi_z}{H}$. Ah! Look at Ⓐ:

$$\underset{\underset{\sim \frac{\xi_z}{H}}{\downarrow}}{\frac{\delta\rho}{\rho}} + \underset{\underset{\sim k\xi_z}{\downarrow}}{i k_z \xi_z} + i k_x \xi_x + \underset{\underset{\sim \frac{\xi_z}{H}}{\downarrow}}{\xi_z \frac{d\ln\rho}{dz}} = 0$$

So, to leading order, we have $\vec{k}\cdot\vec{\xi} = 0$ — incompressibility! Okay, things are consistent, and we have the Boussinesq approx:

$$\frac{\delta p}{p} \sim \frac{1}{kH}\frac{\delta \rho}{\rho} \ll \frac{\delta \rho}{\rho} \sim \frac{\delta u}{a} \ll \frac{k\,\delta u}{\omega} \sim k\xi \sim (kH)\frac{\delta u}{a}.$$

Or, defining the Mach number $\mathcal{M}$ and taking it to be small ($\sim \epsilon$),

$$\frac{\delta u}{a} \sim \frac{\delta \rho}{\rho} \sim \frac{\delta T}{T} \sim \frac{1}{\mathcal{M}}\frac{\delta p}{p} \sim \frac{1}{kH} \sim \epsilon \ll 1.$$

In practice, this means:

1) Assume (near) incompressibility ($\vec{\nabla}\cdot\vec{\delta u} = 0$)

2) Drop δp everywhere EXCEPT the momentum eqn. They are enforcing (near) incompressibility.

3) Keep $\delta \rho$ everywhere EXCEPT the continuity eqn. They interact with gravity to give buoyancy.

Watch how much simpler this is...

$$\begin{tikzcd}
\text{Ⓐ} \arrow[r] & ik_x\xi_x + ik_z\xi_z = 0 \arrow[dr, no head] & \\
\text{Ⓑ} \arrow[r] & -\omega^2\xi_x = -ik_x\frac{\delta p}{\rho} \arrow[r] & \frac{\delta p}{\rho} = \frac{i\omega^2 k_z}{k_x^2}\xi_z \arrow[dd] \\
\text{Ⓒ} \arrow[r] & -\omega^2\xi_z = -ik_z\frac{\delta p}{\rho} - \frac{\delta \rho}{\rho}g \arrow[dr] & \\
\text{Ⓓ} \arrow[r] & 0 = \gamma\frac{\delta \rho}{\rho} - \xi_z\frac{d\ln p\rho^{-\gamma}}{dz} \arrow[dr] & \omega^2\xi_z = \frac{k_x^2}{k^2}g\frac{\delta \rho}{\rho} \arrow[d] \\
 & & \omega^2 = \frac{k_x^2}{k^2}N^2. \text{ Done!}
\end{tikzcd}$$

What we've done here is eliminated the restoring pressure forces that drive sound waves, essentially by assuming that a^2 is so large that sound waves propagate instantaneously. When the restoring force is purely external (e.g., gravity), the flow behaves as though it were incompressible (nearly). Physically, a slow-moving fluid element remains in pressure balance with its surroundings. This readjustment is what makes buoyancy waves and convection possible. Let us see that explicitly.

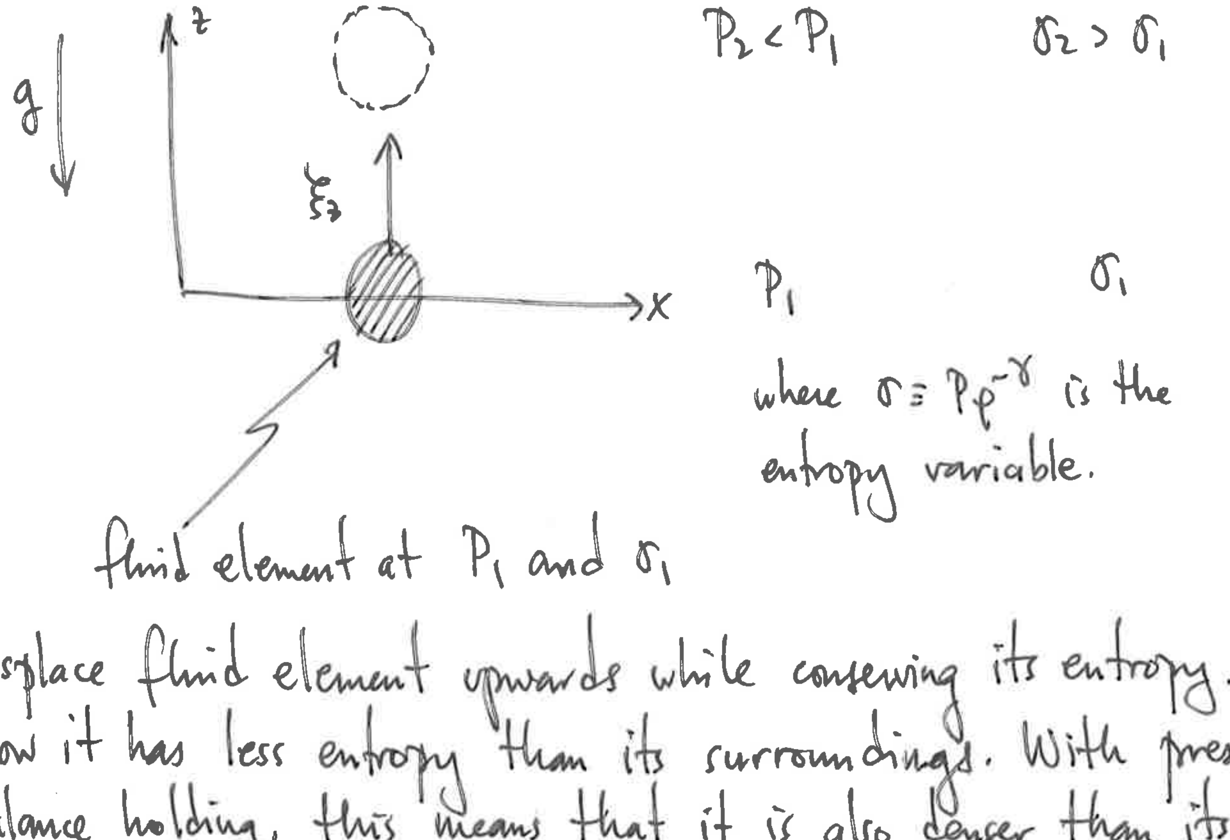

where $\sigma \equiv P\rho^{-\gamma}$ is the entropy variable.

fluid element at P_1 and σ_1

Displace fluid element upwards while conserving its entropy. Now it has less entropy than its surroundings. With pressure balance holding, this means that it is also denser than its surroundings. It must fall back to its equilibrium position. Overshooting, it will oscillate at frequency N. (Mathematically, $\Delta\sigma = 0 \Longrightarrow \Delta p/p = \gamma\,\Delta\rho/\rho \Rightarrow \vec{\xi}\cdot\vec{\nabla}\ln p = \gamma\frac{\delta\rho}{\rho} + \gamma\vec{\xi}\cdot\vec{\nabla}\ln\rho \Rightarrow \frac{\delta\rho}{\rho} = \frac{N^2}{g}\xi_z$.)

Now, consider $\sigma_2 < \sigma_1$. Our upwardly displaced fluid element has *more* entropy than its surroundings, and it will continue to rise $\longrightarrow$ convective instability. The (Karl) *Schwarzschild criterion* for convective stability is $\boxed{N^2 > 0}$.

Bonus: Exact solution to  for an isothermal atmosphere.

Suppose $\frac{d\ln\rho}{dz} = \frac{d\ln p}{dz}$ ($T = \text{const}$) Then $\frac{d\ln p}{dz} = -\frac{\gamma g}{a^2} = \text{const}$.

$\Rightarrow p = p_0 \exp(-z/H)$ with $H \equiv a^2/\gamma g$. Then we have

$$\xi_z'' - \frac{\xi_z'}{H} + \left[\frac{\omega^2 - k_x^2 a^2}{a^2} + \frac{k_x^2 g}{H}\left(1-\frac{1}{\gamma}\right)\frac{1}{\omega^2}\right]\xi_z = 0.$$

Let $\xi_z = f(z)\exp\left(\frac{z}{2H}\right)$. Then

$$\xi_z' = f' e^{z/2H} + \frac{f}{2H} e^{z/2H}$$
$$= f' e^{z/2H} + \xi_z/2H$$
$$\xi_z'' = f'' e^{z/2H} + \frac{f'}{H} e^{z/2H} + \frac{\xi_z}{(2H)^2}$$

$$f'' + \frac{f'}{H} + \frac{f}{(2H)^2} - \frac{f'}{H} - \frac{f}{2H^2} + [\ldots]f = 0.$$

$$f'' + \underbrace{\left[-\frac{1}{4H^2} + \frac{\omega^2 - k_x^2 a^2}{a^2} + \frac{k_x^2 a^2}{\gamma H^2}\left(1-\frac{1}{\gamma}\right)\frac{1}{\omega^2}\right]}_{=\text{ const.}} f = 0.$$

bracket

$\Rightarrow f = \exp(\pm i k_z z)$ with $k_z^2 =$

$$\Rightarrow -k_z^2 - \frac{1}{4H^2} + \frac{\omega^2 - k_x^2 a^2}{a^2} + \frac{k_x^2 a^2}{\omega^2 H^2}\left(\frac{\gamma-1}{\gamma^2}\right) = 0.$$

Mult. by $\omega^2 a^2$ and regroup terms:

$$\omega^4 + \omega^2\left[-k_z^2 a^2 - \frac{a^2}{4H^2} - k_x^2 a^2\right] + k_x^2 a^2\left(\frac{a^2}{H^2}\right)\left(\frac{\gamma-1}{\gamma^2}\right) = 0.$$

$$\Rightarrow \omega^2 = \frac{k^2a^2 + \frac{a^2}{4H^2}}{2} \pm \frac{1}{2}\left[\left(k^2a^2 + \frac{a^2}{4H^2}\right)^2 - 4k_x^2a^2\left(\frac{a^2}{H^2}\right)\left(\frac{\gamma-1}{\gamma^2}\right)\right]^{1/2}.$$

Note that $N^2 \equiv \frac{g}{\gamma}\frac{d\ln P\rho^{-\gamma}}{dz} = \left(\frac{1-\gamma}{\gamma}\right) g \frac{d\ln\rho}{dz} = \frac{a^2}{H^2}\left(\frac{\gamma-1}{\gamma^2}\right).$

So,

$$\boxed{\omega^2 = \frac{k^2a^2 + \frac{\gamma^2}{\gamma-1}N^2}{2} \pm \frac{1}{2}\left[\left(k^2a^2 + \frac{\gamma^2 N^2}{\gamma-1}\right)^2 - 4k_x^2a^2N^2\right]^{1/2}}$$

If $(kH)^2 \gg 1$, this becomes $\omega^2 = k^2a^2$ for the sound wave (plus sign) and $\omega^2 = \frac{k_x^2}{k^2}N^2$ for the g-mode (minus sign). The final term in the square root captures the coupling between these modes.

- A related problem is the <u>Parker Instability</u>, or "magnetic Rayleigh-Taylor instability" (although it is different in detail from RTI and is closer to Schwarzschild Convection). Consider an atmosphere similar to that in our convective instability calculation, but with a magnetic field oriented perpendicularly to gravity with a z-dependence: $\vec{B}_0 = B_0(z)\hat{x}$. The force balance in the equilibrium state now includes a contribution from the magnetic pressure: $g = -\frac{1}{\rho}\left(\frac{dp}{dz} + \frac{dB_0^2}{dz}\right) = \text{const.}$, or

$$\frac{g}{a^2} = -\frac{1}{\gamma}\frac{d\ln P}{dz} - \frac{V_{A0}^2}{a^2}\frac{d\ln B_0}{dz}.$$

Our equations are almost the same:

$$\frac{\delta\rho}{\rho} + ik_x\xi_x + \xi_z' + \xi_z\frac{d\ln\rho}{dz} = 0,$$

$$-\omega^2\xi_x = -ik_x\left(\frac{\delta p}{\rho} + \frac{B_0\,\delta B_x}{4\pi\rho}\right) + \frac{ik_xB_0}{4\pi\rho}\delta B_x + \frac{\delta B_z}{4\pi\rho}\frac{dB_0}{dz},$$

$$-\omega^2\xi_z = -\frac{1}{\rho}\frac{d}{dz}\left(\delta p + \frac{B_0\,\delta B_x}{4\pi}\right) - \frac{\delta\rho}{\rho}g + \frac{ik_xB_0}{4\pi\rho}\delta B_z,$$

$$\frac{\delta p}{p} = \gamma\frac{\delta\rho}{\rho} - \xi_z\frac{d\ln p\rho^{-\gamma}}{dz},$$

but now with magnetic-field perturbations and gradients The former are given by $\vec{\delta B} = \vec{\nabla}\times(\vec{\xi}\times\vec{B}_0) \Rightarrow \delta B_x = -\frac{d}{dz}(\xi_z B_0)$

$$\delta B_z = ik_xB_0\xi_z$$

First, note that $\dfrac{\delta p + B_0\,\delta B_x/4\pi}{\rho}$

$$= a^2\frac{\delta\rho}{\rho} - \frac{a^2}{\gamma}\frac{d\ln p\rho^{-\gamma}}{dz}\xi_z + \frac{B_0}{4\pi\rho}\left(-\frac{d}{dz}\right)(\xi_z B_0)$$

$$= a^2\Big[-ik_x\xi_x - \xi_z' - \xi_z\frac{d\ln\rho}{dz} - \frac{1}{\gamma}\frac{d\ln p\rho^{-\gamma}}{dz}\xi_z$$

$$- \frac{V_{A0}^2}{a^2}\left(\xi_z' + \xi_z\frac{d\ln B_0}{dz}\right)\Big]$$

$$= a^2\left[-ik_x\xi_x - \xi_z'\left(1+\frac{V_{A0}^2}{a^2}\right) + \frac{g}{a^2}\xi_z\right].$$

Then
$$-\omega^2\xi_x = -ik_x a^2\left[-ik_x\xi_x - \xi_z'\left(1+\frac{V_{A0}^2}{a^2}\right) + \frac{g}{a^2}\xi_z\right]$$

$$+ \frac{ik_xB_0}{4\pi\rho}\left[-\xi_z' B_0 - \xi_z B_0\frac{d\ln B_0}{dz}\right] + \frac{ik_xB_0}{4\pi\rho}\xi_z\frac{dB_0}{dz}$$

$$\Rightarrow (-\omega^2 + k_x^2a^2)\xi_x = ik_xa^2\xi_z'\left(1+\cancel{\frac{V_{A0}^2}{a^2}}\right) - ik_xg\xi_z - \cancel{ik_xV_{A0}^2\xi_z'}$$

$$- \cancel{ik_xV_{A0}^2\frac{d\ln B_0}{dz}\xi_z} + \cancel{ik_xV_{A0}^2\frac{d\ln B_0}{dz}\xi_z}$$

$$\Rightarrow \boxed{(-\omega^2 + k_x^2a^2)\xi_x = ik_xa^2\xi_z' - ik_x\xi_z g}$$

Same as (#) w/o B field!

$$\Rightarrow \frac{\delta\rho}{\rho} = -\xi_z' - \xi_z\frac{d\ln\rho}{dz} - ik_x\frac{[ik_xa^2\xi_z' - ik_x\xi_z g]}{(-\omega^2 + k_x^2a^2)}$$

$$\boxed{\frac{\delta\rho}{\rho} = \frac{\omega^2 \xi_z' + \left[(\omega^2 - k_x^2 a^2) \frac{d\ln\rho}{dz} - k_x^2 g \right] \xi_z}{k_x^2 a^2 - \omega^2}}$$

same as ◎ w/o B field!

Buoyancy is fundamentally the same as in the hydro case. Plugging all of this into the z-component of the momentum eqn. gives (with $\frac{\delta p + \delta B^2/8\pi}{p} = \frac{\omega^2}{\omega^2 - k_x^2 a^2}\left[\frac{\gamma g}{a^2}\xi_z - \gamma \xi_z'\right] - \frac{\gamma v_{A0}^2}{a^2}\xi_z'$)

$$-\omega^2 \xi_z = -\frac{1}{\rho}\frac{d}{dz}\left[\frac{p\,\omega^2}{\omega^2 - k_x^2 a^2}\left(\frac{\gamma g}{a^2}\xi_z - \gamma\xi_z'\right) - \frac{B_0^2}{4\pi}\xi_z'\right]$$

$$- g\left\{\frac{\omega^2 \xi_z' + \left[(\omega^2 - k_x^2 a^2)\frac{d\ln\rho}{dz} - k_x^2 g\right]\xi_z}{k_x^2 a^2 - \omega^2}\right\}$$

$$+ \frac{i k_x B_0}{4\pi\rho}\left(i k_x B_0 \xi_z\right)$$

$$\Rightarrow \left(-\omega^2 + k_x^2 v_{A0}^2\right)\xi_z = -\frac{a^2}{\gamma}\frac{d\ln p}{dz}\frac{\omega^2}{\omega^2 - k_x^2 a^2}\left(\frac{\gamma g \xi_z}{a^2} - \gamma\xi_z'\right)$$

$$- \frac{a^2}{\gamma}\frac{\omega^2 k_x^2 a^2}{(\omega^2 - k_x^2 a^2)^2}\frac{d\ln T}{dz}\left(\frac{\gamma g \xi_z}{a^2} - \gamma\xi_z'\right) + v_{A0}^2 \xi_z'' + \xi_z' v_{A0}^2 \frac{d\ln B_0^2}{dz}$$

$$- \frac{a^2}{\gamma}\frac{\omega^2}{\omega^2 - k_x^2 a^2}\left(\cancel{\frac{\gamma g}{a^2}\xi_z'} - \frac{\gamma g \xi_z}{a^2}\frac{d\ln T}{dz} - \gamma\xi_z''\right)$$

$$+ \frac{g}{\omega^2 - k_x^2 a^2}\left\{\cancel{\omega^2 \xi_z'} + \left[(\omega^2 - k_x^2 a^2)\frac{d\ln\rho}{dz} - k_x^2 g\right]\xi_z\right\}$$

After some straightforward algebra, we find

$$\xi_z''\left(v_{A0}^2 + \frac{a^2\omega^2}{\omega^2-k_x^2a^2}\right)$$

$$+\,\xi_z'\left[v_{A0}^2\frac{d\ln B_0^2}{dz} + \frac{a^2\omega^2}{(\omega^2-k_x^2a^2)^2}\left(\omega^2\frac{d\ln p}{dz} - k_x^2a^2\frac{d\ln\rho}{dz}\right)\right]$$

$$+\,\xi_z\left[\frac{g}{\gamma}\frac{k_x^2a^2}{\omega^2-k_x^2a^2}\left(\frac{d\ln p\rho^{-\gamma}}{dz} + \frac{\gamma v_{A0}^2}{a^2}\frac{d\ln B_0}{dz}\right) - \frac{g\,\omega^2k_x^2a^2}{(\omega^2-k_x^2a^2)^2}\frac{d\ln T}{dz} + \omega^2 - k_x^2v_{A0}^2\right]$$

All extra terms are $\propto v_{A0}^2$. For $k_z \to 0$, $k_x^2a^2 \gg 1$, this becomes

$$\boxed{\omega^2 \simeq \underbrace{k_x^2v_{A0}^2}_{\text{magnetic tension}} + \frac{g}{\gamma}\left(\underbrace{\frac{d\ln p\rho^{-\gamma}}{dz}}_{\text{thermal buoyancy}} + \underbrace{\frac{1}{\beta}\frac{d\ln B_0^2}{dz}}_{\text{magnetic buoyancy}}\right)} \quad \text{w/}\ \beta = \frac{B_0^2}{8\pi p}.$$

Now, $\frac{d\ln p\rho^{-\gamma}}{dz} + \frac{1}{\beta}\frac{d\ln B_0^2}{dz} > 0$ for stability. But the physics is the same as in Schwarzschild convection — just the pressure balance is different.

Nonlinear MHD waves: Reduced MHD

The dissipationless, single-fluid, ideal MHD equations are:

$$\frac{\mathrm{d}\rho}{\mathrm{d}t} = -\rho \boldsymbol{\nabla} \boldsymbol{\cdot} \boldsymbol{u}, \tag{I.1}$$

$$\frac{\mathrm{d}\boldsymbol{u}}{\mathrm{d}t} = -\frac{1}{\rho} \boldsymbol{\nabla} \left(p + \frac{B^2}{8\pi} \right) + \frac{\boldsymbol{B} \boldsymbol{\cdot} \boldsymbol{\nabla} \boldsymbol{B}}{4\pi\rho}, \tag{I.2}$$

$$\frac{\mathrm{d}s}{\mathrm{d}t} = 0, \tag{I.3}$$

$$\frac{\mathrm{d}\boldsymbol{B}}{\mathrm{d}t} = \boldsymbol{B} \boldsymbol{\cdot} \boldsymbol{\nabla} \boldsymbol{u} - \boldsymbol{B} \boldsymbol{\nabla} \boldsymbol{\cdot} \boldsymbol{u}, \tag{I.4}$$

where $s \doteq \ln p\rho^{-\gamma}$ is the entropy and

$$\frac{\mathrm{d}}{\mathrm{d}t} \doteq \frac{\partial}{\partial t} + \boldsymbol{u} \boldsymbol{\cdot} \boldsymbol{\nabla} \tag{I.5}$$

is the Lagrangian (or comoving) derivative. Before generalizing these equations for non-ideal MHD and investigating more waves and instabilities, there is one final topic on MHD waves that I think is worth documenting here: nonlinear MHD waves and the so-called *reduced magnetohydrodynamics*.

Reduced MHD (RMHD) is a nonlinear system of fluid equations used to describe anisotropic fluctuations in magnetized plasmas at lengthscales ℓ much larger than the gyroradii of the particles and frequencies ω much smaller than the gyrofrequencies of these particles. It was initially used to model elongated structures in tokamaks (Kadomtsev & Pogutse 1974; Strauss 1976, 1977), but has since become a standard paradigm in astrophysical contexts such as solar-wind turbulence (Zank & Matthaeus 1992*a*,*b*; Bhattacharjee *et al.* 1998) and the solar corona (Oughton *et al.* 2003; Perez & Chandran 2013). In this section, the RMHD system of equations is formulated for both Alfvénic and compressive fluctuations. The presentation of its derivation is useful for (at least) two reasons: first, RMHD makes clear how such fluctuations nonlinearly interact (which is important for understanding modern theories of MHD turbulence) and, second, its derivation offers a relatively simple pedagogical exercise on how to apply an asymptotic ordering to obtain a simplified set of equations (which is important for building your toolkit and your character).

I.0.1. *RMHD ordering*

While one may formulate different versions of RMHD, here I will confine the discussion solely to ideally conducting fluids whose equilibrium state is homogeneous ($\rho_0 = \text{const}$, $p_0 = \text{const}$), stationary ($\boldsymbol{u}_0 = 0$), and threaded by a uniform mean magnetic field oriented along the z axis ($\boldsymbol{B}_0 = B_0\hat{\boldsymbol{z}}$). The fluid is perturbed with small displacements, which we take to satisfy the ordering

$$\frac{\delta\rho}{\rho_0} \sim \frac{\delta p}{p_0} \sim \frac{u_\perp}{c_\mathrm{s}} \sim \frac{u_\parallel}{c_\mathrm{s}} \sim \frac{\delta B_\perp}{B_0} \sim \frac{\delta B_\parallel}{B_0} \sim \frac{k_\parallel}{k_\perp} \doteq \epsilon \ll 1, \tag{I.6}$$

where the sound speed $c_\mathrm{s} \doteq (\gamma p_0/\rho_0)^{1/2}$ is of order the Alfvén speed $v_\mathrm{A} \doteq B_0/(4\pi\rho_0)^{1/2}$. In other words, the plasma beta parameter

$$\beta \doteq \frac{8\pi p_0}{B_0^2} = \frac{2}{\gamma} \frac{c_\mathrm{s}^2}{v_\mathrm{A}^2} \tag{I.7}$$

is taken to be of order unity; subsidiary limits in high and low β may be taken after the ϵ expansion is performed. The fluctuations are therefore sub-sonic, sub-Alfvénic, and spatially anisotropic with respect to the magnetic-field direction, with a characteristic length scale parallel to the field ($\sim k_\parallel^{-1}$) that is much larger than across the field ($\sim k_\perp^{-1}$). The characteristic frequency of the fluctuations $\omega \sim k_\parallel v_{\rm A}$, so that $\omega \sim \epsilon k_\perp v_{\rm A}$; as a result of this ordering, fast magnetosonic modes are ordered out of the equations.

The ordering (I.7) is applied to each of the ideal MHD equations and the result examined order by order in ϵ. This will afford a manageable set of reduced equations (RMHD) that describes non-linear Alfvén waves and their interactions. Before doing so, note that the Lagrangian derivative

$$\frac{\mathrm{d}}{\mathrm{d}t} = \underbrace{\frac{\partial}{\partial t}}_{\sim\omega} + \underbrace{u_\parallel \nabla_\parallel}_{\sim\epsilon\omega} + \underbrace{\boldsymbol{u}_\perp \boldsymbol{\cdot} \boldsymbol{\nabla}_\perp}_{\sim\omega} = \frac{\partial}{\partial t} + \boldsymbol{u}_\perp \boldsymbol{\cdot} \boldsymbol{\nabla}_\perp + \mathcal{O}(\epsilon\omega),$$

so that fluctuations are nonlinearly advected to leading order by the $\boldsymbol{E}\times\boldsymbol{B}$ flow. This is important, as it indicates that, while the fluctuations are assumed small, they are *not* infinitesimally small. Let us proceed.

I.0.2. *Alfvénic fluctuations*

First, the continuity equation (I.1):

$$\underbrace{\frac{\mathrm{d}}{\mathrm{d}t}\frac{\delta\rho}{\rho_0}}_{①} = -\underbrace{\nabla_\parallel u_\parallel}_{①} - \underbrace{\boldsymbol{\nabla}_\perp \boldsymbol{\cdot} \boldsymbol{u}_\perp}_{⓪}, \tag{I.8}$$

where the order in ϵ at which each term enters relative to ω is indicated. To leading order, we have

$$\boxed{\boldsymbol{\nabla}_\perp \boldsymbol{\cdot} \boldsymbol{u}_\perp = 0} \tag{I.9}$$

i.e., the perpendicular dynamics is incompressible. This implies that $\boldsymbol{u}_\perp$ can be written in terms of a stream function:

$$\boldsymbol{u}_\perp = \hat{\boldsymbol{z}} \times \boldsymbol{\nabla}_\perp \mathit{\Phi}. \tag{I.10}$$

Likewise, the solenoidality constraint on the magnetic field allows us to write $\delta\boldsymbol{B}_\perp$ in terms of a flux function:

$$\frac{\delta\boldsymbol{B}_\perp}{\sqrt{4\pi\rho_0}} = \hat{\boldsymbol{z}} \times \boldsymbol{\nabla}_\perp \mathit{\Psi}. \tag{I.11}$$

Thus, the Alfvénic fluctuations can be described in terms of two scalar functions. The evolution equations for the compressive fluctuations are worked out below in §I.0.3, and so let me avoid for now any discussion of the higher-order terms in the continuity equation and proceed directly to obtaining evolution equations for $\mathit{\Phi}$ and $\mathit{\Psi}$.

The latter results from applying the RMHD ordering (I.7) to the induction equation (I.4):

$$\underbrace{\frac{\mathrm{d}}{\mathrm{d}t}\frac{\delta\boldsymbol{B}}{B_0}}_{①} = \underbrace{\frac{\partial\boldsymbol{u}}{\partial z}}_{①} + \underbrace{\left(\frac{\delta\boldsymbol{B}_\perp}{B_0}\boldsymbol{\cdot}\boldsymbol{\nabla}_\perp\right)\boldsymbol{u}}_{①} + \underbrace{\left(\frac{\delta B_\parallel}{B_0}\nabla_\parallel\right)\boldsymbol{u}}_{②} - \underbrace{\hat{\boldsymbol{z}}(\boldsymbol{\nabla}\boldsymbol{\cdot}\boldsymbol{u})}_{①} - \underbrace{\frac{\delta\boldsymbol{B}}{B_0}(\boldsymbol{\nabla}\boldsymbol{\cdot}\boldsymbol{u})}_{②}.$$

To leading order, the perpendicular magnetic-field fluctuations satisfy

$$\frac{\mathrm{d}}{\mathrm{d}t}\frac{\delta\boldsymbol{B}_\perp}{B_0} = \left(\frac{\partial}{\partial z} + \frac{\delta\boldsymbol{B}_\perp}{B_0}\boldsymbol{\cdot}\boldsymbol{\nabla}_\perp\right)\boldsymbol{u}_\perp. \tag{I.12}$$

The term in parentheses in (I.12) is just $\hat{\boldsymbol{b}}\boldsymbol{\cdot}\boldsymbol{\nabla}$ written out to $\mathcal{O}(\epsilon k_\perp)$, and so field-parallel gradients in the perpendicular flow drive (Lagrangian) changes in the perpendicular magnetic-field fluctuations. Using the expressions (I.10) and (I.11) for $\boldsymbol{u}_\perp$ and $\delta\boldsymbol{B}_\perp$, respectively, equation (I.12) implies

$$\boxed{\frac{\partial\varPsi}{\partial t} + \{\varPhi,\varPsi\} = v_\mathrm{A}\frac{\partial\varPhi}{\partial z}} \tag{I.13}$$

where the Poisson bracket

$$\{\varPhi,\varPsi\} \doteq \hat{\boldsymbol{z}}\boldsymbol{\cdot}(\boldsymbol{\nabla}_\perp\varPhi\times\boldsymbol{\nabla}_\perp\varPsi) = \frac{\partial\varPhi}{\partial x}\frac{\partial\varPsi}{\partial y} - \frac{\partial\varPhi}{\partial y}\frac{\partial\varPsi}{\partial x}. \tag{I.14}$$

The evolution equation for $\varPhi$ is obtained from the perpendicular component of the momentum equation (I.2):

$$\begin{aligned}
&\underbrace{\frac{\mathrm{d}\boldsymbol{u}_\perp}{\mathrm{d}t}}_{\textcircled{1}} + \underbrace{(u_\parallel\nabla_\parallel)\boldsymbol{u}_\perp}_{\textcircled{2}} + \underbrace{\frac{\delta\rho}{\rho_0}\frac{\mathrm{d}\boldsymbol{u}_\perp}{\mathrm{d}t}}_{\textcircled{2}} + \underbrace{\frac{\delta\rho}{\rho_0}(u_\parallel\nabla_\parallel)\boldsymbol{u}_\perp}_{\textcircled{3}} = \underbrace{-\boldsymbol{\nabla}_\perp\left(c_\mathrm{s}^2\frac{\delta p}{\gamma p_0} + v_\mathrm{A}^2\frac{\delta B_\parallel}{B_0}\right)}_{\textcircled{0}} \\
&\quad\underbrace{-\,v_\mathrm{A}^2\boldsymbol{\nabla}_\perp\frac{|\delta\boldsymbol{B}|^2}{2B_0^2}}_{\textcircled{1}} + \underbrace{v_\mathrm{A}^2\frac{\partial}{\partial z}\frac{\delta\boldsymbol{B}_\perp}{B_0}}_{\textcircled{1}} + \underbrace{v_\mathrm{A}^2\left(\frac{\delta\boldsymbol{B}_\perp}{B_0}\boldsymbol{\cdot}\boldsymbol{\nabla}_\perp\right)\frac{\delta\boldsymbol{B}_\perp}{B_0}}_{\textcircled{1}} + \underbrace{v_\mathrm{A}^2\left(\frac{\delta B_\parallel}{B_0}\nabla_\parallel\right)\frac{\delta\boldsymbol{B}_\perp}{B_0}}_{\textcircled{2}},
\end{aligned} \tag{I.15}$$

where the order in ϵ at which each term enters relative to ωc_s is indicated. At $\mathcal{O}(1)$, we have perpendicular pressure balance:

$$-\boldsymbol{\nabla}_\perp\left(c_\mathrm{s}^2\frac{\delta p}{\gamma p_0} + v_\mathrm{A}^2\frac{\delta B_\parallel}{B_0}\right) = 0 \quad\Longrightarrow\quad \frac{\delta p}{p_0} = -\frac{2}{\beta}\frac{\delta B_\parallel}{B_0}. \tag{I.16}$$

At $\mathcal{O}(\epsilon)$,

$$\frac{\mathrm{d}\boldsymbol{u}_\perp}{\mathrm{d}t} = -\boldsymbol{\nabla}_\perp\left(c_\mathrm{s}^2\frac{\delta p_2}{\gamma p_0} + v_\mathrm{A}^2\frac{|\delta\boldsymbol{B}|^2}{2B_0^2}\right) + v_\mathrm{A}^2\frac{\partial}{\partial z}\frac{\delta\boldsymbol{B}_\perp}{B_0} + v_\mathrm{A}^2\left(\frac{\delta\boldsymbol{B}_\perp}{B_0}\boldsymbol{\cdot}\boldsymbol{\nabla}_\perp\right)\frac{\delta\boldsymbol{B}_\perp}{B_0}, \tag{I.17}$$

where δp_2 is the second-order pressure fluctuation. Fortunately, δp_2 need not be determined, since its only role is to enforce incompressibility, equation (I.9). Indeed, taking the curl of (I.17) eliminates the entire pressure term, leaving

$$\boldsymbol{\nabla}_\perp\times\left[\frac{\mathrm{d}\boldsymbol{u}_\perp}{\mathrm{d}t} = v_\mathrm{A}^2\frac{\partial}{\partial z}\frac{\delta\boldsymbol{B}_\perp}{B_0} + v_\mathrm{A}^2\left(\frac{\delta\boldsymbol{B}_\perp}{B_0}\boldsymbol{\cdot}\boldsymbol{\nabla}_\perp\right)\frac{\delta\boldsymbol{B}_\perp}{B_0}\right] \tag{I.18}$$

Noting that

$$\begin{gathered}
\boldsymbol{\nabla}_\perp\times(\hat{\boldsymbol{z}}\times\boldsymbol{\nabla}_\perp\varPhi) = -\hat{\boldsymbol{z}}\,\nabla_\perp^2\varPhi, \\
\boldsymbol{\nabla}_\perp\times(\hat{\boldsymbol{z}}\times\boldsymbol{\nabla}_\perp\varPsi) = -\hat{\boldsymbol{z}}\,\nabla_\perp^2\varPsi, \\
\boldsymbol{\nabla}_\perp\times\big[(\hat{\boldsymbol{z}}\times\boldsymbol{\nabla}_\perp\varPhi)\boldsymbol{\cdot}\boldsymbol{\nabla}_\perp(\hat{\boldsymbol{z}}\times\boldsymbol{\nabla}_\perp\varPhi)\big] = -\hat{\boldsymbol{z}}\,\hat{\boldsymbol{z}}\boldsymbol{\cdot}(\boldsymbol{\nabla}_\perp\varPhi\times\boldsymbol{\nabla}_\perp\nabla_\perp^2\varPhi), \\
\boldsymbol{\nabla}_\perp\times\big[(\hat{\boldsymbol{z}}\times\boldsymbol{\nabla}_\perp\varPsi)\boldsymbol{\cdot}\boldsymbol{\nabla}_\perp(\hat{\boldsymbol{z}}\times\boldsymbol{\nabla}_\perp\varPsi)\big] = -\hat{\boldsymbol{z}}\,\hat{\boldsymbol{z}}\boldsymbol{\cdot}(\boldsymbol{\nabla}_\perp\varPsi\times\boldsymbol{\nabla}_\perp\nabla_\perp^2\varPsi),
\end{gathered}$$

the $-\hat{\boldsymbol{z}}$ component of (I.18) may be written as

$$\boxed{\frac{\partial}{\partial t}\nabla_\perp^2\varPhi + \{\varPhi, \nabla_\perp^2\varPhi\} = v_{\rm A}\frac{\partial}{\partial z}\nabla_\perp^2\varPsi + \{\varPsi, \nabla_\perp^2\varPsi\}} \tag{I.19}$$

This is essentially an equation for the flow vorticity.

Equations (I.13) and (I.19) form a closed set of equations for the Alfvénic fluctuations:

$$\frac{{\rm d}\varPsi}{{\rm d}t} = v_{\rm A}\frac{\partial\varPhi}{\partial z}, \tag{I.20a}$$

$$\frac{\rm d}{{\rm d}t}\nabla_\perp^2\varPhi = v_{\rm A}\hat{\boldsymbol{b}}\boldsymbol{\cdot}\boldsymbol{\nabla}\nabla_\perp^2\varPsi, \tag{I.20b}$$

where

$$\frac{\rm d}{{\rm d}t} = \frac{\partial}{\partial t} + \{\varPhi, \dots\} \quad \text{and} \quad \hat{\boldsymbol{b}}\boldsymbol{\cdot}\boldsymbol{\nabla} = \frac{\partial}{\partial z} + \frac{1}{v_{\rm A}}\{\varPsi, \dots\}. \tag{I.21}$$

Note that the compressive fluctuations make no appearance in the equations for the Alfvénic fluctuations, and so the former exert no influence on the latter.

There is an advantageous combination of (I.20) that makes clear the foundation of theories of Alfvén-wave turbulence. Define the Elsässer potentials

$$\zeta^\pm \doteq \varPhi \pm \varPsi. \tag{I.22}$$

Then $\varPhi = (\zeta^+ + \zeta^-)/2$ and $\varPsi = (\zeta^+ - \zeta^-)/2$, and so (I.20) may be written as

$$\frac{\partial}{\partial t}\left(\frac{\zeta^+ - \zeta^-}{2}\right) + \left\{\frac{\zeta^+ + \zeta^-}{2}, \frac{\zeta^+ - \zeta^-}{2}\right\} = v_{\rm A}\frac{\partial}{\partial z}\left(\frac{\zeta^+ + \zeta^-}{2}\right) \tag{I.23a}$$

$$\begin{aligned}\frac{\partial}{\partial t}\nabla_\perp^2\left(\frac{\zeta^+ + \zeta^-}{2}\right) + \left\{\frac{\zeta^+ + \zeta^-}{2}, \nabla_\perp^2\frac{\zeta^+ + \zeta^-}{2}\right\} &= v_{\rm A}\frac{\partial}{\partial z}\nabla_\perp^2\left(\frac{\zeta^+ - \zeta^-}{2}\right)\\ &\quad + \left\{\frac{\zeta^+ - \zeta^-}{2}, \nabla_\perp^2\frac{\zeta^+ - \zeta^-}{2}\right\}.\end{aligned} \tag{I.23b}$$

Noting that $\{\zeta^\pm, \zeta^\pm\} = 0$ and taking $\nabla_\perp^2$ of (I.23a), these become

$$\frac{\partial}{\partial t}\nabla_\perp^2(\zeta^+ - \zeta^-) + \frac{1}{2}\nabla_\perp^2\Bigl(\{\zeta^-, \zeta^+\} - \{\zeta^+, \zeta^-\}\Bigr) = v_{\rm A}\frac{\partial}{\partial z}\nabla_\perp^2(\zeta^+ + \zeta^-),$$

$$\begin{aligned}\frac{\partial}{\partial t}\nabla_\perp^2(\zeta^+ + \zeta^-) + \frac{1}{2}\Bigl(\{\zeta^+, \nabla_\perp^2\zeta^-\} + \{\zeta^-, \nabla_\perp^2\zeta^+\}\Bigr) &= v_{\rm A}\frac{\partial}{\partial z}\nabla_\perp^2(\zeta^+ - \zeta^-)\\ &\quad - \frac{1}{2}\Bigl(\{\zeta^+, \nabla_\perp^2\zeta^-\} + \{\zeta^-, \nabla_\perp^2\zeta^+\}\Bigr),\end{aligned}$$

which may be added to and subtracted from one another to obtain

$$\boxed{\frac{\partial}{\partial t}\nabla_\perp^2\zeta^\pm \mp v_{\rm A}\frac{\partial}{\partial z}\nabla_\perp^2\zeta^\pm = -\frac{1}{2}\Bigl(\{\zeta^+, \nabla_\perp^2\zeta^-\} + \{\zeta^-, \nabla_\perp^2\zeta^+\} \mp \nabla_\perp^2\{\zeta^+, \zeta^-\}\Bigr)} \tag{I.24}$$

The left-hand side of this equation captures the propagation of linear Alvén waves: $\zeta^\pm = f^\pm(x, y, z \mp v_{\rm A}t)$. What is notable is that these solutions are also exact *nonlinear* solutions if either $\zeta^- = 0$ or $\zeta^+ = 0$, since the nonlinearities on the right-hand side of (I.24) then vanish. In fact, in this case the fluctuation (or, indeed, wave packet) may be of arbitrary shape and magnitude, simply propagating along the mean magnetic field at the Alfvén speed. The key here is that only *counterpropagating* fluctuations can interact (Kraichnan 1965). They do so by scattering off each other without exchanging energy; indeed, it is easy to show by multiplying (I.24) by $\rho_0\zeta^\pm$ and integrating by parts that the nonlinear Alfvén-wave energy

$$W^\pm_{\mathrm{AW}} \doteq \frac{1}{2}\int \mathrm{d}^3\boldsymbol{r}\,\rho_0|\boldsymbol{\nabla}_\perp\zeta^\pm|^2 \tag{I.25}$$

is conserved. This conservation law plays an important role in theories of Alfvén-wave turbulence, particularly the fact that, whatever the compressive fluctuations are doing, they are doing it independently of the Alfvén-wave cascade.

I.0.3. *Compressive fluctuations*

The next-order terms in the RMHD equations describe the compressive fluctuations. We have already seen that

$$-\boldsymbol{\nabla}_\perp\left(c_{\mathrm{s}}^2\frac{\delta p}{\gamma p_0} + v_{\mathrm{A}}^2\frac{\delta B_\parallel}{B_0}\right) = 0 \quad\Longrightarrow\quad \frac{\delta p}{p_0} = -\frac{2}{\beta}\frac{\delta B_\parallel}{B_0}; \tag{I.26}$$

i.e., the pressure fluctuations are in perpendicular pressure balance. We have also found that the $\mathcal{O}(\epsilon)$ terms in the continuity equation (I.8) give

$$\boldsymbol{\nabla\cdot u} = -\frac{\mathrm{d}}{\mathrm{d}t}\frac{\delta\rho}{\rho_0}, \tag{I.27}$$

describing the time evolution of the density fluctuations. What of the parallel dynamics? An exercise left to you is to show that the parallel component of the induction equation (I.4) implies

$$\frac{\mathrm{d}}{\mathrm{d}t}\left(\frac{\delta B_\parallel}{B_0} - \frac{\delta\rho}{\rho_0}\right) = \hat{\boldsymbol{b}}\boldsymbol{\cdot\nabla} u_\parallel; \tag{I.28}$$

that the entropy equation (I.3) becomes

$$\frac{\mathrm{d}}{\mathrm{d}t}\frac{\delta s}{s_0} = 0 \tag{I.29}$$

and thus

$$\frac{\mathrm{d}}{\mathrm{d}t}\frac{\delta\rho}{\rho_0} = -\frac{1}{1+c_{\mathrm{s}}^2/v_{\mathrm{A}}^2}\hat{\boldsymbol{b}}\boldsymbol{\cdot\nabla} u_\parallel, \tag{I.30}$$

$$\frac{\mathrm{d}}{\mathrm{d}t}\frac{\delta B_\parallel}{B_0} = +\frac{1}{1+v_{\mathrm{A}}^2/c_{\mathrm{s}}^2}\hat{\boldsymbol{b}}\boldsymbol{\cdot\nabla} u_\parallel; \tag{I.31}$$

and, finally, that the parallel component of the momentum equation (I.2) implies

$$\frac{\mathrm{d}u_\parallel}{\mathrm{d}t} = v_{\mathrm{A}}^2\hat{\boldsymbol{b}}\boldsymbol{\cdot\nabla}\frac{\delta B_\parallel}{B_0}. \tag{I.32}$$

Note that the only nonlinearities in these equations are via the derivatives defined by (I.21), and so the compressive fluctuations are linear along perturbed field lines, i.e., they are nonlinearly mixed by the Alfvénic fluctuations only. Because the compressive fluctuations do not affect the Alfvénic fluctuations, this mixing is entirely passive.

One may go further and define the generalized Elsässer fields for the compressive fluctuations,

$$z^\pm_\parallel \doteq u_\parallel \pm \frac{\delta B_\parallel}{\sqrt{4\pi\rho_0}}\left(1+\frac{v_{\mathrm{A}}^2}{c_{\mathrm{s}}^2}\right)^{1/2}, \tag{I.33}$$

to obtain

$$\frac{\mathrm{d}z^\pm_\parallel}{\mathrm{d}t} = \pm\frac{v_{\mathrm{A}}}{(1+v_{\mathrm{A}}^2/c_{\mathrm{s}}^2)^{1/2}}\hat{\boldsymbol{b}}\boldsymbol{\cdot\nabla} z^\pm_\parallel \tag{I.34}$$

from (I.31) and (I.32). In terms of the Alfvénic Elsässer potential $\zeta^{\pm} \doteq \varPhi \pm \varPsi$, equation (I.34) is equivalent to

$$\frac{\partial z_{\parallel}^{\pm}}{\partial t} \mp \frac{v_{\rm A}}{(1+v_{\rm A}^2/c_{\rm s}^2)^{1/2}}\frac{\partial z_{\parallel}^{\pm}}{\partial z} = -\frac{1}{2}\left[1 \mp \frac{1}{(1+v_{\rm A}^2/c_{\rm s}^2)^{1/2}}\right]\{\zeta^+, z_{\parallel}^{\pm}\}$$
$$- -\frac{1}{2}\left[1 \pm \frac{1}{(1+v_{\rm A}^2/c_{\rm s}^2)^{1/2}}\right]\{\zeta^-, z_{\parallel}^{\pm}\}. \tag{I.35}$$

This form makes evident that the potentials $z_{\parallel}^{\pm}$ represent wave packets of finite-amplitude compressive fluctuations that, in the absence of Alfvénic fluctuations, propagate along the guide field: $z_{\parallel}^{\pm} = f^{\pm}(x, y, z \mp v_{\rm slow})$, where $v_{\rm slow} = v_{\rm A}/(1+v_{\rm A}^2/c_{\rm s}^2)^{1/2}$ is the speed of the slow waves in the $k_{\parallel}/k_{\perp} \ll 1$ limit (see page 9 of these notes). The Alfvénic fluctuations passively mix these wave packets; note that just one propagation direction of the Alfvénic fluctuations is needed. In other words, even if the Alfvénic fluctuations do not interact with one another, the compressive fluctuations are mixed by them. This is because, for general β, the phase speed of the slow waves is smaller than that of the Alfvén waves and, therefore, Alfvén waves can "catch up" and interact with the slow waves that travel in the same direction.

In the high-beta limit, $v_{\rm A} \ll c_{\rm s}$, we may expand $(1+v_{\rm A}^2/c_{\rm s}^2)^{-1/2} \approx 1 - v_{\rm A}^2/2c_{\rm s}^2$ to find

$$\frac{\partial z_{\parallel}^{\pm}}{\partial t} \mp \frac{v_{\rm A}}{(1+v_{\rm A}^2/c_{\rm s}^2)^{1/2}}\frac{\partial z_{\parallel}^{\pm}}{\partial z} = -\{\zeta^{\mp}, z_{\parallel}^{\pm}\} + \mathcal{O}(1/\beta). \tag{I.36}$$

In this case, the compressive fluctuations only interact with the counter-propagating Alfvénic fluctuations. This is because, in the high-beta limit, the slow waves travel at the same speed as the Alfvén waves.

Okay, enough of ideal MHD. Next!

Waves and instabilities in non-ideal MHD

II.1. What is $\boldsymbol{u}$ in a poorly ionized plasma?

Let us revisit the ideal-MHD induction equation, repeated here for convenience:

$$\frac{\partial \boldsymbol{B}}{\partial t} = \boldsymbol{\nabla} \times (\boldsymbol{u} \times \boldsymbol{B}). \tag{II.1}$$

What is $\boldsymbol{u}$? Is it the ion velocity $\boldsymbol{u}_{\rm i}$? the electron velocity $\boldsymbol{u}_{\rm e}$? both? But if $\boldsymbol{u}_{\rm i} = \boldsymbol{u}_{\rm e}$, then where are the currents? You may be remembering that $\boldsymbol{u}$ is the $\boldsymbol{E} \times \boldsymbol{B}$ velocity. Fine, but all charged species drift with the same $\boldsymbol{E} \times \boldsymbol{B}$ velocity, so, again, where are the currents? Or, rather, is $\boldsymbol{u}$ the same center-of-mass velocity $\sum_{\alpha} m_{\alpha} n_{\alpha} \boldsymbol{u}_{\alpha} / \sum_{\alpha} m_{\alpha} n_{\alpha}$ that appears in the momentum equation? But if the plasma is primarily composed of neutrals with, say, number density $n_{\rm n} \sim 10^7\, n_{\rm i}$, then the center-of-mass velocity is dominated by the velocity of the neutral fluid $\boldsymbol{u}_{\rm n}$. So the velocity in the induction equation is the neutral-fluid velocity? That's weird. Why would magnetic flux be frozen into a neutral fluid that doesn't conduct electricity?

In ideal MHD, all of these velocities are basically equivalent, because the interspecies drifts are small. For example, in a quasi-neutral ion–electron plasma,

$$\boldsymbol{u}_{\rm i} - \boldsymbol{u}_{\rm e} = \frac{\boldsymbol{j}}{e n_{\rm i}} = \frac{c \boldsymbol{\nabla} \times \boldsymbol{B}}{4\pi e n_{\rm i}} \quad \Longrightarrow \quad \left| \frac{u_{\rm i} - u_{\rm e}}{v_{\rm A}} \right| \sim \frac{d_{\rm i}}{\ell_B} \lll 1.$$

If there are charge-neutral particles around, then collisions keep them co-moving with the charged species. Let's go back to basics…

Consider a collisional plasma with neutrals, ions, and electrons. The momentum equations for these species are, respectively,

$$m_\mathrm{n} n_\mathrm{n} \frac{\mathrm{d}\boldsymbol{u}_\mathrm{n}}{\mathrm{d}t_\mathrm{n}} = -\boldsymbol{\nabla} p_\mathrm{n} + \boldsymbol{R}_\mathrm{ni} + \boldsymbol{R}_\mathrm{ne}, \tag{II.2}$$

$$m_\mathrm{i} n_\mathrm{i} \frac{\mathrm{d}\boldsymbol{u}_\mathrm{i}}{\mathrm{d}t_\mathrm{i}} = -\boldsymbol{\nabla} p_\mathrm{i} + \boldsymbol{R}_\mathrm{in} + \boldsymbol{R}_\mathrm{ie} + q_\mathrm{i} n_\mathrm{i} \left(\boldsymbol{E} + \frac{\boldsymbol{u}_\mathrm{i}}{c} \times \boldsymbol{B} \right), \tag{II.3}$$

$$m_\mathrm{e} n_\mathrm{e} \frac{\mathrm{d}\boldsymbol{u}_\mathrm{e}}{\mathrm{d}t_\mathrm{e}} = -\boldsymbol{\nabla} p_\mathrm{e} + \boldsymbol{R}_\mathrm{en} + \boldsymbol{R}_\mathrm{ei} - e n_\mathrm{e} \left(\boldsymbol{E} + \frac{\boldsymbol{u}_\mathrm{e}}{c} \times \boldsymbol{B} \right), \tag{II.4}$$

where $\mathrm{d}/\mathrm{d}t_\alpha \doteq \partial/\partial t_\alpha + \boldsymbol{u}_\alpha \boldsymbol{\cdot} \boldsymbol{\nabla}$ is the Lagrangian time derivative in the frame of species α. The electric field here is what ensures $q_\mathrm{i} n_\mathrm{i} - e n_\mathrm{e} = 0$. Indeed, add (II.3) and (II.4):

$$\begin{aligned} m_\mathrm{i} n_\mathrm{i} \frac{\mathrm{d}\boldsymbol{u}_\mathrm{i}}{\mathrm{d}t_\mathrm{i}} + m_\mathrm{e} n_\mathrm{e} \frac{\mathrm{d}\boldsymbol{u}_\mathrm{e}}{\mathrm{d}t_\mathrm{e}} &= -\boldsymbol{\nabla}(p_\mathrm{i} + p_\mathrm{e}) + \boldsymbol{R}_\mathrm{in} + \cancel{\boldsymbol{R}_\mathrm{ie}} + \boldsymbol{R}_\mathrm{en} + \cancel{\boldsymbol{R}_\mathrm{ei}} \\ &\quad + \underbrace{(q_\mathrm{i} n_\mathrm{i} - e n_\mathrm{e})}_{\substack{=\,0 \text{ by quasi-}\\ \text{neutrality}}} \boldsymbol{E} + \underbrace{\frac{1}{c} (q_\mathrm{i} n_\mathrm{i} \boldsymbol{u}_\mathrm{i} - e n_\mathrm{e} \boldsymbol{u}_\mathrm{e})}_{=\,\boldsymbol{j} \text{ by def'n}} \times \boldsymbol{B} \end{aligned} \tag{II.5}$$

Now add (II.2) and (II.5):

$$\begin{aligned} m_\mathrm{n} n_\mathrm{n} \frac{\mathrm{d}\boldsymbol{u}_\mathrm{n}}{\mathrm{d}t_\mathrm{n}} + m_\mathrm{i} n_\mathrm{i} \frac{\mathrm{d}\boldsymbol{u}_\mathrm{i}}{\mathrm{d}t_\mathrm{i}} + m_\mathrm{e} n_\mathrm{e} \frac{\mathrm{d}\boldsymbol{u}_\mathrm{e}}{\mathrm{d}t_\mathrm{e}} &= -\boldsymbol{\nabla}(p_\mathrm{n} + p_\mathrm{i} + p_\mathrm{e}) \\ &\quad + \cancel{\boldsymbol{R}_\mathrm{ni}} + \cancel{\boldsymbol{R}_{ne}} + \cancel{\boldsymbol{R}_\mathrm{in}} + \cancel{\boldsymbol{R}_\mathrm{en}} + \frac{\boldsymbol{j}}{c} \times \boldsymbol{B}. \end{aligned} \tag{II.6}$$

All the friction forces cancel by Newton's third law. The left-hand side of (II.6) may be written as

$$\rho \frac{\mathrm{d}\boldsymbol{u}}{\mathrm{d}t} + \sum_\alpha m_\alpha n_\alpha \mathit{\Delta}\boldsymbol{u}_\alpha \mathit{\Delta}\boldsymbol{u}_\alpha,$$

where $\mathit{\Delta}\boldsymbol{u}_\alpha \doteq \boldsymbol{u}_\alpha - \boldsymbol{u}$ are the species drifts relative to the center-of-mass velocity $\boldsymbol{u}$. Further using Ampère's law to write

$$\frac{\boldsymbol{j}}{c} \times \boldsymbol{B} = \boldsymbol{\nabla} \boldsymbol{\cdot} \left(\frac{\boldsymbol{BB}}{4\pi} - \boldsymbol{I} \frac{B^2}{8\pi} \right). \tag{II.7}$$

equation (II.6) becomes

$$\rho \frac{\mathrm{d}\boldsymbol{u}}{\mathrm{d}t} = -\boldsymbol{\nabla} \boldsymbol{\cdot} \left[\boldsymbol{I} \left(\sum_\alpha p_\alpha + \frac{B^2}{8\pi} \right) + \sum_\alpha m_\alpha n_\alpha \mathit{\Delta}\boldsymbol{u}_\alpha \mathit{\Delta}\boldsymbol{u}_\alpha - \frac{\boldsymbol{BB}}{4\pi} \right]. \tag{II.8}$$

So, collisions between neutrals and charged species is what makes the neutrals see the Lorentz force. By virtue of their large mass and the low degree of ionization in many system, $\boldsymbol{u} \simeq \boldsymbol{u}_\mathrm{n}$, and so it *looks* like the neutrals are magnetized. Not true. They just need to collide often enough with the magnetized particles.

With that borne in mind, let us again return to the induction equation (II.1):

$$\frac{\partial \boldsymbol{B}}{\partial t} = \boldsymbol{\nabla} \times (\boldsymbol{u} \times \boldsymbol{B}).$$

Now, that $\boldsymbol{u}$ *cannot* be the neutral velocity; it would make no sense for the magnetic flux to be frozen into a neutral fluid! Let us instead write

$$\frac{\partial \boldsymbol{B}}{\partial t} = \boldsymbol{\nabla}\times(\boldsymbol{u}_\mathrm{f}\times\boldsymbol{B}), \tag{II.9}$$

where $\boldsymbol{u}_\mathrm{f}$ is the velocity of the field lines. This must be true: field lines are frozen into themselves (i.e., there exists a frame where the electric field vanishes). Now add zero:

$$\frac{\partial \boldsymbol{B}}{\partial t} = \boldsymbol{\nabla}\times\Bigg[\underbrace{(\boldsymbol{u}_\mathrm{f}-\boldsymbol{u}_\mathrm{e})}_{\substack{\text{electron-}\boldsymbol{B}\\ \text{drift}\\ \textcircled{O}}}\times\boldsymbol{B}+\underbrace{(\boldsymbol{u}_\mathrm{e}-\boldsymbol{u}_\mathrm{i})}_{\substack{\text{ion-electron}\\ \text{drift}\\ \textcircled{H}}}\times\boldsymbol{B}+\underbrace{(\boldsymbol{u}_\mathrm{i}-\boldsymbol{u}_\mathrm{n})}_{\substack{\text{ion-neutral}\\ \text{drift}\\ \textcircled{A}}}\times\boldsymbol{B}+\underbrace{\boldsymbol{u}_\mathrm{n}\times\boldsymbol{B}}_{\substack{\text{advection}\\ \text{by neutrals}\\ \textcircled{I}}}\Bigg]. \tag{II.10}$$

(If that derivation of a generalized induction equation was wholly unsatisfactory for you, read §II.5 before proceeding to §II.2.)

The terms in (II.10) labelled Ⓞ (Ohmic), Ⓗ (Hall), and Ⓐ (ambipolar) are formally zero in ideal MHD. Let us estimate their relative sizes:

$$\frac{\textcircled{O}}{\textcircled{I}} \sim \frac{1}{\mathrm{Rm}} \doteq \frac{\eta}{v_\mathrm{A}\ell_B} \sim \underbrace{\left(\frac{d_\mathrm{e}}{\ell_B}\right)}_{\text{small}}\underbrace{\left(\frac{d_\mathrm{e}}{v_\mathrm{A}\tau_\mathrm{en}}\right)}_{\substack{\text{could be}\\ \text{large}}} \tag{II.11}$$

$$\frac{\textcircled{H}}{\textcircled{I}} \sim \left|\frac{\boldsymbol{j}/en_\mathrm{e}}{\boldsymbol{u}_\mathrm{n}}\right| \sim \underbrace{\left(\frac{d_\mathrm{i}}{\ell_B}\right)}_{\text{small}}\underbrace{\left(\frac{\rho}{\rho_\mathrm{i}}\right)^{1/2}}_{\substack{\sim 1,\text{ but}\\ \text{could be}\\ \text{large}}}\underbrace{\left|\frac{v_\mathrm{A}}{u_\mathrm{n}}\right|}_{\sim 1} \tag{II.12}$$

$$\frac{\textcircled{A}}{\textcircled{I}} \sim \left|\frac{\boldsymbol{R}_\mathrm{ni}\tau_\mathrm{ni}}{\rho_\mathrm{n}\boldsymbol{u}_\mathrm{n}}\right| \sim \left|\frac{\boldsymbol{j}\times\boldsymbol{B}}{c}\right|\frac{\tau_\mathrm{ni}}{\rho_\mathrm{n}v_\mathrm{A}}\left|\frac{v_\mathrm{A}}{u_\mathrm{n}}\right| \sim \underbrace{\frac{v_\mathrm{A}\tau_\mathrm{ni}}{\ell_B}}_{\substack{\text{could be}\\ \sim 1}}\underbrace{\left(\frac{\rho}{\rho_\mathrm{n}}\right)^{1/2}}_{\gtrsim 1}\underbrace{\left|\frac{v_\mathrm{A}}{u_\mathrm{n}}\right|}_{\sim 1} \tag{II.13}$$

Note that Ⓗ/Ⓘ is the only ratio not involving collisions. . . we'll come back to this.

The next three sections focus on the above non-ideal effects in reverse order: ambipolar diffusion (§II.2), the Hall effect (§II.3), and Ohmic dissipation (§II.4). While Ohmic dissipation is certainly the easiest to handle of the three – not only because it's probably most familiar to you, but also because it acts isotropically – we'll postpone its discussion until after ambipolar diffusion and the Hall effect are elucidated. The reason is that a discussion of Ohmic dissipation will lead naturally into the lectures on magnetic reconnection.

In each of the sections below, astrophysical examples are provided for when each of these non-ideal MHD effects are important. But there is one particular system where all three non-ideal effects – ambipolar diffusion, the Hall effect, and Ohmic dissipation – are important: a protoplanetary disk. This is because the wide variety of ionization sources, temperatures, and densities give a wide variety of ionization fractions, collision rates, and Alfvén speeds:

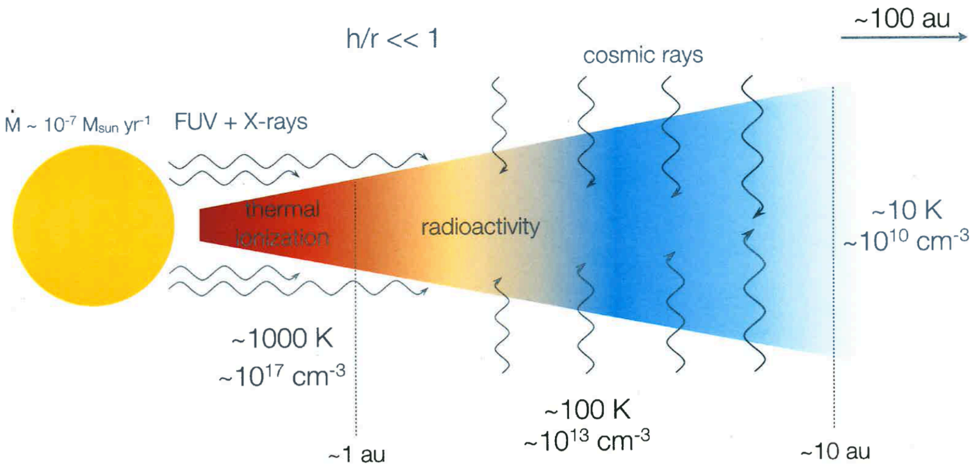

Using the estimates (II.11)–(II.13) with $v_{\rm A}/c_{\rm s} = 0.1$ in a model of the minimum-mass solar nebula (MMSN; Hayashi 1981) leads to the following figure, adapted from Kunz & Balbus (2004), which delineates the regimes in which different non-ideal effects dominate:

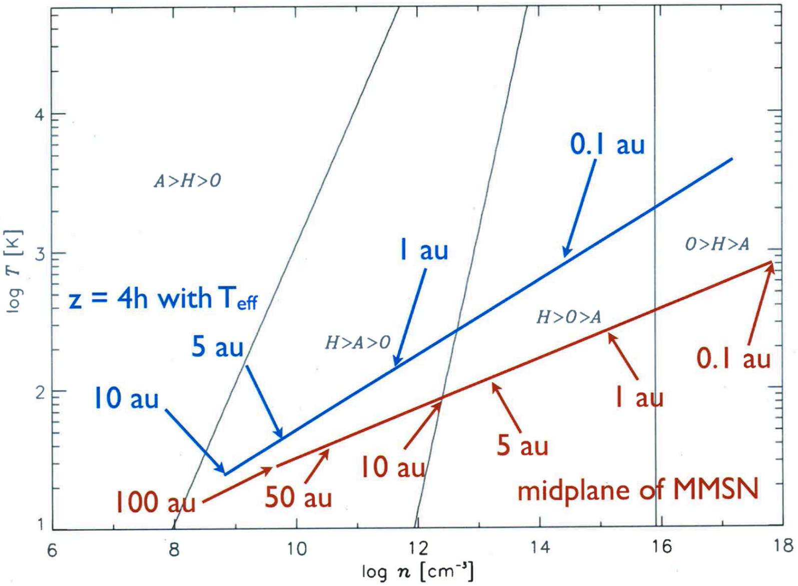

I show this particular plot not because it's the most accurate (it's not) or because it's mine (okay, maybe because it's mine), but because it demonstrates in a very simple way that – even without the myriad complications introduced by the consideration of dust grains, their size spectrum, and their spatial distribution – each non-ideal effect gets their chance to affect the disk dynamics.[1] For more on this topic of "layered accretion", see Gammie (1996), Fromang *et al.* (2002), Wardle (2007), and Armitage (2011).

---

[1] . . . and they do. For linear stability analyses, see Blaes & Balbus (1994), Wardle (1999), Balbus & Terquem (2001), Kunz & Balbus (2004), Desch (2004), Salmeron & Wardle (2003, 2005, 2008), Kunz (2008), and Wardle & Salmeron (2012). For nonlinear numerical simulations, see Hawley & Stone (1998), Sano & Stone (2002*a*,*b*), Bai & Stone (2011, 2013), Simon *et al.* (2013*a*,*b*), Kunz & Lesur (2013), Lesur *et al.* (2014), Bai (2013, 2014, 2015), Simon *et al.* (2015), Gressel *et al.* (2015), Béthune *et al.* (2016), Bai & Stone (2017), Béthune *et al.* (2017), and Bai (2017).

II.2. Ambipolar diffusion

II.2.1. *Astrophysical context and basic theory*

Imagine a poorly ionized gas of neutrals, ions, and electrons. Let us assume $\boldsymbol{u}_\mathrm{i} \simeq \boldsymbol{u}_\mathrm{e}$ (i.e., $d_\mathrm{i}/\ell_B \ll (\rho_\mathrm{i}/\rho)^{1/2}$) and negligible Ohmic dissipation on the scales of interest. To give some physical context for an astrophysical situation where these are fairly good assumptions, consider the cold ($T \sim 10$ K) plasma out of which stars form. Such gas is comprised primarily of neutral molecular hydrogen H_2 ($n_{\mathrm{H}_2} \gtrsim 10^3~\mathrm{cm}^{-3}$) with 20% He by number, along with trace ($\lesssim 10^{-7}$) amounts of electrons, molecular ions (primarily HCO^+), and atomic ions (primarily Na^+, Mg^+, K^+). There are also neutral, negatively charged, and positively charged dust grains, conglomerates of silicate and carbonaceous materials that are between a few molecules to 0.1 μm in size. While dust grains are of critical importance to interstellar chemistry, thermodynamics, and magnetic diffusion, we will ignore them for now.[2] Molecular clouds are poorly ionized because their densities are large enough to screen the most potent sources of ionization (e.g., UV radiation) and their temperatures are low enough to render thermal ionization completely negligible. This leaves only infrequent cosmic rays of energy $\gtrsim$100 MeV (and extremely weak radioactive nuclides like $^{26}\mathrm{Al}$ and $^{40}\mathrm{K}$) to ionize the plasma. So sad.

In molecular clouds, interspecies collisions are strong enough that $T_\mathrm{n} = T_\mathrm{i} = T_\mathrm{e}$. The friction forces are primarily due to elastic collisions and are accurately modeled by

$$\boldsymbol{R}_\mathrm{in} = \frac{m_\mathrm{n} n_\mathrm{n}}{\tau_\mathrm{ni}} (\boldsymbol{u}_\mathrm{n} - \boldsymbol{u}_\mathrm{i}) \quad \text{with} \quad \tau_\mathrm{ni} = \frac{m_\mathrm{n} n_\mathrm{n}}{m_\mathrm{i} n_\mathrm{i}} \tau_\mathrm{in} = 1.23 \, \frac{m_\mathrm{i} + m_{\mathrm{H}_2}}{m_\mathrm{i} n_\mathrm{i} \langle \sigma w \rangle_{\mathrm{iH}_2}}, \tag{II.14}$$

$$\boldsymbol{R}_\mathrm{en} = \frac{m_\mathrm{n} n_\mathrm{n}}{\tau_\mathrm{ne}} (\boldsymbol{u}_\mathrm{n} - \boldsymbol{u}_\mathrm{e}) \quad \text{with} \quad \tau_\mathrm{ne} = \frac{m_\mathrm{n} n_\mathrm{n}}{m_\mathrm{e} n_\mathrm{e}} \tau_\mathrm{en} = 1.21 \, \frac{m_\mathrm{e} + m_{\mathrm{H}_2}}{m_\mathrm{e} n_\mathrm{e} \langle \sigma w \rangle_{\mathrm{eH}_2}}, \tag{II.15}$$

$$\boldsymbol{R}_\mathrm{ie} = \frac{m_\mathrm{e} n_\mathrm{e}}{\tau_\mathrm{ei}} (\boldsymbol{u}_\mathrm{e} - \boldsymbol{u}_\mathrm{i}) \quad \text{with} \quad \tau_\mathrm{ei} = \frac{3\sqrt{m_\mathrm{e}} (k_\mathrm{B} T_\mathrm{e})^{3/2}}{4\sqrt{2\pi} q_\mathrm{i}^2 e^2 n_\mathrm{i} \ln \lambda_\mathrm{ei}}, \tag{II.16}$$

where $\langle \sigma w \rangle_{\alpha \mathrm{H}_2}$ is the mean collisional rate between species α and hydrogen molecules of mass m_{H_2}; the pre-factors of 1.23 and 1.21 account for the presence of He lengthening the slowing-down time relative to the value it would have if only α-H_2 collisions were considered. The mass ratios worth knowing in this context are $m_\mathrm{i}/m_\mathrm{p} = 29$ for HCO^+, $m_\mathrm{i}/m_\mathrm{p} = 23$ for Na^+, $m_\mathrm{i}/m_\mathrm{p} = 24$ for Mg^+, and $m_\mathrm{p}/m_\mathrm{e} = 1836$; the mean mass per particle in molecular clouds is

$$\mu \doteq \frac{\rho}{n} = 2.33 m_\mathrm{p}. \tag{II.17}$$

With $\langle \sigma w \rangle_{\mathrm{iH}_2} = 1.69 \times 10^{-9}~\mathrm{cm}^3~\mathrm{s}^{-1}$ for HCO^+–H_2 collisions (similar values hold for Na^+ and Mg^+) and $\langle \sigma w \rangle_{\mathrm{eH}_2} = 1.3 \times 10^{-9}\,(T/10~\mathrm{K})^{1/2}~\mathrm{cm}^3~\mathrm{s}^{-1}$ for e–H_2 collisions, the above collision timescales become

$$\tau_\mathrm{ni} = 0.23 \left(1 + \frac{m_{\mathrm{H}_2}}{m_\mathrm{i}} \right) \left(\frac{10^{-7}}{x_\mathrm{i}} \right) \left(\frac{10^3~\mathrm{cm}^{-3}}{n_\mathrm{n}} \right) ~\mathrm{Myr}, \tag{II.18}$$

$$\tau_\mathrm{ne} = 0.29 \, \frac{m_{\mathrm{H}_2}}{m_\mathrm{e}} \left(\frac{10^{-7}}{x_\mathrm{e}} \right) \left(\frac{10^3~\mathrm{cm}^{-3}}{n_\mathrm{n}} \right) \left(\frac{10~\mathrm{K}}{T} \right)^{1/2} ~\mathrm{Myr}, \tag{II.19}$$

$$\tau_\mathrm{ei} = 1.2 \left(\frac{10^{-7}}{x_\mathrm{i}} \right) \left(\frac{10^3~\mathrm{cm}^{-3}}{n_\mathrm{n}} \right) \left(\frac{T}{10~\mathrm{K}} \right)^{3/2} ~\mathrm{hr}, \tag{II.20}$$

---

[2] Interstellar grains comprise about 1% of the mass in the interstellar medium (Spitzer 1978). Baker (1979), Elmegreen (1979), and Nakano & Umebayashi (1980) suggested that charged grains may couple to the magnetic field and thereby play a role in ambipolar diffusion and star formation (see also Ciolek & Mouschovias (1993, 1994)).

where $x_\mathrm{i} \doteq n_\mathrm{i}/n_\mathrm{n}$ is the degree of ionization. Because $m_{\mathrm{H}_2}/m_\mathrm{e} \gg 1$, $\boldsymbol{R}_\mathrm{in} + \boldsymbol{R}_\mathrm{en} \simeq \boldsymbol{R}_\mathrm{in}$.

To give the above timescales some context, dynamical timescales in star-forming molecular clouds are $\tau_\mathrm{dyn} \sim 0.1$–$10$ Myr. Magnetic-field strengths are $\sim$10–100 μG, giving an ion cyclotron frequency $\sim$0.1 Hz and an Alfvén speed $\sim$1 km s^{-1}. Every astrophysicist should know that 1 km s^{-1} $\simeq$ 1 pc Myr^{-1}, and so an Alfvén wave crosses a typical molecular cloud of size $\sim$10 pc in $\sim$10 Myr and a typical pre-stellar core of size $\sim$0.1 pc in $\sim$0.1 Myr. Sound travels slower at $\simeq$0.2 km s^{-1}, and so the plasma $\beta \sim 0.01$ or so. The gravitational free-fall time is roughly $\tau_\mathrm{ff} \sim 1$ Myr at the mean density of a molecular cloud, although support against gravitational collapse provided by magnetic tension renders this timescale almost meaningless (Mestel 1965; Mouschovias 1976*a*,*b*).

Under these conditions, equation (II.5) becomes

$$m_\mathrm{i} n_\mathrm{i} \frac{\mathrm{d}\boldsymbol{u}_\mathrm{i}}{\mathrm{d}t_\mathrm{i}} = -\boldsymbol{\nabla}(p_\mathrm{i} + p_\mathrm{e}) + \boldsymbol{R}_\mathrm{in} + \frac{\boldsymbol{j}}{c} \times \boldsymbol{B}. \tag{II.21}$$

Next we make a number of simplifying assumptions, which are certainly not true in all cases of interest but hold rather well in molecular clouds (again, ignoring grains). The left-hand side of (II.21) is typically small, $\sim x_\mathrm{i} \rho v_\mathrm{A}/\tau_\mathrm{dyn}$. Comparing that to the Lorentz force on the right-hand side, $\boldsymbol{j} \times \boldsymbol{B}/c \sim \rho v_\mathrm{A}^2/\ell_B$, the inertial term is indeed smaller by a factor $\sim x_\mathrm{i} \ell_B/(v_\mathrm{A} \tau_\mathrm{dyn})$, which is at most $\sim 10^{-8}(1~\mathrm{Myr}/\tau_\mathrm{dyn})$ in molecular cloud cores. The pressure-gradient terms on the right-hand side of (II.21) are $\sim x_\mathrm{i} \beta \rho v_\mathrm{A}^2/\ell$ and so, as long as the pressure-gradient scales do not differ from the magnetic-gradient scales by more than a factor $\sim x_\mathrm{i}\beta \lesssim 10^{-8}$ (unlikely), the pressure-gradient terms are completely negligible. This leaves the friction force, $\boldsymbol{R}_\mathrm{in}$, and so the dominant balance in (II.21) is

$$\boldsymbol{R}_\mathrm{in} = \frac{\rho_\mathrm{n}}{\tau_\mathrm{ni}}(\boldsymbol{u}_\mathrm{n} - \boldsymbol{u}_\mathrm{i}) \simeq -\frac{\boldsymbol{j}}{c} \times \boldsymbol{B} \quad \Longrightarrow \quad \boldsymbol{u}_\mathrm{i} \simeq \boldsymbol{u}_\mathrm{n} + \frac{\tau_\mathrm{ni}}{\rho_\mathrm{n}} \frac{\boldsymbol{j}}{c} \times \boldsymbol{B}. \tag{II.22}$$

Substituting (II.22) into the non-ideal induction equation (II.10) with the Ohmic and Hall terms neglected, we find

$$\frac{\partial \boldsymbol{B}}{\partial t} = \boldsymbol{\nabla} \times (\boldsymbol{u}_\mathrm{i} \times \boldsymbol{B}) = \boldsymbol{\nabla} \times \left[\boldsymbol{u}_\mathrm{n} \times \boldsymbol{B} + \frac{(\boldsymbol{j} \times \boldsymbol{B}) \times \boldsymbol{B}}{c \rho_\mathrm{n} \nu_\mathrm{ni}} \right], \tag{II.23}$$

where $\nu_\mathrm{ni} \doteq \tau_\mathrm{ni}^{-1}$ is the neutral-ion collision frequency. Thus, there is an electric field in the frame of the neutrals, generated as the field lines slip through the bulk neutral plasma. Note that

$$\frac{(\boldsymbol{j} \times \boldsymbol{B}) \times \boldsymbol{B}}{c \rho_\mathrm{n} \nu_\mathrm{ni}} = -\frac{B^2}{4\pi \rho_\mathrm{n} \nu_\mathrm{ni}} \boldsymbol{j}_\perp = -\frac{v_\mathrm{A}^2}{\nu_\mathrm{ni}} \boldsymbol{j}_\perp$$

only targets perpendicular currents; i.e., ambipolar diffusion is *anisotropic* diffusion. It is also *non-linear* diffusion, in that the magnetic-diffusion coefficient is proportional to B^2. (Note that better coupling, $\nu_\mathrm{ni} \to \infty$, returns the ideal-MHD case.)

Finally, with (II.22) specifying the ion-neutral drift, we have

$$\sum_\alpha m_\alpha n_\alpha \Delta\boldsymbol{u}_\alpha \Delta\boldsymbol{u}_\alpha \simeq m_\mathrm{i} n_\mathrm{i} |\Delta\boldsymbol{u}_\mathrm{i}|^2 \simeq m_\mathrm{i} n_\mathrm{i} \left| \frac{\boldsymbol{j} \times \boldsymbol{B} \tau_\mathrm{ni}}{c \rho_\mathrm{n}} \right|^2 \sim \frac{m_\mathrm{i} n_\mathrm{i}}{\rho_\mathrm{n}} \left| \frac{v_\mathrm{A} \tau_\mathrm{ni}}{\ell_B} \right|^2 \frac{B^2}{4\pi} \ll \frac{B^2}{4\pi},$$

and so the single-fluid momentum equation (II.8) becomes

$$\rho \frac{\mathrm{d}\boldsymbol{u}}{\mathrm{d}t} \simeq m_\mathrm{n} n_\mathrm{n} \frac{\mathrm{d}\boldsymbol{u}_\mathrm{n}}{\mathrm{d}t_\mathrm{n}} = -\boldsymbol{\nabla} p_\mathrm{n} + \frac{\boldsymbol{j}}{c} \times \boldsymbol{B}. \tag{II.24}$$

Therefore, the only substantive change from ideal MHD is an additional (anisotropic) diffusive term in the induction equation.

II.2.2. *Wave-driven ambipolar diffusion*

Ambipolar diffusion is now recognized to be important in a wide range of astrophysical plasmas, many of which are extremely complex, both dynamically and chemically. Let's curb our ambition and simply investigate how ambipolar diffusion affects linear waves in a static, homogeneous background. As usual, separate the fields into their background (adorned by a "0") and fluctuating parts:

$$\boldsymbol{B} = \boldsymbol{B}_0 + \delta\boldsymbol{B}, \quad \boldsymbol{u}_{\rm n} = \delta\boldsymbol{u}, \quad p_{\rm n} = p_0 + \delta p, \quad \rho_{\rm n} = \rho_0 + \delta\rho, \tag{II.25}$$

with $\delta \sim \exp(-\mathrm{i}\omega t + \mathrm{i}\boldsymbol{k}\cdot\boldsymbol{r})$. Working to $\mathcal{O}(\delta)$, our MHD equations including ambipolar diffusion become

$$-\mathrm{i}\omega\delta\rho = -\mathrm{i}\rho_0\boldsymbol{k}\cdot\delta\boldsymbol{u}, \tag{II.26}$$

$$-\mathrm{i}\omega\delta\boldsymbol{u} = -\mathrm{i}\boldsymbol{k}\left(\frac{\delta p}{\rho_0} + \frac{\boldsymbol{B}_0\cdot\delta\boldsymbol{B}}{4\pi\rho_0}\right) + \frac{\mathrm{i}\boldsymbol{k}\cdot\boldsymbol{B}_0}{4\pi\rho_0}\delta\boldsymbol{B}, \tag{II.27}$$

$$-\mathrm{i}\omega\delta\boldsymbol{B} = \mathrm{i}\boldsymbol{k}\cdot\boldsymbol{B}_0\delta\boldsymbol{u} - \boldsymbol{B}_0\mathrm{i}\boldsymbol{k}\cdot\delta\boldsymbol{u} + \mathrm{i}\boldsymbol{k}\times\left[\frac{(\delta\boldsymbol{j}\times\boldsymbol{B}_0)\times\boldsymbol{B}_0}{c\rho_0\nu_{\rm ni}}\right]. \tag{II.28}$$

The final (ambipolar) term may be recast using two vector identities and the linearized Ampére's law, $\delta\boldsymbol{j} = (c/4\pi)(\mathrm{i}\boldsymbol{k}\times\delta\boldsymbol{B})$:

$$\begin{aligned}
\mathrm{i}\boldsymbol{k}\times\left[\frac{(\delta\boldsymbol{j}\times\boldsymbol{B}_0)\times\boldsymbol{B}_0}{c\rho_0\nu_{\rm ni}}\right] &= -\mathrm{i}\boldsymbol{k}\times\left[\frac{B_0^2}{c\rho_0\nu_{\rm ni}}\left(\boldsymbol{I} - \frac{\boldsymbol{B}_0\boldsymbol{B}_0}{B_0^2}\right)\cdot\delta\boldsymbol{j}\right] \\
&= \boldsymbol{k}\times\left[\frac{B_0^2}{4\pi\rho_0\nu_{\rm ni}}\left(\boldsymbol{I} - \frac{\boldsymbol{B}_0\boldsymbol{B}_0}{B_0^2}\right)\cdot(\boldsymbol{k}\times\delta\boldsymbol{B})\right] \\
&= -\frac{k^2v_{\rm A}^2}{\nu_{\rm ni}}\left[\boldsymbol{I} - \frac{(\boldsymbol{k}\times\boldsymbol{B}_0)(\boldsymbol{k}\times\boldsymbol{B}_0)}{k^2B_0^2}\right]\cdot\delta\boldsymbol{B},
\end{aligned}$$

where $v_{\rm A}^2 = B_0^2/4\pi\rho_0$ refers only to the zeroth-order quantities. Equation (II.28) may then be written as

$$\left[\left(-\mathrm{i}\omega + \frac{k^2v_{\rm A}^2}{\nu_{\rm ni}}\right)\boldsymbol{I} - \frac{(\boldsymbol{k}\times\boldsymbol{v}_{\rm A})(\boldsymbol{k}\times\boldsymbol{v}_{\rm A})}{\nu_{\rm ni}}\right]\cdot\delta\boldsymbol{B} = \mathrm{i}\boldsymbol{k}\cdot\boldsymbol{B}_0\delta\boldsymbol{u} - \boldsymbol{B}_0\mathrm{i}\boldsymbol{k}\cdot\delta\boldsymbol{u}. \tag{II.29}$$

Note that, if $\boldsymbol{k} \parallel \boldsymbol{B}_0$, equation (II.29) is the standard linearized induction equation but with $\omega \to \omega + \mathrm{i}k_\parallel^2v_{\rm A}^2/\nu_{\rm ni}$. In this case, if you remember the linear dispersion relation for ideal MHD with $\boldsymbol{k} = k_\parallel\hat{\boldsymbol{b}}_0$, you can skip right to the end by simply replacing ω with $\omega + \mathrm{i}k_\parallel^2v_{\rm A}^2/\nu_{\rm ni}$. The result is

$$\omega\left(\omega + \mathrm{i}\frac{k_\parallel^2v_{\rm A}^2}{\nu_{\rm ni}}\right) = k_\parallel^2v_{\rm A}^2 \quad\Longrightarrow\quad \omega = -\mathrm{i}\frac{k_\parallel^2v_{\rm A}^2}{2\nu_{\rm ni}} \pm \sqrt{k_\parallel^2v_{\rm A}^2 - \left(\frac{k_\parallel^2v_{\rm A}^2}{2\nu_{\rm ni}}\right)^2}\,. \tag{II.30}$$

Easy…damped shear-Alfvén waves. Physically, as the field lines oscillate with the effectively inertialess, flux-frozen ions, the inertia-bearing neutrals get left behind (if $k \gtrsim 2\nu_{\rm ni}/v_{\rm A}$) and frictionally drag on the ions, damping the oscillation. Put differently, if an Alfvénic disturbance in the magnetic field has wavelength $\lambda \lesssim \lambda_{\rm AD} \doteq \pi v_{\rm A}\tau_{\rm ni}$, it diffuses before collisions between neutrals and ions have time to transmit to the neutrals the magnetic force (e.g., Kulsrud & Pearce 1969, Appendix; also, Mouschovias 1991).

To give you a feeling for the numbers involved here,

$$\lambda_{\rm AD} \doteq \pi v_{\rm A} \tau_{\rm ni} \simeq \left(\frac{B}{10~\mu{\rm G}} \right) \left(\frac{n_{\rm H_2}}{10^3~{\rm cm}^{-3}} \right)^{-1/2} \left(\frac{n_{\rm i}}{3.3 \times 10^{-5}~{\rm cm}^{-3}} \right)^{-1} {\rm pc}, \tag{II.31}$$

using $m_{\rm i} = 29 m_{\rm H}$, $\rho_{\rm n} = 2.33 m_{\rm H} n_{\rm n} = 1.4 m_{\rm H_2} n_{\rm H_2}$, and $\langle \sigma w \rangle_{\rm iH_2} = 1.69 \times 10^{-9}~{\rm cm}^3~{\rm s}^{-1}$ (see (II.14)). To obtain $n_{\rm i}$ in terms of $n_{\rm H_2}$, a customary simplification in used in molecular cloud research is to assume a balance between cosmic-ray ionization and dissociative recombination:

$$\zeta_{\rm cr} n_{\rm H_2} = \alpha_{\rm dr} n_{\rm i} n_{\rm e} = \alpha_{\rm dr} n_{\rm i}^2, \tag{II.32}$$

where $\zeta_{\rm cr}$ is the cosmic-ray ionization rate and $\alpha_{\rm dr}$ is the dissociative recombination rate. Using $\zeta_{\rm cr} = 5 \times 10^{-17}~{\rm s}^{-1}$ and $\alpha_{\rm dr} = 2.5 \times 10^{-6}\,(T/10~{\rm K})^{-3/4}~{\rm cm}^3~{\rm s}^{-1}$ (Umebayashi & Nakano 1990) to replace $n_{\rm i}$ in (II.31) by $(\zeta_{\rm cr} n_{\rm H_2}/\alpha_{\rm dr})^{1/2}$, we find

$$\lambda_{\rm AD} \simeq 0.23 \left(\frac{B}{10~\mu{\rm G}} \right) \left(\frac{n_{\rm H_2}}{10^3~{\rm cm}^{-3}} \right)^{-1} {\rm pc}, \tag{II.33}$$

a suggestive number given that prestellar cores in molecular clouds are observed to be quiescent with thermalized linewidths (e.g. Goodman *et al.* 1998; Bacmann *et al.* 2000; Caselli *et al.* 2002; Tafalla *et al.* 2004).

The general case is more interesting physically. Take $\mathrm{i}\boldsymbol{k} \boldsymbol{\cdot}$ (II.27):

$$\underbrace{\omega \boldsymbol{k} \boldsymbol{\cdot} \delta \boldsymbol{u}}_{\substack{= \omega^2 \delta\rho/\rho_0 \\ \text{using} \\ \text{(II.26)}}} = k^2 \left(\frac{\delta p}{\rho_0} + \frac{\boldsymbol{B}_0 \boldsymbol{\cdot} \delta \boldsymbol{B}}{4\pi\rho_0} \right) - \frac{\boldsymbol{k} \boldsymbol{\cdot} \boldsymbol{B}_0}{4\pi\rho_0} \cancelto{0}{\boldsymbol{k} \boldsymbol{\cdot} \delta \boldsymbol{B}}$$

$$\Longrightarrow \quad \omega^2 \frac{\delta\rho}{\rho_0} = k^2 \left(\frac{\delta p}{\rho_0} + \frac{\boldsymbol{B}_0 \boldsymbol{\cdot} \delta \boldsymbol{B}}{4\pi\rho_0} \right) = k^2 a^2 \frac{\delta\rho}{\rho_0} + k^2 \frac{\boldsymbol{B}_0 \boldsymbol{\cdot} \delta \boldsymbol{B}}{4\pi\rho_0}$$

$$\Longrightarrow \quad \frac{\delta\rho}{\rho_0} = \frac{1}{a^2} \frac{\delta p}{\rho_0} = \frac{k^2}{\omega^2 - k^2 a^2} \frac{\boldsymbol{B}_0 \boldsymbol{\cdot} \delta \boldsymbol{B}}{4\pi\rho_0}. \tag{II.34}$$

Substituting (II.34) back into (II.27) and re-arranging leads to

$$-\mathrm{i}\omega \delta \boldsymbol{u} = -\mathrm{i}\boldsymbol{k} \frac{\boldsymbol{B}_0 \boldsymbol{\cdot} \delta \boldsymbol{B}}{4\pi\rho_0} \frac{\omega^2}{\omega^2 - k^2 a^2} + \frac{\mathrm{i}\boldsymbol{k} \boldsymbol{\cdot} \boldsymbol{B}_0}{4\pi\rho_0} \delta \boldsymbol{B}, \tag{II.35}$$

which may then be fed into (II.29) to obtain

$$\boldsymbol{M} \boldsymbol{\cdot} \delta \boldsymbol{B} \doteq \left\{ \left[\omega^2 + \mathrm{i}\omega \frac{k^2 v_{\rm A}^2}{\nu_{\rm ni}} - (\boldsymbol{k} \boldsymbol{\cdot} \boldsymbol{v}_{\rm A})^2 \right] \boldsymbol{I} - \mathrm{i}\omega \frac{(\boldsymbol{k} \times \boldsymbol{v}_{\rm A})(\boldsymbol{k} \times \boldsymbol{v}_{\rm A})}{\nu_{\rm ni}} \right.$$

$$\left. + \frac{\omega^2}{\omega^2 - k^2 a^2} \left(\boldsymbol{k} \boldsymbol{\cdot} \boldsymbol{v}_{\rm A} \boldsymbol{k} \boldsymbol{v}_{\rm A} - k^2 \boldsymbol{v}_{\rm A} \boldsymbol{v}_{\rm A} \right) \right\} \boldsymbol{\cdot} \delta \boldsymbol{B} = 0. \tag{II.36}$$

Taking the determinant of $\boldsymbol{M}$ and setting it to zero gives the dispersion relation. The algebra is aided greatly by a good choice of coordinate system:

$$\boldsymbol{B}_0 = B_0 \hat{\boldsymbol{z}}, \quad \boldsymbol{k} = k_\parallel \hat{\boldsymbol{z}} + k_\perp \hat{\boldsymbol{x}}, \quad \delta \boldsymbol{B} = \delta B_\parallel \hat{\boldsymbol{z}} + \delta B_x \hat{\boldsymbol{x}} + \delta B_y \hat{\boldsymbol{y}}. \tag{II.37}$$

Then we have

$$\boldsymbol{k} \times \boldsymbol{v}_{\rm A} = -\hat{\boldsymbol{y}} k_\perp v_{\rm A} \quad \text{and} \quad \delta \boldsymbol{v}_{\rm A} \boldsymbol{\cdot} \delta \boldsymbol{B} = -v_{\rm A} \frac{k_\perp}{k_\parallel} \delta B_x. \tag{II.38}$$

Introducing

$$\widetilde{\omega}^2 \doteq \omega^2 - (\boldsymbol{k}\cdot\boldsymbol{v}_{\rm A})^2, \tag{II.39}$$

equation (II.36) may be written as

$$\begin{bmatrix} \widetilde{\omega}^2 + {\rm i}\omega\dfrac{k^2v_{\rm A}^2}{\nu_{\rm ni}} - \dfrac{\omega^2k_\perp^2v_{\rm A}^2}{\omega^2-k^2a^2} & 0 \\ 0 & \widetilde{\omega}^2 + {\rm i}\omega\dfrac{k_\parallel^2v_{\rm A}^2}{\nu_{\rm ni}} \end{bmatrix}\begin{bmatrix} \delta B_x \\ \delta B_y \end{bmatrix} = 0. \tag{II.40}$$

The dispersion relation is thus

$$\underbrace{\left(\omega^2 + {\rm i}\omega\frac{k_\parallel^2v_{\rm A}^2}{\nu_{\rm ni}} - k_\parallel^2v_{\rm A}^2\right)}_{\text{damped Alfvén waves}}\underbrace{\left(\omega^2 + {\rm i}\omega\frac{k^2v_{\rm A}^2}{\nu_{\rm ni}} - k_\parallel^2v_{\rm A}^2 - \frac{\omega^2k_\perp^2v_{\rm A}^2}{\omega^2-k^2a^2}\right)}_{\text{damped magnetosonic waves}} = 0, \tag{II.41}$$

where the two branches have been labelled. For the Alfvén-wave branch, we recover (II.30) – damped Alfvén waves. But for the magnetosonic branch, we have

$$\underbrace{\omega^4 - \omega^2k^2\left(a^2+v_{\rm A}^2\right) + k^2a^2k_\parallel^2v_{\rm A}^2}_{\text{fast and slow modes}} = \underbrace{-\,{\rm i}\omega\frac{k^2v_{\rm A}^2}{\nu_{\rm ni}}\left(\omega^2-k^2a^2\right)}_{\substack{\text{damping by}\\ \text{ambipolar diffusion}}}. \tag{II.42}$$

Notice that the magnetosonic modes are damped at a different rate than the Alfvén waves! This is because ambipolar diffusion affects only *perpendicular* currents, a feature that is particularly important in the context of planar shear flows and differentially rotating accretion disks (Kunz & Balbus 2004; Kunz 2008).

II.2.3. *Ambipolar diffusion heats plasma*

As ambipolar diffusion relaxes perpendicular currents and allows the redistribution of mass in magnetic flux tubes, heat is generated equivalent to the work done by the ion-neutral friction force:

$$(\boldsymbol{u}_{\rm n}-\boldsymbol{u}_{\rm i})\cdot\boldsymbol{R}_{\rm in} = \frac{\tau_{\rm ni}}{\rho_{\rm n}}\frac{\boldsymbol{j}}{c}\times\boldsymbol{B}\cdot\frac{\boldsymbol{j}}{c}\times\boldsymbol{B} = \frac{4\pi}{c^2}v_{\rm A}^2\tau_{\rm ni}|\boldsymbol{j}_\perp|^2 \doteq \eta_{\rm A}|\boldsymbol{j}_\perp|^2, \tag{II.43}$$

where $\eta_{\rm A}$ is the ambipolar resistivity. Note that $\eta_{\rm A}\propto(n_{\rm n}n_{\rm i})^{-1}$ – denser gas gets heated less. This heating was first considered in the context of magnetic star formation by Scalo (1977) to put constraints on how the magnetic-field strength scales with density during protostellar core contraction. Zweibel & Josafatsson (1983) considered what constraints heating by wave damping (including ambipolar diffusion) places on the properties of the turbulent fluctuations observed in molecular clouds (see also Arons & Max (1975)). Draine *et al.* (1983) considered heating by ambipolar diffusion occurring in so-called "*C*-type shock waves" in turbulent molecular clouds.

II.3. The Hall effect

II.3.1. *Astrophysical context and basic theory*

Now suppose that $|\boldsymbol{u}_{\rm i}-\boldsymbol{u}_{\rm n}|\ll u_{\rm n}$, so that ambipolar diffusion is ignorable, but that $(d_{\rm i}/\ell_B)(\rho/\rho_{\rm i})^{1/2}\sim 1$ (recall (II.12)). That is, the ions appreciably drift with respect to the electrons on the scales of interest. (In what follows, we will also ignore Ohmic dissipation, postponing its discussion to §II.4.) In a fully ionized plasma, this is only true if the magnetic field has structure on scales ℓ_B comparable to the ion skin depth $d_{\rm i}$. But in a poorly ionized plasma, the ion skin depth is effectively larger by a factor of $(\rho/\rho_{\rm i})^{1/2}$, which is potentially huge in protostellar cores and protoplanetary disks. This is an inertial effect: as a magnetic fluctuation oscillates in a plasma, for the ions to be responsive to that fluctuation they must cope with the sluggishness of not only their inertial mass but also the inertial mass of the more abundant neutrals to which they are collisionally coupled. This makes for a larger *Hall length scale*,

$$\ell_{\rm H} \doteq d_{\rm i} \left(\frac{\rho}{\rho_{\rm i}} \right)^{1/2} = \frac{v_{\rm A}}{\omega_{\rm H}}, \tag{II.44}$$

where

$$\omega_{\rm H} \doteq \frac{q_{\rm i} B}{\mu c} \frac{n_{\rm e}}{n} \tag{II.45}$$

is the *Hall frequency* (e.g., Kunz & Lesur 2013). (Recall the definition of μ, the mean mass per particle: (II.17)). Note that $\ell_{\rm H}$ is independent of the magnetic-field strength. At scales $\ell_B \lesssim \ell_{\rm H}$, the Hall effect is important.

An example of an astrophysical system in which the Hall effect is very important is a protoplanetary disk, ∼1–10 au from the central protostar in particular. While such systems are chemically rich, for the sake of obtaining a simple estimate let us assume the customary balance between cosmic-ray ionization and dissociative recombination, equation (II.32). Setting $m_{\rm i} = 39 m_{\rm p}$ (appropriate for K^+ being the dominant ion) and $\mu = 2.33 m_{\rm p}$, and using $\zeta_{\rm cr} = 5\times10^{-17}~{\rm s}^{-1}$ and $\alpha_{\rm dr} = 2.5\times10^{-6}\,(T/10~{\rm K})^{-3/4}~{\rm cm}^3~{\rm s}^{-1}$ as in §II.2.2, equation (II.44) becomes

$$\ell_{\rm H} \simeq 2.5\times10^{-6} \frac{n_{\rm H_2}^{1/2}}{n_{\rm i}}~{\rm au} \simeq 0.24 \left(\frac{T}{100~{\rm K}} \right)^{-3/8}~{\rm au}, \tag{II.46}$$

independent of density. Comparing this to the disk scale height in the minimum-mass solar nebula (MMSN; Hayashi 1981),

$$h \simeq 0.033 \left(\frac{R}{1~{\rm au}} \right)^{5/4}~{\rm au} \quad {\rm with} \quad T \simeq 280 \left(\frac{R}{1~{\rm au}} \right)^{-1/2}~{\rm K},$$

we have

$$\frac{\ell_{\rm H}}{h} \approx 5 \left(\frac{R}{1~{\rm au}} \right)^{-17/16} \quad \Longrightarrow \quad \ell_{\rm H} \approx H ~{\rm at}~ R \approx 5~{\rm au}. \tag{II.47}$$

Given the uncertainties in these numbers, the radial location in a protoplanetary disk at which scales comparable to the disk scale height are subject to Hall electromotive forces likely ranges between ∼1–10 au. (Within ∼1 au, cosmic rays are attenuated, the ionization fraction drops precipitously, and Ohmic dissipation becomes the dominant diffusion mechanism.) Dust grains complicate this estimate greatly, especially since they tend to be the dominant charge carriers around $n_{\rm H_2} \gtrsim 10^{12}~{\rm cm}^{-3}$ (e.g., Umebayashi & Nakano 1990; Desch & Mouschovias 2001; Kunz & Mouschovias 2010).

Under these conditions, and again specializing to a quasi-neutral ion-electron-neutral plasma devoid of dust grains, the non-ideal induction equation (II.10) becomes

$$\frac{\partial \boldsymbol{B}}{\partial t} = \boldsymbol{\nabla} \times \left(\boldsymbol{u} \times \boldsymbol{B} - \frac{\boldsymbol{j} \times \boldsymbol{B}}{e n_{\rm e}} \right), \tag{II.48}$$

where $\boldsymbol{u} \simeq \boldsymbol{u}_{\rm n} \simeq \boldsymbol{u}_{\rm i}$ and $\boldsymbol{j} = e n_{\rm e} (\boldsymbol{u}_{\rm i} - \boldsymbol{u}_{\rm e})$.

II.3.2. *Wave-driven Hall diffusion*

As in §II.2.2, let us temper our ambition and focus first on the linear theory of waves in a static, homogeneous plasma, subject to Hall diffusion. The linearized continuity and momentum equations are identical to (II.26) and (II.27), respectively. The linearized induction equation (II.48) becomes

$$-\,\mathrm{i}\omega\delta\boldsymbol{B} = \mathrm{i}\boldsymbol{k}\cdot\boldsymbol{B}_0\delta\boldsymbol{u} - \boldsymbol{B}_0\mathrm{i}\boldsymbol{k}\cdot\delta\boldsymbol{u} - \mathrm{i}\boldsymbol{k}\times\left(\frac{\delta\boldsymbol{j}\times\boldsymbol{B}_0}{en_{\mathrm{e}0}}\right). \tag{II.49}$$

The final (Hall) term may be recast using two vector identities and the linearized Ampére's law, $\delta\boldsymbol{j} = (c/4\pi)(\mathrm{i}\boldsymbol{k}\times\delta\boldsymbol{B})$:

$$\begin{aligned}
\mathrm{i}\boldsymbol{k}\times\left(\frac{\delta\boldsymbol{j}\times\boldsymbol{B}_0}{en_{\mathrm{e}0}}\right) &= \mathrm{i}\boldsymbol{k}\cdot\boldsymbol{B}_0\left(\frac{\delta\boldsymbol{j}}{en_{\mathrm{e}0}}\right) - \mathrm{i}\boldsymbol{k}\cdot\left(\frac{\delta\boldsymbol{j}}{en_{\mathrm{e}0}}\right)\boldsymbol{B}_0 \\
&= \mathrm{i}\boldsymbol{k}\cdot\boldsymbol{B}_0\left(\frac{c\mathrm{i}\boldsymbol{k}\times\delta\boldsymbol{B}}{4\pi en_{\mathrm{e}0}}\right) - \cancelto{0}{\mathrm{i}\boldsymbol{k}\cdot\left(\frac{c\mathrm{i}\boldsymbol{k}\times\delta\boldsymbol{B}}{4\pi en_{\mathrm{e}0}}\right)}\boldsymbol{B}_0 \\
&= -\frac{c\boldsymbol{k}\cdot\boldsymbol{B}_0}{4\pi en_{\mathrm{e}0}}(\boldsymbol{k}\times\delta\boldsymbol{B})
\end{aligned}$$

Equation (II.49) may then be written as

$$-\,\mathrm{i}\omega\delta\boldsymbol{B} - \frac{c\boldsymbol{k}\cdot\boldsymbol{B}_0}{4\pi en_{\mathrm{e}0}}(\boldsymbol{k}\times\delta\boldsymbol{B}) = \mathrm{i}\boldsymbol{k}\cdot\boldsymbol{B}_0\delta\boldsymbol{u} - \boldsymbol{B}_0\mathrm{i}\boldsymbol{k}\cdot\delta\boldsymbol{u}. \tag{II.50}$$

Before using the linearized continuity and momentum equations in (II.50) to obtain the dispersion relation, let's do something extremely simple yet incredibly enlightening. Set $\delta\boldsymbol{u} = 0$, i.e., stationary ions and neutrals. Using $\boldsymbol{k}\cdot\delta\boldsymbol{B} = 0$, equation (II.50) then becomes

$$-\,\mathrm{i}\omega\delta\boldsymbol{B} - \left(\frac{c\boldsymbol{k}\cdot\boldsymbol{B}_0}{4\pi en_{\mathrm{e}0}}\right)^2\frac{k^2}{\mathrm{i}\omega}\delta\boldsymbol{B} = 0 \quad\Longrightarrow\quad \omega = \pm\frac{ck\boldsymbol{k}\cdot\boldsymbol{B}_0}{4\pi en_{\mathrm{e}0}}. \tag{II.51}$$

This is the linear dispersion relation for a *whistler wave*. Note that is it a *dispersive* wave, in that different wavelengths travel at different speeds. Note further that there is no dissipation involved. Why? For $\boldsymbol{k}\parallel\boldsymbol{B}_0$ and $\boldsymbol{B}_0 = B_0\hat{\boldsymbol{z}}$, equation (II.50) with $\delta\boldsymbol{u} = 0$ may be written as

$$-\,\mathrm{i}\omega\begin{bmatrix}\delta B_x\\ \delta B_y\end{bmatrix} - \frac{ck k_{\parallel}B_0}{4\pi en_{\mathrm{e}0}}\begin{bmatrix}0 & -1\\ 1 & 0\end{bmatrix}\begin{bmatrix}\delta B_x\\ \delta B_y\end{bmatrix} = 0. \tag{II.52}$$

The Hall effect is just rotating the perpendicular magnetic-field fluctuations about the guide field! Indeed, eigenvector corresponding to (II.51) is $\delta B_y/\delta B_x = \pm\mathrm{i}$. That there is a rotation involved should have been clear from the $(\boldsymbol{k}\times\delta\boldsymbol{B})$ in (II.50).

Now let's restore the ion/neutral motion:

$$\begin{aligned}
-\mathrm{i}\omega\delta\boldsymbol{B} - \frac{c\boldsymbol{k}\cdot\boldsymbol{B}_0}{4\pi en_{\mathrm{e}0}}(\boldsymbol{k}\times\delta\boldsymbol{B}) = \mathrm{i}\boldsymbol{k}\cdot\boldsymbol{B}_0&\left(\frac{\omega\boldsymbol{k}}{\omega^2-k^2a^2}\frac{\boldsymbol{B}_0\cdot\delta\boldsymbol{B}}{4\pi\rho_0} - \frac{1}{\omega}\frac{\boldsymbol{k}\cdot\boldsymbol{B}_0}{4\pi\rho_0}\delta\boldsymbol{B}\right) \\
-\boldsymbol{B}_0\mathrm{i}\boldsymbol{k}\cdot&\left(\frac{\omega\boldsymbol{k}}{\omega^2-k^2a^2}\frac{\boldsymbol{B}_0\cdot\delta\boldsymbol{B}}{4\pi\rho_0} - \frac{1}{\omega}\frac{\boldsymbol{k}\cdot\boldsymbol{B}_0}{4\pi\rho_0}\delta\boldsymbol{B}\right).
\end{aligned} \tag{II.53}$$

Multiplying by $-\mathrm{i}\omega$, using $\boldsymbol{k}\cdot\delta\boldsymbol{B}=0$, and rearranging (II.53),

$$\left\{\left[\omega^2-(\boldsymbol{k}\cdot\boldsymbol{v}_\mathrm{A})^2\right]\mathsf{\boldsymbol{I}}+\frac{\omega^2}{\omega^2-k^2a^2}\left(\boldsymbol{k}\cdot\boldsymbol{v}_\mathrm{A}\boldsymbol{k}\boldsymbol{v}_\mathrm{A}-k^2\boldsymbol{v}_\mathrm{A}\boldsymbol{v}_\mathrm{A}\right)\right\}\cdot\delta\boldsymbol{B}=\frac{\mathrm{i}\omega c\boldsymbol{k}\cdot\boldsymbol{B}_0}{4\pi en_\mathrm{e0}}\boldsymbol{k}\times\delta\boldsymbol{B}. \tag{II.54}$$

Using the same coordinate system as in (II.37), the dispersion relation emerges after a few lines of algebra:

$$\left(\omega^2+\omega\frac{ckk_\parallel B_0}{4\pi en_\mathrm{e0}}-k_\parallel^2v_\mathrm{A}^2\right)\left(\omega^2-\omega\frac{ckk_\parallel B_0}{4\pi en_\mathrm{e0}}-k_\parallel^2v_\mathrm{A}^2\right)=\frac{\omega^2k_\perp^2v_\mathrm{A}^2}{\omega^2-k^2a^2}\left(\omega^2-k_\parallel^2v_\mathrm{A}^2\right) \tag{II.55}$$

Let us focus on incompressible fluctuations, which may be extracted by taking $a^2\to\infty$ (i.e., pressure fluctuations propagate instantaneously). The right-hand side of (II.55) then drops out and we find that the positive-frequency solutions satisfy

$$\omega=\mp\frac{ckk_\parallel B_0}{8\pi en_\mathrm{e0}}+\frac{ckk_\parallel B_0}{8\pi en_\mathrm{e0}}\sqrt{1+\frac{16\pi e^2n_\mathrm{e0}^2}{c^2k^2\rho_0}}=\frac{1}{2}k_\parallel v_\mathrm{A}k\ell_\mathrm{H}\left[\mp1+\sqrt{1+\left(\frac{2\omega_\mathrm{H}}{kv_\mathrm{A}}\right)^2}\right] \tag{II.56a}$$

$$\to\begin{cases}k_\parallel v_\mathrm{A} & (\mp,\ \text{Alfvén wave}) \quad \text{if } kd_\mathrm{i}\ll1\\ \dfrac{k_\parallel}{k}\omega_\mathrm{H} & (-,\ \text{left-handed ion-cyclotron wave}) \quad \text{if } kd_\mathrm{i}\gg1\\ k_\parallel v_\mathrm{A}k\ell_\mathrm{H} & (+,\ \text{right-handed whistler wave}) \quad \text{if } kd_\mathrm{i}\gg1,\end{cases} \tag{II.56b}$$

where $\mu\doteq\rho/n$.

For $k=k_\parallel$, the dispersion relation looks like this:

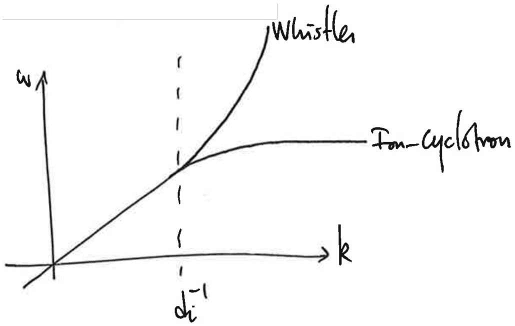

with the long-wavelength Alfvén waves bifurcating at $kd_\mathrm{i}\sim1$ according to their handedness. The ion-cyclotron wave gets "cut off" at the Hall frequency, at which the rotating electric field associated with the left-handed wave resonates with the ion gyro-motion. At this resonance, wave energy is converted into perpendicular kinetic energy of the ions. (The right-handed whistler wave gets cut off at the electron Larmor frequency for a similar reason.) This difference in handedness of can be obtained from (II.54) in the $k\ell_\mathrm{H}\gg1$ limit:

$$\frac{\delta B_y}{\delta B_x}\approx\pm\frac{\mathrm{i}}{\omega}k^2v_\mathrm{A}\ell_\mathrm{H}. \tag{II.57}$$

For an ion-cyclotron wave, $\delta B_y/\delta B_x\approx-\mathrm{i}(k/k_\parallel)(k\ell_\mathrm{H})^2$, whereas for a whistler wave, $\delta B_y/\delta B_x\approx\mathrm{i}(k/k_\parallel)$. Graphically,

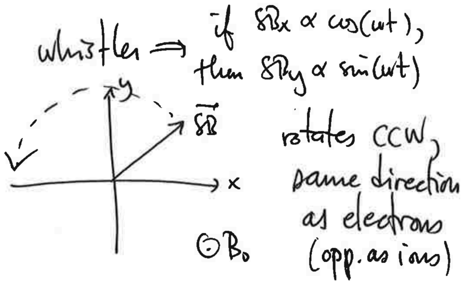

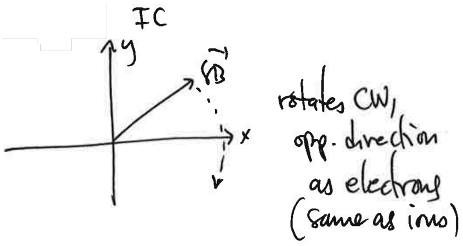

Whistler waves have been studied in the magnetosphere for more than 100 years, starting with passive ground observations of very-low-frequency radio waves from the ionosphere. (The following historical tidbits are taken from Stenzel (1999).) Preece (1894) reported that operators on the Liverpool-Hamburg telephone lines heard strange rumblings. Barkhausen (1919) described observations of "Pfeiftöne" (whistling tones) on long wire antennas and related their occurrence to lighting and auroral activity. After World War II, a lot of research into whistler waves started (not surprisingly). Whistlers have a distinct pattern in observed frequency versus time:

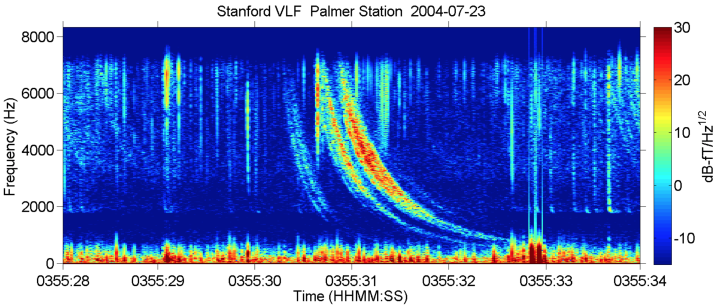

Because $\omega \propto k^2$ implies a phase velocity $\propto k$, the highest-wavenumber/frequency waves arrive first, leading to the descending tone. Such observations can be used to measure the electron density of the ionosphere.

II.3.3. *The Hall effect does not heat plasma*

From (II.56), it is clear that the Hall effect results in wave dispersion but *not* wave dissipation. Indeed, the electromagnetic work done by the Hall electric field, $\boldsymbol{j} \cdot \boldsymbol{E}_{\rm H} \propto \boldsymbol{j} \cdot (\boldsymbol{j} \times \boldsymbol{B}) = 0$. This makes sense from the physical discussion in the previous section: the Hall effect only *rotates* magnetic-field fluctuations; it does not damp their energy. Because of this, it is a bit of a misnomer to refer to "Hall diffusion", as it's not really diffusion in the usual dissipative sense of the word. Because collisions are not involved, there is nothing irreversible about the Hall effect (despite the $\eta_{\rm H}$ notation used in §II.5). It is simply a result of differences in the field-perpendicular fluid motion of oppositely charged species caused by their disparate inertia.[3]

II.3.4. *Lorentz force, Hall effect, and canonical vorticity*

This is an aside, not focused on waves and instabilities *per se*; but what's covered in this subsection is nevertheless interesting enough and so rarely discussed in textbooks that it's worth documenting here.

The differences between the ion/neutral and electron fluid motion result in an inter-

---

[3] Disparate inertia is key. There is no Hall effect in a pair plasma.

esting change to Kelvin's circulation theorem. It is straightforward to show from the ideal-MHD equations that, for $p = p(\rho)$, the fluid vorticity $\boldsymbol{\omega} = \boldsymbol{\nabla} \times \boldsymbol{u}$ satisfies

$$\frac{\partial \boldsymbol{\omega}}{\partial t} = \boldsymbol{\nabla} \times \left(\boldsymbol{u} \times \boldsymbol{\omega} + \frac{\boldsymbol{j} \times \boldsymbol{B}}{c\rho} \right), \tag{II.58}$$

so that the circulation $\varGamma \doteq \int_S \boldsymbol{\omega} \boldsymbol{\cdot} \mathrm{d}\boldsymbol{S}$ within a fluid element is conserved but for the rotational influence of the Lorentz force:

$$\frac{\mathrm{d}\varGamma}{\mathrm{d}t} = \oint_{\partial S} \left(\frac{\boldsymbol{j} \times \boldsymbol{B}}{c\rho} \right) \boldsymbol{\cdot} \mathrm{d}\boldsymbol{\ell}. \tag{II.59}$$

The version of this without the Lorentz force is called *Kelvin's circulation theorem.* (The enclosed area S must be such that we can shrink the boundary ∂S to a point without leaving the region, i.e., the closed contour must be *simply connected.* A region with a hole (like a bathtub drain) is *not* simply connected.)

Now, when the Hall effect is important, the induction equation (II.48) reads

$$\frac{\partial \boldsymbol{B}}{\partial t} = \boldsymbol{\nabla} \times \left(\boldsymbol{u} \times \boldsymbol{B} - \frac{\boldsymbol{j} \times \boldsymbol{B}}{en_{\mathrm{e}}} \right). \tag{II.60}$$

Compare (II.58) and (II.60). Clearly there is some special symmetry here that is saying something important. Just as the Lorentz force changes the number of vortex lines threading a fluid element, the Hall effect changes the number of magnetic-field lines threading a fluid element. Indeed, the origin of the Hall term is the differential motion between the electrons, to which the magnetic-field lines are tied (modulo Ohmic losses), and the drifting ions, which we take to be collisionally well coupled to the bulk neutral fluid.

Since the divergences of both the vorticity and the magnetic field are zero, any new vortex and magnetic-field lines that are made must be created as continuous curves that grow out of points or lines where the vorticity and magnetic field, respectively, vanish. Put simply, just as the effect of the Lorentz force on the vorticity is non-dissipative, so too is the Hall effect on the magnetic field; vorticity and magnetic flux can only be *redistributed* by these processes. We now prove that they must be redistributed in a specific way.

Consider the canonical momentum

$$\wp_{\mathrm{can}} \doteq m\boldsymbol{u} + \frac{e\boldsymbol{A}}{c} \frac{n_{\mathrm{e}}}{n}, \tag{II.61}$$

and the associated *canonical vorticity*

$$\boldsymbol{\omega}_{\mathrm{can}} \doteq \frac{1}{m} \boldsymbol{\nabla} \times \wp_{\mathrm{can}} = \boldsymbol{\omega} + \frac{e\boldsymbol{B}}{mc} \frac{n_{\mathrm{e}}}{n}, \tag{II.62}$$

where $\boldsymbol{A}$ is the vector potential satisfying $\boldsymbol{B} = \boldsymbol{\nabla} \times \boldsymbol{A}$. The final term in (II.62) should look familiar. Combining (II.58) and (II.60), we find that the canonical vorticity satisfies

$$\frac{\partial \boldsymbol{\omega}_{\mathrm{can}}}{\partial t} = \boldsymbol{\nabla} \times (\boldsymbol{u} \times \boldsymbol{\omega}_{\mathrm{can}}). \tag{II.63}$$

This equation states that, in the absence of dissipative sinks[4], the canonical vorticity is frozen into the fluid. As a result, the combined number of vortex and magnetic-field lines threading a material surface is conserved; i.e., the *canonical circulation*

$$\varGamma_{\mathrm{can}} \doteq \oint_{\partial S} \wp_{\mathrm{can}} \boldsymbol{\cdot} \mathrm{d}\boldsymbol{\ell} \quad \left(= \frac{1}{m} \int_S \boldsymbol{\omega}_{\mathrm{can}} \boldsymbol{\cdot} \mathrm{d}\boldsymbol{S} \right) \tag{II.64}$$

---

[4] . . . which add $\nabla^2(\nu\boldsymbol{\omega} + \eta\boldsymbol{\omega}_{\mathrm{H}})$ to the right-hand side of (II.63).

around a simple closed contour $\partial \boldsymbol{S}$ bounding a material surface S is a constant. This is simply Kelvin's (1869) circulation theorem generalized for Hall-MHD. An important consequence is that *a local increase in magnetic flux must be accompanied by a local decrease in vorticity flux and vice versa.*

Such behavior is absent in ideal MHD, in which the magnetic flux is conserved for each fluid element independent of how the vorticity is advected. The difference is due to the fact that, in Hall-MHD, the ion-neutral fluid drifts relative to the field lines and, as such, has its momentum augmented by the magnetic field through which it travels. One may think of this as a consequence of Lenz's law. This property received special attention in work by Kunz & Lesur (2013) on the magneto-rotational instability in poorly ionized protostellar accretion disks, with surprising consequences for its saturation and the global self-organization of the magnetic field.

II.3.5. *Hall shear instability*

There is a relatively simple instability that highlights the rotational nature of the Hall effect. To extract it, we begin by noting that the equations of Hall-MHD admit a very simple equilibrium solution consisting of a linear shear flow $\boldsymbol{u}_0 = -Sx\hat{\boldsymbol{y}}$ (where $S > 0$ is a constant), uniform density and pressure, and a uniform magnetic field $\boldsymbol{B}_0 = B_0\hat{\boldsymbol{z}}$, which we take be to be oriented along the same axis as the equilibrium vorticity $\boldsymbol{\omega}_0 = -S\hat{\boldsymbol{z}}$. Perturb the magnetic field with $\delta\boldsymbol{B}(t)\exp(\mathrm{i}kz)$ on scales $k\ell_{\mathrm{H}} \gg 1$, such that the ion flow is entirely unresponsive. The Hall-MHD induction equation then reads

$$\frac{\mathrm{d}}{\mathrm{d}t}\begin{pmatrix}\delta B_x\\ \delta B_y\end{pmatrix} = \begin{pmatrix}0 & -\varOmega\\ \varOmega - S & 0\end{pmatrix}\begin{pmatrix}\delta B_x\\ \delta B_y\end{pmatrix}, \tag{II.65}$$

where $\varOmega \doteq k_{\|}v_{\mathrm{A}}k\ell_{\mathrm{H}}$ is the whistler-wave frequency (see (II.56)). Resist the urge to compute the dispersion relation and just look at what we have here: the Hall effect rotates δB_y into δB_x, while the background shear stretches δB_x into δB_y. For every bit of field-line stretching in the y direction due to shear, Hall forces rotate this increased field back into the x direction, only to be stretched further by shear. This results in a feedback loop that will lead to exponential growth. Indeed, taking $\mathrm{d}/\mathrm{d}t$ of (II.65) leads to

$$\frac{\mathrm{d}^2\delta\boldsymbol{B}_\perp}{\mathrm{d}t^2} = -\varOmega(\varOmega - S)\,\delta\boldsymbol{B}_\perp, \tag{II.66}$$

whose solutions are exponentially growing if $S/\varOmega > 1$. This is the *Hall shear instability* (Kunz 2008). In the more general case where the background magnetic field $\boldsymbol{B}_0 = B_{0y}\hat{\boldsymbol{y}} + B_{0z}\hat{\boldsymbol{z}}$, the perturbation wavevector $\boldsymbol{k} = k_x\hat{\boldsymbol{x}} + k_z\hat{\boldsymbol{z}}$, and the ion dynamics are retained, the dispersion relation is

$$\big[\omega^2 + \omega\varOmega - (\boldsymbol{k}\cdot\boldsymbol{v}_{\mathrm{A}})^2\big]\big[\omega^2 - \omega\varOmega - (\boldsymbol{k}\cdot\boldsymbol{v}_{\mathrm{A}})^2\big] = -\frac{k_z}{k}S\varOmega\big[\omega^2 - (\boldsymbol{k}\cdot\boldsymbol{v}_{\mathrm{A}})^2\big]; \tag{II.67}$$

i.e., whistler/ion-cyclotron waves coupled by shear. The system is then unstable when $(\boldsymbol{k}\cdot\boldsymbol{B}_0)(\boldsymbol{k}\cdot\boldsymbol{\omega}_0) < 0$. The maximum growth rate in this case is $S/2$ and occurs for $\boldsymbol{k} = k_z\hat{\boldsymbol{z}}$.

This instability may be simply understood as a alternating succession of rotations and shears applied to an initial δB_y. See the figure below, in which (a) an initial vector $|r_0\rangle$ (black arrow) evolves under a counter-clockwise rotation $\boldsymbol{R}|r_0\rangle$ by an angle θ (gray arrow) and then (b) is sheared along the y-axis into $|r_1\rangle$ (white arrow). Mathematically iterating this process every time step $\varDelta t$ leads to a recursion relation between successive state vectors, $|r_n\rangle - (2\cos\theta + \varepsilon\sin\theta)|r_{n-1}\rangle + |r_{n-2}\rangle = 0$, where $\theta = \varOmega\varDelta t$ and $\varepsilon = S\varDelta t$. The $\varDelta t \to 0$ continuous limit of this equation is $\ddot{r} = -\varOmega(\varOmega - S)r$, precisely equation (II.66).

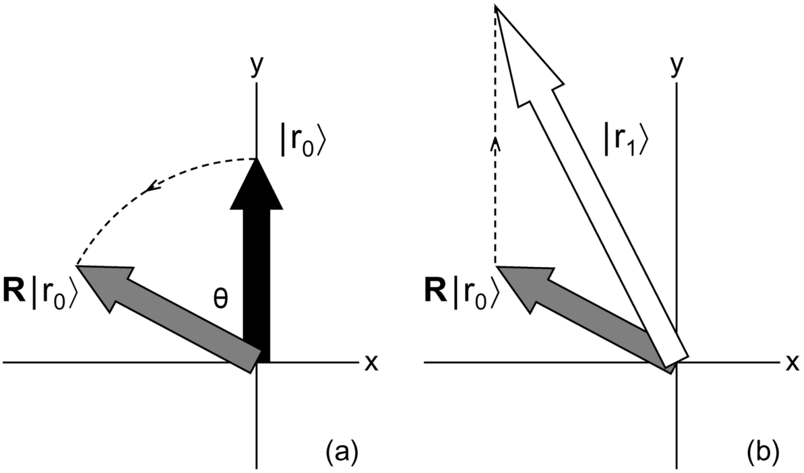

A similar instability – the *ambipolar-diffusion shear instability* – may be obtained by an iterative combination of projections and shears (Kunz 2008). Apparently, shear + anisotropic diffusion generically produces instabilities.

II.4. Ohmic dissipation

II.4.1. *Astrophysical context and basic theory*

Up to now, we've assumed that there is always at least one a species that is infinitely conducting, i.e., there is a species into whose fluid velocity the magnetic field is frozen. We know relax that assumption and, in so doing, introduce a finite conductivity σ that relates the current density $\boldsymbol{j}$ to the electric field $\boldsymbol{E}'$ in the rest frame of the plasma:

$$\boldsymbol{j} = \sigma \boldsymbol{E}'. \tag{II.68}$$

I speak of a "plasma rest frame", as I am no longer distinguishing between the fluid velocity of the neutrals and that of the charged species. Finite σ implies finite resistivity η, which in a collisional plasma is driven primarily by the friction force between the ions and electrons (see (II.4) with (II.16)):

$$\begin{aligned} 0 \approx \boldsymbol{R}_{\rm ei} - en_{\rm e}\boldsymbol{E}' &= \frac{m_{\rm e}n_{\rm e}}{\tau_{\rm ei}}(\boldsymbol{u}_{\rm i} - \boldsymbol{u}_{\rm e}) - en_{\rm e}\boldsymbol{E}' = \frac{m_{\rm e}n_{\rm e}}{\tau_{\rm ei}}\frac{\boldsymbol{j}}{en_{\rm e}} - en_{\rm e}\boldsymbol{E}' \\ \implies \quad \boldsymbol{j} &= \frac{e^2 n_{\rm e}\tau_{\rm ei}}{m_{\rm e}}\boldsymbol{E}' \doteq \sigma\boldsymbol{E}' \doteq \frac{1}{\eta}\boldsymbol{E}'. \end{aligned} \tag{II.69}$$

Using Ampére's law, the non-ideal induction equation then reads

$$\frac{\partial \boldsymbol{B}}{\partial t} = \boldsymbol{\nabla} \times (\boldsymbol{u} \times \boldsymbol{B}) - \boldsymbol{\nabla} \times \left(\frac{c^2\eta}{4\pi} \boldsymbol{\nabla} \times \boldsymbol{B} \right). \tag{II.70}$$

The first term is the familiar advection term. The second term might look more familiar to you if we take the resistivity to be spatially uniform and use $\boldsymbol{\nabla} \times (\boldsymbol{\nabla} \times \boldsymbol{B}) = -\nabla^2 \boldsymbol{B}$ to obtain

$$\frac{\partial \boldsymbol{B}}{\partial t} = \boldsymbol{\nabla} \times (\boldsymbol{u} \times \boldsymbol{B}) + \frac{c^2\eta}{4\pi}\nabla^2 \boldsymbol{B},$$

in which case the resistive term leads to a diffusion equation with diffusion coefficient $c^2\eta/4\pi$. Because this factor of $c^2/4\pi$ is often a nuisance to carry around, I will henceforth absorb this factor into the definition of the resistivity and regard η as a diffusion coefficient (with units of length^2 per time).

The relative importance of the advection and diffusion terms in (II.70) is quantified using the dimensionless *magnetic Reynolds number*,

$$\mathrm{Rm} \doteq \frac{UL}{\eta}, \tag{II.71}$$

where U and L are characteristic scales for the flow velocity and spatial gradients, respectively. For example,

$$\begin{aligned}
\text{liquid metals in industrial contexts: } & \mathrm{Rm} \sim 10^{-3} \dots 10^{-1}, \\
\text{laboratory plasma-astrophysics experiments: } & \mathrm{Rm} \sim 1 \dots 100 \text{ (and growing)}, \\
\text{planetary interiors: } & \mathrm{Rm} \sim 100 \dots 300, \\
\text{solar convective zone: } & \mathrm{Rm} \sim 10^{6} \dots 10^{9}, \\
\text{warm phase of the interstellar medium: } & \mathrm{Rm} \sim 10^{18}, \\
\text{intracluster medium of galaxy clusters: } & \mathrm{Rm} \sim 10^{29}.
\end{aligned}$$

But be careful: even in situations with $\mathrm{Rm} \ggg 1$ on the macroscopic scales, resistivity may still be important if sufficiently small spatial scales are produced, say, by a turbulent cascade or in a forming current sheet. Both of these topics – turbulence and reconnection – will be covered elsewhere in this school. For now, let's focus only on linear theory.

II.4.2. *Wave-driven Ohmic dissipation*

Regarding the linear theory of waves on a static, homogeneous background, there is nothing particularly special about the Ohmic decay of Alfvén waves versus the Ohmic decay of magnetosonic waves. Because the diffusion operator is isotropic, all modes suffer the same rate of magnetic diffusion, dependent only upon the magnitude of the wavenumber. Indeed, the linearized induction equation is

$$-\mathrm{i}\omega\delta\boldsymbol{B} = \mathrm{i}\boldsymbol{k}\boldsymbol{\cdot}\boldsymbol{B}_0\delta\boldsymbol{u} - \boldsymbol{B}_0\mathrm{i}\boldsymbol{k}\boldsymbol{\cdot}\delta\boldsymbol{u} - k^2\eta\delta\boldsymbol{B}. \tag{II.72}$$

In the final term, there is no projection onto the plane perpendicular to $\boldsymbol{k}\times\boldsymbol{B}_0$ (as in ambipolar diffusion), nor is there a $\boldsymbol{k}$-dependent rotation of the magnetic perturbation (as in the Hall effect). There is only a simple, isotropic decay at a rate $k^2\eta$. For a shear Alfvén wave with $\delta\boldsymbol{u} = -(\boldsymbol{k}\boldsymbol{\cdot}\boldsymbol{B}_0/\omega)(\delta\boldsymbol{B}/4\pi\rho)$, equation (II.72) becomes

$$\big[\omega(\omega + \mathrm{i}k^2\eta) - k_\parallel^2 v_\mathrm{A}^2\big]\delta\boldsymbol{B} = 0, \tag{II.73}$$

whose solutions satisfy

$$\omega = -\mathrm{i}\frac{k^2\eta}{2} \pm k_\parallel v_\mathrm{A}\sqrt{1 - \left(\frac{k^2\eta}{2k_\parallel v_\mathrm{A}}\right)^2}. \tag{II.74}$$

For $\mathrm{Rm} \sim v_\mathrm{A}/(k\eta) \gg 1$, these solutions become $\omega \approx \pm k_\parallel v_\mathrm{A} - \mathrm{i}k^2\eta/2$, i.e., weakly damped shear-Alfvén waves. Magnetic-field fluctuations produce currents, currents are associated with drifts between the charged species, and these interspecies drifts are damped by collisional friction.

II.4.3. *Ohmic dissipation heats plasma*

Think back to grade-school physics when you played with circuits… power is current squared times resistance, $P = RI^2$. In the language of non-ideal MHD, $\boldsymbol{j}\boldsymbol{\cdot}\boldsymbol{E}' = \eta|\boldsymbol{j}|^2$. It is straightforward to show by dotting (II.70) with $\boldsymbol{B}/4\pi$ that this is precisely the rate at which the total magnetic energy decays:

$$\frac{\mathrm{d}}{\mathrm{d}t}\int \mathrm{d}V\,\frac{B^2}{8\pi} = \underbrace{-\int \mathrm{d}V\,\boldsymbol{u}\cdot\left(\frac{\boldsymbol{j}}{c}\times\boldsymbol{B}\right)}_{\substack{\text{minus the work of the}\\ \text{Lorentz force on the flow}}} - \underbrace{\frac{c}{4\pi}\oint \mathrm{d}\boldsymbol{S}\cdot(\boldsymbol{E}\times\boldsymbol{B})}_{\text{Poynting flux}} - \underbrace{\int \mathrm{d}V\,\eta|\boldsymbol{j}|^2}_{\substack{\text{Ohmic}\\ \text{dissipation}}}. \tag{II.75}$$

This liberated magnetic energy must go somewhere, of course, and it does:

$$\frac{p}{\gamma-1}\frac{\mathrm{d}}{\mathrm{d}t}\ln\frac{p}{\rho^\gamma} = \eta|\boldsymbol{j}|^2, \tag{II.76}$$

Voila. Joule heating.

II.4.4. *Tearing instability*

Magnetic reconnection refers to the topological rearrangement of magnetic-field lines that converts magnetic energy to plasma energy. Here we briefly explore the case when such a rearrangement is facilitated by a spatially constant Ohmic resistivity, as might occur in a well-ionized collisional fluid:

$$\frac{\partial\boldsymbol{B}}{\partial t} = \boldsymbol{\nabla}\times(\boldsymbol{u}\times\boldsymbol{B}) + \eta\nabla^2\boldsymbol{B}.$$

This assumption is obviously not warranted in hot, dilute astrophysical systems, such as the collisionless solar wind, or in poorly ionized systems, like molecular clouds and pre-stellar cores. But let us assume this anyhow, knowing that (i) the physics of reconnection in even the simplest of systems is surprisingly rich and complex, and (ii) there is a huge amount of literature on all aspects of magnetic reconnection in a wide variety of environments. What follows is not intended as a replacement of that literature, nor a synopsis of current research in the field (particularly in the laboratory and the Earth's magnetosheath). Rather, I offer an incomplete presentation of a few key highlights in the theory of magnetic reconnection, focusing exclusively on the linear mechanism of instability. Hopefully this provides enough pedagogical value and inspiration to encourage you to dig into the literature further. For that, I recommend that you start with the excellent review articles by Zweibel & Yamada (2009), Yamada *et al.* (2010), and Loureiro & Uzdensky (2016).

II.4.4.1. *Formulation of the problem*

We begin by analyzing the stability of a simple stationary equilibrium in which the magnetic field reverses across $x = 0$:

$$\boldsymbol{B}_0 = B_y(x)\hat{\boldsymbol{y}} + B_\mathrm{g}\hat{\boldsymbol{z}}, \tag{II.77}$$

where $B_y(x)$ is an odd function and $B_\mathrm{g} = \mathrm{const}$ denotes the guide field. A oft-employed profile for $B_y(x)$ is the Harris (1962) sheet:

$$B_y(x) = B_\mathrm{r}\tanh\left(\frac{x}{a}\right), \tag{II.78}$$

where B_r is the asymptotic value of the reconnecting field and a is the characteristic scale length of the current sheet. Its profile, and the associated current density $j_z = (B_\mathrm{r}/a)\,\mathrm{sech}^2(x/a)$, are shown in the figure below:

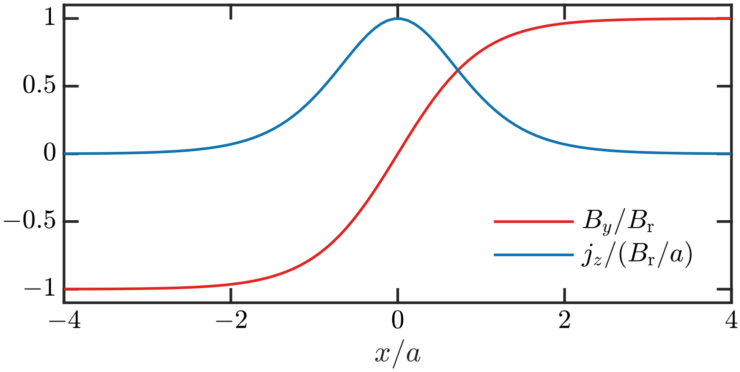

The quickest route through the tearing calculation employs the reduced MHD (RMHD) equations governing the evolution of the stream and flux functions $\varPhi$ and $\varPsi$, respectively, whose gradients describe the (incompressible) velocity and magnetic fields perpendicular to the guide-field axis, $\hat{\boldsymbol{z}}$:

$$\boldsymbol{u}_\perp = \hat{\boldsymbol{z}} \times \boldsymbol{\nabla}_\perp \varPhi, \qquad \frac{\boldsymbol{B}_\perp}{\sqrt{4\pi\rho}} = \hat{\boldsymbol{z}} \times \boldsymbol{\nabla}_\perp \varPsi. \tag{II.79}$$

Thus, $B_y(x)/\sqrt{4\pi\rho} = \varPsi_0'$ for some equilibrium $\varPsi_0(x)$. If $B_y(x)$ is taken to be the Harris-sheet profile (II.78), then $\varPsi_0 = a v_{\rm A,r} \ln[\cosh(x/a)]$, where $v_{\rm A,r} \doteq B_{\rm r}/\sqrt{4\pi\rho}$ is the Alfvén speed associated with the reconnecting field. Because this lecture focuses on linear waves and instabilities, the RMHD equations are simply stated here, as if they fell from above:

$$\frac{\partial}{\partial t}\varPsi + \{\varPhi, \varPsi\} = v_{\rm A} \frac{\partial}{\partial z}\varPhi + \eta \nabla_\perp^2 \varPsi, \tag{II.80}$$

$$\frac{\partial}{\partial t}\nabla_\perp^2 \varPhi + \left\{\varPhi, \nabla_\perp^2 \varPhi\right\} = v_{\rm A} \frac{\partial}{\partial z}\nabla_\perp^2 \varPsi + \left\{\varPsi, \nabla_\perp^2 \varPsi\right\} \tag{II.81}$$

where the Poisson bracket

$$\{\varPhi, \varPsi\} \doteq \hat{\boldsymbol{z}} \boldsymbol{\cdot} \left(\boldsymbol{\nabla}_\perp \varPhi \times \boldsymbol{\nabla}_\perp \varPsi\right) \tag{II.82}$$

captures the nonlinearities. The first of these equations, (II.80), is the un-curled induction equation, with the inclusion of a constant Ohmic diffusivity η. The second equation, (II.81), is obtained from the component of the fluid momentum equation perpendicular to the guide field; it is equivalent to an evolution equation for the flow vorticity.

Using these equations, the equilibrium (II.77) is perturbed by small fluctuations having no variation along the guide field and a sinusoidal variation along the reconnecting field:

$$\varPhi = \phi(x) {\rm e}^{{\rm i}ky + \gamma t}, \quad \varPsi = \varPsi_0(x) + \psi(x) {\rm e}^{{\rm i}ky + \gamma t}, \tag{II.83}$$

where k is the wavenumber and γ is the rate at which perturbations will grow or decay. Substituting (II.83) into (II.81) and (II.80) and retaining terms of only linear order in the fluctuation amplitudes, we have

$$\gamma \left(\frac{{\rm d}^2}{{\rm d}x^2} - k^2\right)\phi = {\rm i}k\varPsi_0' \left(\frac{{\rm d}^2}{{\rm d}x^2} - k^2\right)\psi - {\rm i}k\psi\varPsi_0''', \tag{II.84}$$

$$\gamma\psi - {\rm i}k\phi\varPsi_0' = \eta \left(\frac{{\rm d}^2}{{\rm d}x^2} - k^2\right)\psi. \tag{II.85}$$

The trick to solving this set of equations is to realize that, as η tends towards zero, the derivative on the right-hand side of (II.85) must grow to balance the terms on the left-hand side. In other words, a boundary layer forms about $x = 0$, outside of which the system satisfies the ideal-MHD equations and inside of which the resistivity is important. The width of this boundary layer is customarily denoted $\delta_{\rm in}$, and much of reconnection theory rests on determining its size given the various attributes of the host plasma. To do so, we will first solve (II.84) and (II.85) in the "outer region", where the resistivity is negligible and the system behaves as though it were ideal. Then they will be solved in the "inner region", where the resistivity dominates and $k \sim a^{-1} \ll {\rm d}/{\rm d}x \sim \delta_{\rm in}^{-1}$. The two solutions must asymptotically join onto one another; this matching, along with boundary conditions at $x = 0$ and $\pm\infty$, will determine the full solution.

Before proceeding with this program, it will be advantageous to define the resistive and Alfvén timescales,

$$\tau_\eta \doteq \frac{a^2}{\eta} \quad \text{and} \quad \tau_{\rm A} \doteq \frac{1}{ka\varPsi_0''(0)} = \frac{1}{kv_{\rm A,r}}, \tag{II.86}$$

respectively. We will assume $\tau_\eta^{-1} \ll \gamma \ll \tau_{\rm A}^{-1}$, i.e. the tearing mode grows faster than it takes for the entirety of the current sheet to resistively diffuse but slower than it takes for an Alfvén wave to cross k^{-1}. Physically, this implies that the outer solution results from neglecting the plasma's inertia and Ohmic resistivity.

II.4.4.2. *Outer equation*

Adopting the ordering $\tau_\eta^{-1} \ll \gamma \ll \tau_{\rm A}^{-1}$, equations (II.84) and (II.85) reduce to

$$\left(\frac{{\rm d}^2}{{\rm d}x^2} - k^2 - \frac{\varPsi_0'''}{\varPsi_0'}\right)\psi_{\rm out} = 0 \quad \text{and} \quad \phi_{\rm out} = \frac{\gamma}{{\rm i}k\varPsi_0'}\psi_{\rm out}. \tag{II.87}$$

Note that $\varPsi_0'''/\varPsi_0' = B_y''/B_y$ measures the gradient of the current density, and so different current-sheet profiles will result in different solutions to (II.87). Regardless of the exact current-sheet profile, however, both $\phi_{\rm out}$ and $\psi_{\rm out}$ must tend to zero as $x \to \pm\infty$. Also, since the y-component of the perturbed magnetic field must reverse direction at $x = 0$, $\psi_{\rm out}$ must have a discontinuous derivative there, corresponding to a singular current. Indeed, it is this discontinuity that characterizes the free energy available to reconnect, quantified by the tearing-instability parameter

$$\varDelta' \doteq \frac{1}{\psi_{\rm out}(0)} \frac{{\rm d}\psi_{\rm out}}{{\rm d}x}\bigg|_{-0}^{+0}, \tag{II.88}$$

and that ultimately warrants consideration of a resistive inner layer.

II.4.4.3. *Inner equation*

In the inner region where $k \ll {\rm d}/{\rm d}x \sim \delta_{\rm in}^{-1}$, the dominant terms in (II.84) and (II.85) are

$$\gamma\frac{{\rm d}^2\phi_{\rm in}}{{\rm d}x^2} = {\rm i}k\varPsi_0'\frac{{\rm d}^2\psi_{\rm in}}{{\rm d}x^2}, \tag{II.89}$$

$$\gamma\psi_{\rm in} - {\rm i}k\phi_{\rm in}\varPsi_0' = \eta\frac{{\rm d}^2\psi_{\rm in}}{{\rm d}x^2}. \tag{II.90}$$

These equations may be solved analytically provided some amenable form of $\varPsi_0'$. Because we are deep within the current sheet, the leading-order term in a Taylor expansion will suffice, *viz.*, $\varPsi_0' \approx \varPsi_0''(0)x = v_{\rm A,r}(x/a)$. Then (II.89) and (II.90) may be straightforwardly combined to obtain

$$\frac{{\rm d}^2\psi_{\rm in}}{{\rm d}x^2} = -\left[\frac{\gamma}{k\varPsi_0''(0)}\right]^2 \frac{1}{x}\frac{{\rm d}^2}{{\rm d}x^2}\left[\frac{1}{x}\left(1 - \frac{\eta}{\gamma}\frac{{\rm d}^2}{{\rm d}x^2}\right)\psi_{\rm in}\right]. \tag{II.91}$$

With some effort, this equation can actually be solved for $\psi_{\rm in}$ analytically. I'll show you how below. But even without that effort, equation (II.91) may be used to estimate the width of the boundary layer, $\delta_{\rm in}$:

$$1 \sim (\gamma a \tau_{\rm A})^2 \frac{\eta}{\gamma \delta_{\rm in}^4} \quad \Longrightarrow \quad \frac{\delta_{\rm in}}{a} \sim \left(\frac{\gamma \tau_{\rm A}^2}{\tau_\eta}\right)^{1/4}. \tag{II.92}$$

Note that $\delta_{\rm in}$ depends on k – each tearing mode k has a different boundary-layer width; because of this, each k will correspond to a different $\varDelta'$.

Normalizing lengthscales to $\delta_{\rm in}$ by introducing $\xi \doteq x/\delta_{\rm in}$, equation (II.91) may be written as

$$\frac{{\rm d}^2\psi_{\rm in}}{{\rm d}\xi^2} = -\frac{1}{\xi}\frac{{\rm d}^2}{{\rm d}\xi^2}\left[\frac{1}{\xi}\left(\varLambda - \frac{{\rm d}^2}{{\rm d}\xi^2}\right)\psi_{\rm in}\right], \tag{II.93}$$

where the eigenvalue $\varLambda \doteq \gamma^{3/2}\tau_{\rm A}\tau_\eta^{1/2} = \gamma\delta_{\rm in}^2/\eta$ is the growth rate of the tearing mode normalized by the rate of resistive diffusion across a layer of width $\delta_{\rm in}$. Provided we can solve (II.93), the solution $\psi_{\rm in}$ must be matched onto the outer solution $\psi_{\rm out}$. This is done by equating the discontinuity in $\psi_{\rm out}$, quantified by $\varDelta'$ (see (II.88)), to the total change in ${\rm d}\psi_{\rm in}/{\rm d}x$ across the inner region, *viz.*,

$$\varDelta' = \frac{2}{\delta_{\rm in}}\int_0^1 {\rm d}\xi\, \frac{1}{\psi_{\rm in}(0)}\frac{{\rm d}^2\psi_{\rm in}}{{\rm d}\xi^2}.$$

(The factor of 2 is because the solution is odd, and so the total change across the $x = 0$ surface is twice the change measured for $x > 0$.) The upper limit on the integral can be extended to $+\infty$ by committing only a ~10% error:

$$\varDelta' = \frac{2}{\delta_{\rm in}}\int_0^\infty {\rm d}\xi\, \frac{1}{\psi_{\rm in}(0)}\frac{{\rm d}^2\psi_{\rm in}}{{\rm d}\xi^2}. \tag{II.94}$$

So, find $\psi(\xi)$ by solving the inner equation (II.93), compute the integral in (II.94), and invert the answer to obtain the growth rate in terms of $\varDelta'$.

Before carrying out that program, it will be useful to further simply (II.93) by introducing

$$\chi(\xi) \doteq \xi^2 \frac{\rm d}{{\rm d}\xi}\left[\frac{\psi_{\rm in}(\xi)}{\xi}\right], \tag{II.95}$$

so that

$$\frac{\rm d}{{\rm d}\xi}\left[\frac{\rm d}{{\rm d}\xi}\left(\frac{1}{\xi^2}\frac{{\rm d}\chi}{{\rm d}\xi}\right) - \left(1 + \frac{\varLambda}{\xi^2}\right)\chi\right] = 0. \tag{II.96}$$

Integrating this equation once and, for reasons that will eventually become apparent, setting the integration constant to $-\chi_\infty$, we find

$$\xi^2 \frac{\rm d}{{\rm d}\xi}\left(\frac{1}{\xi^2}\frac{{\rm d}\chi}{{\rm d}\xi}\right) - \left(\xi^2 + \varLambda\right)\chi = -\chi_\infty \xi^2. \tag{II.97}$$

Once this equation is solved, the inner solution is obtained using (cf. (II.95))

$$\psi_{\rm in}(\xi) = -\xi\int_\xi^\infty {\rm d}x\, \frac{\chi(x)}{x^2} = -\xi\int_\xi^\infty {\rm d}x\, \frac{\chi'(x)}{x} - \chi(\xi), \tag{II.98}$$

which may then be plugged into (II.94) to compute $\varDelta'$.

II.4.4.4. *Approximate solutions*

There are a few ways to solve (II.87) and (II.97), none of which are particularly obvious. However, it's possible to obtain scaling laws for $\varDelta'$ and the tearing-mode growth rate

γ without actually doing so. In fact, the answers obtained in this way differ from those obtained by a more mathematically rigorous solution (see §II.4.4.5) by only order-unity coefficients. Nice.

We start with (II.87), the outer equation. With some knowledge that the fastest-growing modes occur at long wavelengths ($ka \ll 1$), we can make some progress by simply dropping the middle term in (II.87). Then, so long as B_y varies faster within $|x| \lesssim a$ than it does at $|x| \gg a$, we can estimate

$$\varDelta' \sim \frac{1}{ka^2}. \tag{II.99}$$

(This scaling is exact for the Harris-sheet profile, solved for in §II.4.4.5.) One may formalize this estimate somewhat (Loureiro *et al.* 2007, 2013) by quantifying what "varies faster within $|x| \lesssim a$ than it does at $|x| \gg a$" means, but not much is gained intuitively by going that route, and the estimate (II.99) will suffice.

As for the inner equation (II.93), we know from (II.97) that, whatever its solution, $\psi_{\text{in}}(\xi)$ only depends on the parameter $\varLambda$. Thus, equation (II.94) may be written as

$$\varDelta'\delta_{\text{in}} = f(\varLambda) \tag{II.100}$$

for some function $f(\varLambda)$. Combining (II.99) and (II.100) yields an expression for the growth rate, provided we can invert $f(\varLambda)$. Fortunately, we can, at least in certain limits.

The first limit is the so-called "constant-ψ approximation" or "FKR regime", which corresponds to $f(\varLambda) \sim \varLambda \ll 1$ (Furth *et al.* 1963). Then (II.100) gives $\varDelta'\delta_{\text{in}} \sim \varLambda$, so that

$$\boxed{\gamma_{\text{FKR}} \sim \tau_{\text{A}}^{-2/5}\tau_{\eta}^{-3/5}(\varDelta' a)^{4/5}, \quad \frac{\delta_{\text{in}}}{a} \sim \left(\frac{\tau_{\text{A}}}{\tau_{\eta}}\right)^{2/5}(\varDelta' a)^{1/5}} \tag{II.101}$$

With $\varDelta' \sim 1/ka^2$ (see (II.99)), these become

$$\frac{\gamma_{\text{FKR}}}{v_{\text{A,r}}/a} \sim (ka)^{-2/5} S_a^{-3/5}, \quad \frac{\delta_{\text{in}}}{a} \sim (ka)^{-3/5} S_a^{-2/5}, \tag{II.102}$$

where we have introduced the *Lundquist number*

$$S_a \doteq \frac{a v_{\text{A,r}}}{\eta}. \tag{II.103}$$

Note that longer wavelengths have faster growth rates (the divergence as $k \to 0$ will be cured in the "Coppi" regime, in which the small-$\varDelta'$ assumption breaks down – see below). This approximation results from setting $\psi_{\text{in}} = \psi_{\text{in}}(0)$ on the left-hand side of (II.90), so that the inner equation (II.90) becomes

$$\gamma\psi_{\text{in}}(0) - \mathrm{i}k\phi_{\text{in}}\varPsi_0''(0)x = \eta\frac{\mathrm{d}^2\psi_{\text{in}}}{\mathrm{d}x^2}, \tag{II.104}$$

and so (cf. (II.97))

$$\xi^2\frac{\mathrm{d}}{\mathrm{d}\xi}\left(\frac{1}{\xi^2}\frac{\mathrm{d}\chi}{\mathrm{d}\xi}\right) - \xi^2(\chi - \chi_\infty) = -\varLambda\psi_{\text{in}}(0). \tag{II.105}$$

In effect, we are assuming that the resistive diffusion time across the inner-layer thickness is much shorter than the instability growth time, i.e., $\gamma \ll \eta/\delta_{\text{in}}^2$, so that ψ_{in} can be approximated as constant on the dynamical time scale. Using (II.102) in this inequality requires $S_a \gg (\varDelta' a)^4$. This is sometimes called the "small-$\varDelta'$ regime".

The second limit is the "Coppi regime" or "large-$\varDelta'$ regime", in which the constant-ψ

approximation breaks down and $\gamma \sim \eta/\delta_{\text{in}}^2$. This occurs for $\Lambda \sim 1^-$, at which $f(\Lambda) \to \infty$. The growth rate then becomes independent of Δ' and we have

$$\boxed{\gamma_{\text{Coppi}} \sim \tau_{\text{A}}^{-2/3}\tau_\eta^{-1/3}, \quad \frac{\delta_{\text{in}}}{a} \sim \left(\frac{\tau_{\text{A}}}{\tau_\eta}\right)^{1/3}} \tag{II.106}$$

In terms of the tearing-mode wavenumber k and the Lundquist number S_a,

$$\frac{\gamma_{\text{Coppi}}}{v_{\text{A,r}}/a} \sim (ka)^{2/3}S_a^{-1/3}, \quad \frac{\delta_{\text{in}}}{a} \sim (ka)^{-1/3}S_a^{-1/3}. \tag{II.107}$$

In this limit, the shorter wavelengths have faster growth rates, opposite to the FKR scaling (II.102). This suggests a maximally growing mode, whose growth rate $\gamma_{\max}$ and wavenumber $k_{\max}$ may be estimated by matching the FKR solution (II.102) to the Coppi one (II.107):

$$\gamma_{\text{FKR}} \sim \gamma_{\text{Coppi}} \quad \Longrightarrow \quad k_{\max}a \sim S_a^{-1/4}, \quad \frac{\gamma_{\max}}{v_{\text{A,r}}/a} \sim S_a^{-1/2}, \quad \frac{\delta_{\text{in}}}{a} \sim S_a^{-1/4}. \tag{II.108}$$

Note that the FKR (Coppi) regime corresponds to $k > k_{\max}$ ($k < k_{\max}$).

Of course, all of these scalings make sense only if the modes can fit into the current sheet, i.e., $kL \gtrsim 1$, where L is the length of the current sheet. For the maximally growing mode to be viable thus requires a current-sheet aspect ratio of $L/a \gtrsim S_a^{1/4}$. If this inequality is not satisfied, then the fastest-growing mode will be the FKR mode (II.102) with the smallest possible allowed wavenumber, $kL \sim 1$. Thus, low-aspect-ratio sheets with $L/a \ll S_a^{1/4}$ will develop tearing perturbations comprising just one or two islands; the high-aspect-ratio sheets, in which the Coppi regime is accessible, will instead spawn whole chains comprising $\sim k_{\max}L$ islands.

II.4.4.5. *Exact solution for a Harris sheet*

This is advanced material detailing a more rigorous derivation of the tearing-mode dispersion relation.

The solutions obtained in the last section should suffice for most. But with some (read: a lot of) effort, one can be more precise. For that task, let us adopt the equilibrium flux function $\varPsi_0 = av_{\text{A,r}}\ln[\cosh(x/a)]$, corresponding to the Harris-sheet profile (II.78). Then (II.87) becomes

$$\left[\frac{\mathrm{d}^2}{\mathrm{d}x^2} - k^2 + \frac{2}{a^2}\operatorname{sech}^2\left(\frac{x}{a}\right)\right]\psi_{\text{out}} = 0 \quad \text{and} \quad \phi_{\text{out}} = -\mathrm{i}\gamma\tau_{\text{A}}\coth\left(\frac{x}{a}\right)\psi_{\text{out}}. \tag{II.109}$$

The former equation can be solved by changing variables to $\mu = \tanh(x/a)$, so that $\operatorname{sech}^2(x/a) = (1-\mu^2)^{-1}$ and

$$\frac{\mathrm{d}}{\mathrm{d}x} = \frac{1-\mu^2}{a}\frac{\mathrm{d}}{\mathrm{d}\mu}, \quad \frac{\mathrm{d}^2}{\mathrm{d}x^2} = \frac{1-\mu^2}{a}\frac{\mathrm{d}}{\mathrm{d}\mu}\frac{1-\mu^2}{a}\frac{\mathrm{d}}{\mathrm{d}\mu}.$$

Then (II.109) becomes

$$\left[\frac{\mathrm{d}}{\mathrm{d}\mu}(1-\mu^2)\frac{\mathrm{d}}{\mathrm{d}\mu} + 2 - \frac{k^2a^2}{1-\mu^2}\right]\psi_{\text{out}} = 0 \quad \text{and} \quad \phi_{\text{out}} = -\mathrm{i}\gamma\tau_{\text{A}}\frac{\psi_{\text{out}}}{\mu}, \tag{II.110}$$

the first of which you might recognize as the associated Legendre equation

$$\left[\frac{\mathrm{d}}{\mathrm{d}\mu}(1-\mu^2)\frac{\mathrm{d}}{\mathrm{d}\mu} + \ell(\ell+1) - \frac{m^2}{1-\mu^2}\right]P_\ell^m(\mu) = 0$$

with $\ell = 1$ and $m = ka$. Transforming the boundary conditions $\psi(\pm\infty) = 0$ into $\psi(\mu = \pm 1) = 0$ and enforcing $\psi(\mu) = \psi(-\mu)$, the solution to (II.110) is thus

$$\psi_{\text{out}} = C_{1m} P_1^m(\mu), \tag{II.111}$$

with $C_{1m} = \text{const}$. If you can't picture in your head what the first associated Legendre polynomial with non-integer m looks like – I know I can't – you may like to know that the outer solution may be equivalently written as

$$\psi_{\text{out}}(x) = C'_{1m} \mathrm{e}^{-kx} \left[1 + \frac{1}{ka} \tanh\left(\frac{x}{a}\right) \right] \tag{II.112}$$

for $\xi \geqslant 0$, where $C'_{1m} = \text{const}$. (Note that $\psi_{\text{out}}(-\xi) = \psi_{\text{out}}(\xi)$.) Visually:

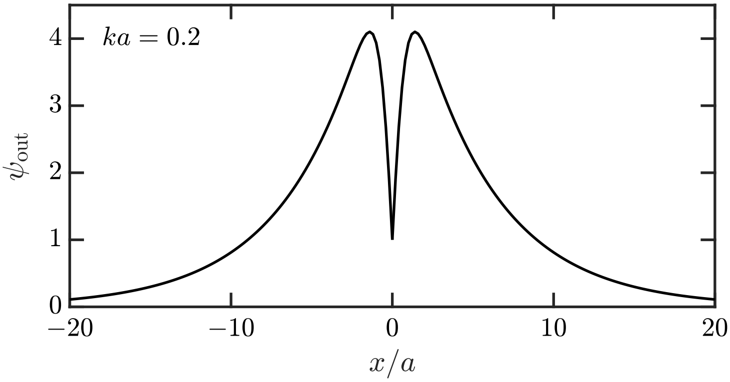

Recall that Δ' measures the discontinuity of $\mathrm{d}\psi_{\text{out}}/\mathrm{d}x$ at $x = 0$ (see (II.88)). Solving for C_{1m} (or C'_{1m}) requires matching onto the inner solution, but even before doing that we can compute Δ' using $\psi_{\text{out}} \propto P_1^m(\mu)$ in (II.88):[5]

$$\begin{aligned} \Delta' a &= \frac{1}{P_1^m(0)} \frac{\mathrm{d}P_1^m}{\mathrm{d}\mu} \bigg|_{-0}^{+0} = \frac{2}{P_1^m(0)} \frac{\mathrm{d}P_1^m}{\mathrm{d}\mu} \bigg|_{\mu=0} = 2\left(\frac{1}{m} - m\right) \\ &= 2\left(\frac{1}{ka} - ka\right). \end{aligned} \tag{II.113}$$

Note that $\Delta' > 0$ requires $ka < 1$ – any unstable mode must have an extent at least as large as the current-sheet thickness. This places an upper limit on the wavenumber of the FKR modes (II.102).

As for the inner equation, let us use its compact form (II.97), repeated here for convenience:

$$\xi^2 \frac{\mathrm{d}}{\mathrm{d}\xi}\left(\frac{1}{\xi^2}\frac{\mathrm{d}\chi}{\mathrm{d}\xi}\right) - \left(\xi^2 + \Lambda\right)\chi = -\chi_\infty \xi^2, \tag{II.114}$$

where $\Lambda \doteq \gamma^{3/2} \tau_{\mathrm{A}} \tau_\eta^{1/2}$. There are a few ways to solve (II.114), none of which are particularly obvious. One way, explained in Appendix A of Ara *et al.* (1978), is as follows. Write

$$\chi = \chi_\infty \sum_{n=0}^{\infty} a_n L_n^{(-3/2)}(\xi^2)\, \mathrm{e}^{-\xi^2/2}, \tag{II.115}$$

---

[5] See `https://dlmf.nist.gov/14.5` for information on $P_\ell^m(0)$ and $\mathrm{d}P_\ell^m/\mathrm{d}\mu|_{\mu=0}$.

where $L_n^\alpha(z)$ are the associated Laguerre (or "Sonine") polynomials satisfying

$$z\frac{\mathrm{d}^2L_n^{(\alpha)}}{\mathrm{d}z^2}+(\alpha+1-z)\frac{\mathrm{d}L_n^{(\alpha)}}{\mathrm{d}z}+nL_n^{(\alpha)}=0. \tag{II.116}$$

Substitute this decomposition into (II.97) and use the recursion relations

$$\frac{\mathrm{d}L_n^\alpha}{\mathrm{d}z}=-L_{n-1}^{\alpha+1}(z) \text{ if } 1\leqslant n \ (=0 \text{ otherwise}),$$
$$nL_n^{(-3/2)}(z)=-\left(z+\frac{1}{2}\right)L_{n-1}^{(-1/2)}(z)-zL_{n-2}^{(1/2)}(z),$$

to obtain

$$\sum_{n=0}^\infty a_n\,\xi^{-2}\,\mathrm{e}^{-\xi^2/2}L_n^{(-3/2)}(\xi^2)\big(4n+\mathit{\Lambda}-1\big)=1. \tag{II.117}$$

Multiply this by $\mathrm{e}^{-\xi^2/2}\xi^{-1}L_m^{-3/2}$, integrate, and use the orthogonality relation

$$\int_0^\infty \mathrm{d}z\,\mathrm{e}^{-z}z^\alpha L_m^\alpha L_n^\alpha=\delta_{mn}\frac{\mathit{\Gamma}(n+\alpha+1)}{\mathit{\Gamma}(n+1)}$$

to find that

$$\begin{aligned}a_n\frac{(n-3/2)!}{n!}(4n+\mathit{\Lambda}-1)&=\int_0^\infty \mathrm{d}z\,z^{-1/2}\mathrm{e}^{-z/2}L_n^{-3/2}\\&=\int_0^\infty \mathrm{d}z\,z^{-1/2}\mathrm{e}^{-z/2}(L_n^{-1/2}-L_{n-1}^{-1/2})\\&=\sqrt{2}(-1)^n\left[\frac{\mathit{\Gamma}(n+1/2)}{\mathit{\Gamma}(n+1)}+\frac{\mathit{\Gamma}(n-1/2)}{\mathit{\Gamma}(n)}\right]\\\implies\quad a_n&=\frac{(-1)^n}{\sqrt{2}}\frac{4n-1}{4n+\mathit{\Lambda}-1}.\end{aligned}$$

Thus, equation (II.115) becomes[6]

$$\chi=\frac{\chi_\infty}{\sqrt{2}}\,\mathrm{e}^{-\xi^2/2}\sum_{n=0}^\infty(-1)^nL_n^{-3/2}(\xi^2)\frac{4n-1}{4n+\mathit{\Lambda}-1}=\xi^2\frac{\mathrm{d}}{\mathrm{d}\xi}\frac{\psi_{\mathrm{in}}}{\xi}, \tag{II.118}$$

which may be solved for ψ_{in} following (II.98).

Actually doing so and plugging the solution into (II.94) to compute $\mathit{\Delta}'$ ain't easy, as it involves a lot of non-standard math. I may LaTeX those steps up one day, but, for now, I'll just skip to the answer:

$$\mathit{\Delta}'\delta_{\mathrm{in}}=f(\mathit{\Lambda})\doteq\frac{\pi}{2}\frac{\mathit{\Gamma}[(\mathit{\Lambda}+3)/4]}{\mathit{\Gamma}[(\mathit{\Lambda}+5)/4]}\frac{\mathit{\Lambda}}{1-\mathit{\Lambda}}. \tag{II.119}$$

This is an implicit equation for $\mathit{\Gamma}$, which may be solved numerically (see figure below). But it's possible to recover our approximate results (II.101) and (II.106) in their respective limits. For $\mathit{\Lambda}\ll 1$,

$$f(\mathit{\Lambda})\approx\frac{\pi}{2}\frac{\mathit{\Gamma}(3/4)}{\mathit{\Gamma}(5/4)}\mathit{\Lambda}\simeq 2.124\,\mathit{\Lambda}\quad\implies\quad\gamma\approx 0.547\,\tau_{\mathrm{A}}^{-2/5}\tau_\eta^{-3/5}(\mathit{\Delta}'a)^{4/5}. \tag{II.120}$$

Our approximate result for this FKR regime, equation (II.101), is off by only a factor of

---

[6] Note that we cannot use the expansion (II.115) if $\mathit{\Lambda}=1$.

0.547 – not too bad. For $\varLambda = 1^-$,

$$f(\varLambda) \approx \frac{\pi}{2}\frac{\varGamma(1)}{\varGamma(3/2)}\frac{1}{1-\varLambda} = \frac{\sqrt{\pi}}{1-\varLambda} \quad\Longrightarrow\quad \gamma \approx \tau_{\mathrm{A}}^{-2/3}\tau_{\eta}^{-1/3} - \mathcal{O}\left(\frac{kv_{\mathrm{A,r}}}{\varDelta' a}\right). \tag{II.121}$$

This matches our Coppi-regime estimate, (II.106). These asymptotic solutions actually do rather well across the full range of wavenumbers:

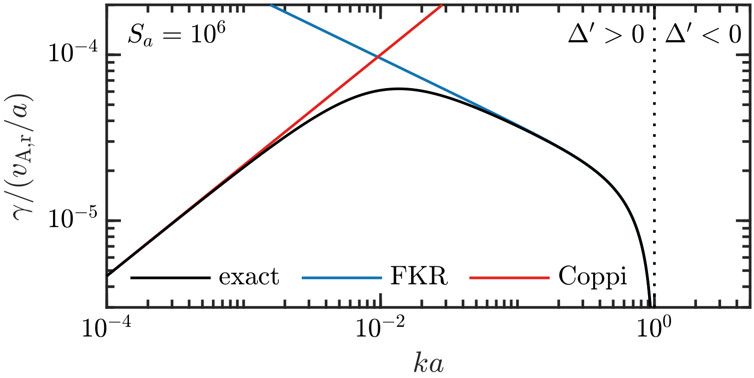

It also appears that we are well justified in estimating the maximally growing mode by matching the FKR and Coppi expressions (as in (II.108)). These regimes also occur where we anticipated, with $f(\varLambda) = \varDelta'\delta_{\mathrm{in}}$ being $\ll 1$ ($\gg 1$) in the FKR (Coppi) regime:

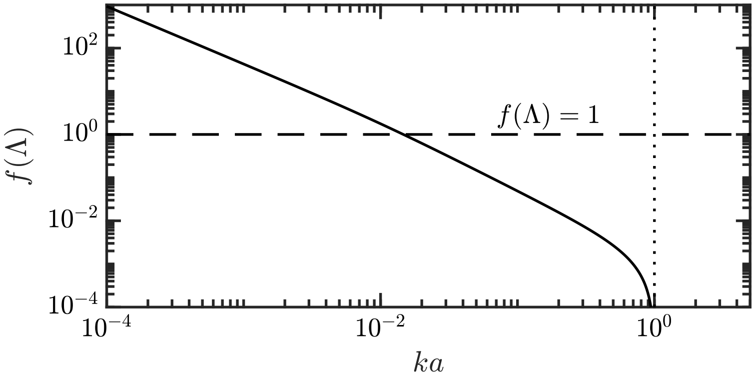

Thus the “small-$\varDelta'$” / “large-$\varDelta'$” phraseology.

How long does this linear phase, in which the tearing modes grow exponentially, last? That depends on the $\varDelta'$ of the mode. But I’ll provide nothing further on this topic in these notes, as it would take us quite outside of linear theory – and certainly outside of my restricted definition of “waves and instabilities” for the purposes of this school.

II.5. A more rigorous derivation of a generalized Ohm’s law

Finally, for completeness, I include here a more rigorous derivation of the non-ideal induction equation including ambipolar diffusion, the Hall effect, and Ohmic dissipation.

Consider the (inertia- and pressure-less) force equation for the charged species:

$$0 = q_\alpha n_\alpha \left(\boldsymbol{E} + \frac{\boldsymbol{u}_\alpha}{c}\times\boldsymbol{B}\right) + \boldsymbol{R}_{\alpha\mathrm{n}}, \tag{II.122}$$

where $\alpha = \mathrm{i}, \mathrm{e}, \mathrm{g}_+, \mathrm{g}_-$. With the friction force due to collisions with the neutrals given by

$$\boldsymbol{R}_{\alpha\mathrm{n}} = \frac{\rho_\mathrm{n}}{\tau_{\mathrm{n}\alpha}}(\boldsymbol{u}_\mathrm{n} - \boldsymbol{u}_\alpha) = \frac{\rho_\alpha}{\tau_{\alpha\mathrm{n}}}(\boldsymbol{u}_\mathrm{n} - \boldsymbol{u}_\alpha),$$

equation (II.122) becomes

$$0 = q_\alpha n_\alpha \left(\boldsymbol{E} + \frac{\boldsymbol{u}_\alpha}{c} \times \boldsymbol{B}\right) + \frac{\rho_\alpha}{\tau_{\alpha\mathrm{n}}}(\boldsymbol{u}_\mathrm{n} - \boldsymbol{u}_\alpha). \tag{II.123}$$

We are going to use this system of equations to obtain $\boldsymbol{E}$. We'll only consider elastic collisions with the neutrals, since these are the dominant collisions in most of the parameter space in molecular clouds and their cores. The collision time scales for ion–neutral and electron–neutral collisions were already provided in (II.14) and (II.15); for collisions between grains with radius a_gr and neutrals,

$$\tau_\mathrm{ng} = \frac{m_\mathrm{n} n_\mathrm{n}}{m_\mathrm{g} n_\mathrm{g}} \tau_\mathrm{gn} = 1.09\,\frac{m_\mathrm{g} + m_{\mathrm{H}_2}}{m_\mathrm{g} n_\mathrm{g} \langle \sigma w \rangle_{\mathrm{gH}_2}}, \tag{II.124}$$

where the mean collisional rate between the grain species and H_2 is

$$\langle \sigma w \rangle_{\mathrm{gH}_2} = \pi a_\mathrm{gr}^2 \left(\frac{8 k_\mathrm{B} T}{\pi m_{\mathrm{H}_2}}\right)^{1/2} \quad \text{for } |\boldsymbol{u}_\mathrm{n} - \boldsymbol{u}_\mathrm{g}| < C. \tag{II.125}$$

Collisions between, say, ions and electrons can be readily incorporated at the expense of algebraic discomfort. For an inclusion of inelastic grain-grain collisions, see the Appendix of Kunz & Mouschovias (2009).

The derivation begins by shifting to the frame of the neutrals by introducing $\boldsymbol{w}_\alpha \doteq \boldsymbol{u}_\alpha - \boldsymbol{u}_\mathrm{n}$ and $\boldsymbol{E}_\mathrm{n} \doteq \boldsymbol{E} + \boldsymbol{u}_\mathrm{n} \times \boldsymbol{B}/c$, so that (II.123) becomes

$$0 = q_\alpha n_\alpha \left(\boldsymbol{E}_\mathrm{n} + \frac{\boldsymbol{w}_\alpha}{c} \times \boldsymbol{B}\right) - \frac{\rho_\alpha}{\tau_{\alpha\mathrm{n}}} \boldsymbol{w}_\alpha. \tag{II.126}$$

Using quasi-neutrality, the current density $\boldsymbol{j} = \sum_\alpha q_\alpha n_\alpha \boldsymbol{u}_\alpha = \sum_\alpha q_\alpha n_\alpha \boldsymbol{w}_\alpha$. Thus, if we can write $\boldsymbol{w}_\alpha$ in terms of the electric field $\boldsymbol{E}$, we can invert this equation to obtain $\boldsymbol{E} = \boldsymbol{E}(\boldsymbol{j})$ – a generalized Ohm's law.

To solve (II.126) for the relative species velocities $\boldsymbol{w}_\alpha$, start by taking its cross product with $\boldsymbol{B}$ and multiplying by $q_\alpha \tau_{\alpha\mathrm{n}}/m_\alpha c$ to find

$$0 = \frac{q_\alpha^2 n_\alpha \tau_{\alpha\mathrm{n}}}{m_\alpha c} \left(\boldsymbol{E}_\mathrm{n} \times \boldsymbol{B} - \frac{\boldsymbol{w}_{\alpha\perp}}{c} B^2\right) - q_\alpha n_\alpha \frac{\boldsymbol{w}_\alpha}{c} \times \boldsymbol{B}. \tag{II.127}$$

Adding (II.127) to (II.126) and multiplying by $\tau_{\alpha\mathrm{n}}/\rho_\alpha$,

$$0 = \frac{q_\alpha \tau_{\alpha\mathrm{n}}}{m_\alpha} \boldsymbol{E}_\mathrm{n} + (\mathit{\Omega}_\alpha \tau_{\alpha\mathrm{n}})^2 \left(\frac{c}{B} \boldsymbol{E}_\mathrm{n} \times \hat{\boldsymbol{b}} - \boldsymbol{w}_{\alpha\perp}\right) - \boldsymbol{w}_\alpha. \tag{II.128}$$

Note that if the entire plasma is well magnetized, *viz.* $(\mathit{\Omega}_\alpha \tau_{\alpha\mathrm{n}})^2 \gg 1$ for each α, then the leading-order motion of all species consists of the same $\boldsymbol{E} \times \boldsymbol{B}$ drift.

We solve (II.128) by examining its parallel and perpendicular components separately. The former gives

$$\boldsymbol{w}_{\alpha\|} = \frac{q_\alpha \tau_{\alpha\mathrm{n}}}{m_\alpha} \boldsymbol{E}_{\mathrm{n}\|} \quad \Longrightarrow \quad \boldsymbol{j}_\| = \left(\sum_\alpha \frac{q_\alpha^2 n_\alpha \tau_{\alpha\mathrm{n}}}{m_\alpha}\right) \boldsymbol{E}_{\mathrm{n}\|} \doteq \left(\sum_\alpha \sigma_\alpha\right) \boldsymbol{E}_{\mathrm{n}\|} \doteq \sigma_\| \boldsymbol{E}_{\mathrm{n}\|}, \tag{II.129}$$

where the parallel conductivity $\sigma_\|$ has been defined *in situ*. The perpendicular component of (II.128) may be rearranged to obtain

$$\boldsymbol{w}_{\alpha\perp} = \frac{q_\alpha \tau_{\alpha\mathrm{n}}}{m_\alpha} \left[\frac{1}{1+(\Omega_\alpha \tau_{\alpha\mathrm{n}})^2} \boldsymbol{E}_{\mathrm{n}\perp} + \frac{\Omega_\alpha \tau_{\alpha\mathrm{n}}}{1+(\Omega_\alpha \tau_{\alpha\mathrm{n}})^2} \boldsymbol{E}_\mathrm{n} \times \hat{\boldsymbol{b}} \right]$$

$$\begin{aligned} \implies \quad \boldsymbol{j}_\perp &= \left[\sum_\alpha \frac{\sigma_\alpha}{1+(\Omega_\alpha \tau_{\alpha\mathrm{n}})^2} \right] \boldsymbol{E}_{\mathrm{n}\perp} + \left[\sum_\alpha \frac{\sigma_\alpha \Omega_\alpha \tau_{\alpha\mathrm{n}}}{1+(\Omega_\alpha \tau_{\alpha\mathrm{n}})^2} \right] \boldsymbol{E}_\mathrm{n} \times \hat{\boldsymbol{b}} \\ &\doteq \sigma_\perp \boldsymbol{E}_{\mathrm{n}\perp} - \sigma_\mathrm{H} \boldsymbol{E}_\mathrm{n} \times \hat{\boldsymbol{b}}, \end{aligned} \tag{II.130}$$

where the perpendicular conductivity $\sigma_\perp$ and Hall conductivity σ_H have been defined *in situ*. Combining (II.129) and (II.130), the total current density

$$\boldsymbol{j} = \sigma_\parallel \boldsymbol{E}_{\mathrm{n}\parallel} + \sigma_\perp \boldsymbol{E}_{\mathrm{n}\perp} - \sigma_\mathrm{H} \boldsymbol{E}_\mathrm{n} \times \hat{\boldsymbol{b}}, \tag{II.131}$$

which may be inverted to find

$$\boldsymbol{E}_\mathrm{n} = \eta_\parallel \boldsymbol{j}_\parallel + \eta_\perp \boldsymbol{j}_\perp + \eta_\mathrm{H} \boldsymbol{j} \times \hat{\boldsymbol{b}}, \tag{II.132}$$

where the parallel, perpendicular, and Hall resistivities are

$$\eta_\parallel \doteq \frac{1}{\sigma_\parallel}, \quad \eta_\perp \doteq \frac{\sigma_\perp}{\sigma_\perp^2 + \sigma_\mathrm{H}^2}, \quad \eta_\mathrm{H} \doteq \frac{\sigma_\mathrm{H}}{\sigma_\perp^2 + \sigma_\mathrm{H}^2}, \tag{II.133}$$

respectively. Knowing that Ohmic dissipation affects the total current while ambipolar diffusion affects only the perpendicular component, the Ohmic (O) and ambipolar (A) resistivities are

$$\eta_\mathrm{O} \doteq \eta_\parallel \quad \text{and} \quad \eta_\mathrm{A} \doteq \eta_\perp - \eta_\parallel, \tag{II.134}$$

respectively. Thus,

$$\boldsymbol{E} = -\frac{\boldsymbol{u}_\mathrm{n}}{c} \times \boldsymbol{B} + \eta_\mathrm{O} \boldsymbol{j} + \eta_\mathrm{A} \boldsymbol{j}_\perp + \eta_\mathrm{H} \boldsymbol{j} \times \hat{\boldsymbol{b}} \tag{II.135}$$

is the generalized Ohm's law. Note that an arbitrary number of species may be included in this expression, so long as their abundance is small enough that they may be considered inertia- and pressure-less and so long as the dominant collisional processes affecting their dynamics involve only the neutrals. (Regarding this final point, the inclusion of inelastic collisions between charged grains, neutral grains, ions, and electrons does not change the basic form of (II.135) – see Kunz & Mouschovias (2009).)

REFERENCES

Ara, G., Basu, B., Coppi, B., Laval, G., Rosenbluth, M. N. & Waddell, B. V. 1978 Magnetic reconnection and m = 1 oscillations in current carrying plasmas. *Annals of Physics* **112**, 443–476.

Armitage, P. J. 2011 Dynamics of Protoplanetary Disks. *Ann. Rev. Astron. Astrophys.* **49**, 195–236.

Arons, J. & Max, C. E. 1975 Hydromagnetic Waves in Molecular Clouds. *Astrophys. J. Lett.* **196**, L77.

Bacmann, A., André, P., Puget, J.-L., Abergel, A., Bontemps, S. & Ward-Thompson, D. 2000 An ISOCAM absorption survey of the structure of pre-stellar cloud cores. *Astron. Astrophys.* **361**, 555–580.

Bai, X.-N. 2013 Wind-driven Accretion in Protoplanetary Disks. II. Radial Dependence and Global Picture. *Astrophys. J.* **772**, 96.

Bai, X.-N. 2014 Hall-effect-Controlled Gas Dynamics in Protoplanetary Disks. I. Wind Solutions at the Inner Disk. *Astrophys. J.* **791**, 137.

Bai, X.-N. 2015 Hall Effect Controlled Gas Dynamics in Protoplanetary Disks. II. Full 3D Simulations toward the Outer Disk. *Astrophys. J.* **798**, 84.

Bai, X.-N. 2017 Global Simulations of the Inner Regions of Protoplanetary Disks with Comprehensive Disk Microphysics. *Astrophys. J.* **845**, 75.

Bai, X.-N. & Stone, J. M. 2011 Effect of Ambipolar Diffusion on the Nonlinear Evolution of Magnetorotational Instability in Weakly Ionized Disks. *Astrophys. J.* **736**, 144.

Bai, X.-N. & Stone, J. M. 2013 Wind-driven Accretion in Protoplanetary Disks. I. Suppression of the Magnetorotational Instability and Launching of the Magnetocentrifugal Wind. *Astrophys. J.* **769**, 76.

Bai, X.-N. & Stone, J. M. 2017 Hall Effect-Mediated Magnetic Flux Transport in Protoplanetary Disks. *Astrophys. J.* **836**, 46.

Baker, P. L. 1979 On the magnetic field in interstellar molecular clouds. *Astron. Astrophys.* **75**, 54–60.

Balbus, S. A. & Terquem, C. 2001 Linear Analysis of the Hall Effect in Protostellar Disks. *Astrophys. J.* **552**, 235–247.

Béthune, W., Lesur, G. & Ferreira, J. 2016 Self-organisation in protoplanetary discs. Global, non-stratified Hall-MHD simulations. *Astron. Astrophys.* **589**, A87.

Béthune, W., Lesur, G. & Ferreira, J. 2017 Global simulations of protoplanetary disks with net magnetic flux. I. Non-ideal MHD case. *Astron. Astrophys.* **600**, A75.

Bhattacharjee, A., Ng, C. S. & Spangler, S. R. 1998 Weakly Compressible Magnetohydrodynamic Turbulence in the Solar Wind and the Interstellar Medium. *Astrophys. J.* **494**, 409–418.

Blaes, O. M. & Balbus, S. A. 1994 Local shear instabilities in weakly ionized, weakly magnetized disks. *Astrophys. J.* **421**, 163–177.

Caselli, P., Benson, P. J., Myers, P. C. & Tafalla, M. 2002 Dense Cores in Dark Clouds. XIV. N_2H^+ (1-0) Maps of Dense Cloud Cores. *Astrophys. J.* **572**, 238–263.

Ciolek, G. E. & Mouschovias, T. C. 1993 Ambipolar Diffusion, Interstellar Dust, and the Formation of Cloud Cores and Protostars. I. Basic Physics and Formulation of the Problem. *Astrophys. J.* **418**, 774.

Ciolek, G. E. & Mouschovias, T. C. 1994 Ambipolar diffusion, interstellar dust, and the formation of cloud cores and protostars. 3: Typical axisymmetric solutions. *Astrophys. J.* **425**, 142–160.

Desch, S. J. 2004 Linear Analysis of the Magnetorotational Instability, Including Ambipolar Diffusion, with Application to Protoplanetary Disks. *Astrophys. J.* **608**, 509–525.

Desch, S. J. & Mouschovias, T. C. 2001 The Magnetic Decoupling Stage of Star Formation. *Astrophys. J.* **550**, 314–333.

Draine, B. T., Roberge, W. G. & Dalgarno, A. 1983 Magnetohydrodynamic shock waves in molecular clouds. *Astrophys. J.* **264**, 485–507.

Elmegreen, B. G. 1979 Magnetic diffusion and ionization fractions in dense molecular clouds - The role of charged grains. *Astrophys. J.* **232**, 729–739.

Fromang, S., Terquem, C. & Balbus, S. A. 2002 The ionization fraction in α models of protoplanetary discs. *Mon. Not. R. Astron. Soc.* **329**, 18–28.

Furth, H. P., Killeen, J. & Rosenbluth, M. N. 1963 Finite-Resistivity Instabilities of a Sheet Pinch. *Physics of Fluids* **6**, 459–484.

Gammie, C. F. 1996 Layered Accretion in T Tauri Disks. *Astrophys. J.* **457**, 355.

Goodman, A. A., Barranco, J. A., Wilner, D. J. & Heyer, M. H. 1998 Coherence in Dense Cores. II. The Transition to Coherence. *Astrophys. J.* **504**, 223–246.

Gressel, O., Turner, N. J., Nelson, R. P. & McNally, C. P. 2015 Global Simulations of Protoplanetary Disks With Ohmic Resistivity and Ambipolar Diffusion. *Astrophys. J.* **801**, 84.

Harris, E. G. 1962 On a plasma sheath separating regions of oppositely directed magnetic field. *Il Nuovo Cimento* **23**, 115–121.

Hawley, J. F. & Stone, J. M. 1998 Nonlinear Evolution of the Magnetorotational Instability in Ion-Neutral Disks. *Astrophys. J.* **501**, 758–771.

Hayashi, C. 1981 Structure of the Solar Nebula, Growth and Decay of Magnetic Fields and Effects of Magnetic and Turbulent Viscosities on the Nebula. *Progress of Theoretical Physics Supplement* **70**, 35–53.

Kadomtsev, B. B. & Pogutse, O. P. 1974 Nonlinear helical perturbations of a plasma in the tokamak. *Soviet Journal of Experimental and Theoretical Physics* **38**, 283–290.

Kraichnan, R. H. 1965 Inertial-Range Spectrum of Hydromagnetic Turbulence. *Physics of Fluids* **8**, 1385–1387.

Kulsrud, R. & Pearce, W. P. 1969 The Effect of Wave-Particle Interactions on the Propagation of Cosmic Rays. *Astrophys. J.* **156**, 445.

Kunz, M. W. 2008 On the linear stability of weakly ionized, magnetized planar shear flows. *Mon. Not. R. Astron. Soc.* **385**, 1494–1510.

Kunz, M. W. & Balbus, S. A. 2004 Ambipolar diffusion in the magnetorotational instability. *Mon. Not. R. Astron. Soc.* **348**, 355–360.

Kunz, M. W. & Lesur, G. 2013 Magnetic self-organization in Hall-dominated magnetorotational turbulence. *Mon. Not. R. Astron. Soc.* **434**, 2295–2312.

Kunz, M. W. & Mouschovias, T. C. 2009 The Nonisothermal Stage of Magnetic Star Formation. I. Formulation of the Problem and Method of Solution. *Astrophys. J.* **693**, 1895–1911.

Kunz, M. W. & Mouschovias, T. C. 2010 The non-isothermal stage of magnetic star formation - II. Results. *Mon. Not. R. Astron. Soc.* **408**, 322–341.

Lesur, G., Kunz, M. W. & Fromang, S. 2014 Thanatology in protoplanetary discs. The combined influence of Ohmic, Hall, and ambipolar diffusion on dead zones. *Astron. Astrophys.* **566**, A56.

Loureiro, N. F., Schekochihin, A. A. & Cowley, S. C. 2007 Instability of current sheets and formation of plasmoid chains. *Phys. Plasmas* **14** (10), 100703–100703.

Loureiro, N. F., Schekochihin, A. A. & Uzdensky, D. A. 2013 Plasmoid and Kelvin-Helmholtz instabilities in Sweet-Parker current sheets. *Phys. Rev. E* **87** (1), 013102.

Loureiro, N. F. & Uzdensky, D. A. 2016 Magnetic reconnection: from the Sweet-Parker model to stochastic plasmoid chains. *Plasma Phys. Controlled Fusion* **58** (1), 014021.

Mestel, L. 1965 Problems of Star Formation - II. *Quarterly J. R. Astron. Soc.* **6**, 265.

Mouschovias, T. C. 1976*a* Nonhomologous contraction and equilibria of self-gravitating, magnetic interstellar clouds embedded in an intercloud medium: Star formation. I Formulation of the problem and method of solution. *Astrophys. J.* **206**, 753–767.

Mouschovias, T. C. 1976*b* Nonhomologous contraction and equilibria of self-gravitating, magnetic interstellar clouds embedded in an intercloud medium: Star formation. II - Results. *Astrophys. J.* **207**, 141–158.

Mouschovias, T. C. 1991 Magnetic braking, ambipolar diffusion, cloud cores, and star formation - Natural length scales and protostellar masses. *Astrophys. J.* **373**, 169–186.

Nakano, T. & Umebayashi, T. 1980 Behavior of Grains in the Drift of Plasma and Magnetic Field in Dense Interstellar Clouds. *Pub. Astron. Soc. Japan* **32**, 613.

Oughton, S., Dmitruk, P. & Matthaeus, W. H. 2003 Coronal Heating and Reduced MHD. In *Turbulence and Magnetic Fields in Astrophysics* (ed. E. Falgarone & T. Passot), *Lecture Notes in Physics, Berlin Springer Verlag*, vol. 614, pp. 28–55.

Perez, J. C. & Chandran, B. D. G. 2013 Direct Numerical Simulations of Reflection-driven, Reduced Magnetohydrodynamic Turbulence from the Sun to the Alfvén Critical Point. *Astrophys. J.* **776**, 124.

Salmeron, R. & Wardle, M. 2003 Magnetorotational instability in stratified, weakly ionized accretion discs. *Mon. Not. R. Astron. Soc.* **345**, 992–1008.

Salmeron, R. & Wardle, M. 2005 Magnetorotational instability in protoplanetary discs. *Mon. Not. R. Astron. Soc.* **361**, 45–69.

Salmeron, R. & Wardle, M. 2008 Magnetorotational instability in protoplanetary discs: the effect of dust grains. *Mon. Not. R. Astron. Soc.* **388**, 1223–1238.

Sano, T. & Stone, J. M. 2002*a* The Effect of the Hall Term on the Nonlinear Evolution of the Magnetorotational Instability. I. Local Axisymmetric Simulations. *Astrophys. J.* **570**, 314–328.

Sano, T. & Stone, J. M. 2002*b* The Effect of the Hall Term on the Nonlinear Evolution of the Magnetorotational Instability. II. Saturation Level and Critical Magnetic Reynolds Number. *Astrophys. J.* **577**, 534–553.

Scalo, J. M. 1977 Heating of dense interstellar clouds by magnetic ion slip - A constraint on cloud field strengths. *Astrophys. J.* **213**, 705–711.

Simon, J. B., Bai, X.-N., Armitage, P. J., Stone, J. M. & Beckwith, K. 2013*a* Turbulence in the Outer Regions of Protoplanetary Disks. II. Strong Accretion Driven by a Vertical Magnetic Field. *Astrophys. J.* **775**, 73.

Simon, J. B., Bai, X.-N., Stone, J. M., Armitage, P. J. & Beckwith, K. 2013*b* Turbulence in the Outer Regions of Protoplanetary Disks. I. Weak Accretion with No Vertical Magnetic Flux. *Astrophys. J.* **764**, 66.

Simon, J. B., Lesur, G., Kunz, M. W. & Armitage, P. J. 2015 Magnetically driven accretion in protoplanetary discs. *Mon. Not. R. Astron. Soc.* **454**, 1117–1131.

Spitzer, L. 1978 *Physical processes in the interstellar medium*. Wiley-Interscience.

Stenzel, R. L. 1999 Whistler waves in space and laboratory plasmas. *J. Geophys. Res.* **104**, 14379–14396.

Strauss, H. R. 1976 Nonlinear, three-dimensional magnetohydrodynamics of noncircular tokamaks. *Phys. Fluids* **19**, 134–140.

Strauss, H. R. 1977 Dynamics of high beta Tokamaks. *Phys. Fluids* **20**, 1354–1360.

Tafalla, M., Myers, P. C., Caselli, P. & Walmsley, C. M. 2004 On the internal structure of starless cores. I. Physical conditions and the distribution of CO, CS, N_2H^+, and NH_3 in L1498 and L1517B. *Astron. Astrophys.* **416**, 191–212.

Umebayashi, T. & Nakano, T. 1990 Magnetic flux loss from interstellar clouds. *Mon. Not. R. Astron. Soc.* **243**, 103–113.

Wardle, M. 1999 The Balbus-Hawley instability in weakly ionized discs. *Mon. Not. R. Astron. Soc.* **307**, 849–856.

Wardle, M. 2007 Magnetic fields in protoplanetary disks. *Astrophys. Space Sci.* **311**, 35–45.

Wardle, M. & Salmeron, R. 2012 Hall diffusion and the magnetorotational instability in protoplanetary discs. *Mon. Not. R. Astron. Soc.* **422**, 2737–2755.

Yamada, M., Kulsrud, R. & Ji, H. 2010 Magnetic reconnection. *Rev. Mod. Phys.* **82**, 603–664.

Zank, G. P. & Matthaeus, W. H. 1992*a* The equations of reduced magnetohydrodynamics. *J. Plasma Phys.* **48**, 85.

Zank, G. P. & Matthaeus, W. H. 1992*b* Waves and turbulence in the solar wind. *J. Geophys. Res.* **97**, 17189.

Zweibel, E. G. & Josafatsson, K. 1983 Hydromagnetic wave dissipation in molecular clouds. *Astrophys. J.* **270**, 511–518.

Zweibel, E. G. & Yamada, M. 2009 Magnetic Reconnection in Astrophysical and Laboratory Plasmas. *Ann. Rev. Astron. Astrophys.* **47**, 291–332.